

THE UNIVERSITY OF HULL

**Exploration of the Bioadhesivity of
Sporopollenin microcapsules and their use to
Encapsulate and Release Drugs and Vitamin D**

being a Thesis submitted for the Degree of

Doctor of Philosophy

in the University of Hull

by

Farooq Almutairi, BSc, MSc.

November 2015

Acknowledgements

Firstly, I would like to acknowledge this work to the most important people, who helped me a lot during the time of this project and tried to find a time for me in their busy schedule, Dr. Andrew Boa and Dr. Grahame Mackenzie. Also, I want to say that both of them were valuable for the accomplishment of this thesis. Million Thanks go to Prof. Steve Archibald for his support and guidance during the time of this thesis writing up.

Also, I would like to thank Dr. Colin Thompson (School of Pharmacy and Life Sciences, Robert Gordon University) for his help and guidance in the mucoadhesion part of this report, Dr. Mark Lorch for his help in using the NMR, Dr. Kevin Welham for his help in mass spectrometry, Dr. Alberto Diego-Taboada for his technical assistance in the beginning of my Ph.D lab work and to my best friend Dr. Youkui Huang.

Many thanks for Mr. Tony Sinclair, Mr. Bob Knight and Mrs. Carol Kennedy for obtaining the SEM images, ICP and elemental analysis, respectively.

Also, great thanks go to project students who brought enjoyment to the work, thanks Ryan, Leila and Marie.

I dedicate this thesis to my family for their precious support, and to the Ministry of Higher Education in the Kingdom of Saudi Arabia for their scholarship.

Abstract

Sporopollenin is the polymeric fabric of the outer shell (known as exine) of plant spores and pollen grains. It is a highly cross-linked polymer composed of carbon, hydrogen and oxygen. It contains functional groups such as phenols, carboxylic acids and aliphatic alcohols as well as hydrophobic saturated and unsaturated alkyl chains. Sporopollenin is one of the most extraordinarily resistant polymers known in the organic world. It has the ability to resist harsh biological, chemical and physical environments, as intact sporopollenin exines have been found intact in some sedimentary rocks that are 500 million years old.

This hydrophobic biopolymer has interesting properties, as its lipids (which are 20 % w/w of the total mass of extracted spores) possess liquid-like behavior in a dry solid polymer. This biopolymer has the ability to transform the liquid simple C18 fatty acids into “dry liquid” state when adsorbed or attached chemically to the surface.

Sporopollenin exine capsules (SECs) have potential as a microparticle for vitamin and drug microencapsulation offering protection, controlled release and absorption enhancement. SECs have been shown to be able to encapsulate hydrophilic and hydrophobic drugs and vitamins and they have the ability to control the release of the encapsulated actives depending on the pH.

In this study vitamin D, diclofenac sodium salt and mesalamine were encapsulated in *L. clavatum* SECs, and then released into buffer solutions at different pHs that mimic the GIT pHs. The release of such kind of vitamin and drugs showed the direct effect of pH factor on the release of the SECs contents. Vitamin D was released in pH 7.4, but was not in acidic pH. This was an interesting point, especially, for protecting the

encapsulated vitamin D from the harsh acidic environment of stomach and release it in the mildly basic environment of small intestine. Also, diclofenac sodium was released fully in pH 7.4 within 12 hours, whereas less than 40 % was released in pH 1.5. However, the mesalamine showed a full release in acidic pH which showed that SECs need coating to be used for mesalamine. The adsorption of the drugs to the SECs was shown to be very low (0.4 %), which means that almost all the drug will be released and would not adsorb to the SECs surface, especially in the GIT when they would be flushed with fluid continuously.

It is proposed that the ability of SECs to enhance the absorption is related to the mucoadhesivity that they possess, which was shown to be higher than chitosan and lower than carbopol. The mucoadhesion strength for *L. clavatum* powder polymer was statistically significant either with their lipids in (p-value = 0.03), or when their lipids were removed (p-value = 0.01).

Also, the “dry liquid” C16 and C18 fatty acids of SECs might play role in absorption enhancement by disturbing the tight junction of the paracellular pathway transport, were most of the hydrophilic small molecules pass through to blood stream.

The disintegration time of SECs tablets gives an idea about the best extraction protocol to use to increase the time of disintegration or decrease it depending in the site of absorption. For example, AH-SECs of *L. clavatum* was disintegrated within 2 h and lost 23.33 % of their mass, which is a preferable SECs type to be used for drug release in intestine within 2 h from the time of SECs tablet ingestion.

Keywords: *Spores; Pollen grains; Sporopollenin; Exines; Lycopodium clavatum; Dry liquid; Microencapsulation; Drug delivery; Vitamin D; Diclofenac; Mesalamine; Mucoadhesion; Absorption enhancer.*

Content:

<u>Abstract</u>	iii
<u>Content</u>	v
<u>Abbreviations</u>	xi
<u>List of Figures</u>	xv
Chapter 1. Sporopollenin: Definitions, Properties and Structure	1
1.1 Spores and Pollen.....	1
1.1.1 Spores from <i>Lycopodium clavatum</i>	4
1.2 Sporopollenin.....	5
1.3 Morphology of <i>L. clavatum</i> spores	6
1.3.1 Nanochannels of <i>L. clavatum</i> spores.....	7
1.4 Physical Characteristics of Sporopollenin	8
1.4.1 Chemical Resistance	8
1.4.2 Thermal Resistance	9
1.4.3 Biological Resistance	9
1.5 Extraction of Sporopollenin from Raw spores and pollen grains	10
1.5.1 Treatment with Alkali and Phosphoric acid.....	11
1.5.2 Acetolysis.....	11
1.5.3 Anhydrous Hydrofluoric acid.....	11
1.5.4 Enzymes	12
1.5.5 4-Methylmorpholine- <i>N</i> -oxide	12

1.5.6 Hydrochloric acid.....	12
1.6 Overview of Sporopollenin Chemical Structure.....	13
1.6.1 NMR Spectroscopy of Sporopollenin	14
1.6.1.1 Liquid-state ¹ H-NMR	14
1.6.1.2 MAS SS- ¹³ C-NMR	16
Chapter 2. Sporopollenin: Ingestion, Toxicology and Applications	21
2.1 Ingestion and Absorption of Sporopollenin.....	21
2.2 Digestion of Sporopollenin.....	21
2.3 Toxicology of Sporopollenin.....	22
2.4 Applications of Sporopollenin SECs	22
2.4.1 Microencapsulation	23
2.4.1.1 Currently available drug delivery system.....	24
2.4.2 SECs in Taste Masking	25
2.4.3 SECs as Absorption Enhancers	27
2.4.4 SECs as Sequestrators	29
2.4.5 Micro-reactors and Bio-reactors.....	29
2.4.6 SECs in Drug Delivery.....	32
2.4.6.1 Mucoadhesion.....	34
2.4.6.1.1 Mucoadhesion Mechanism	34
2.4.6.1.2 Mucoadhesive Polymers	37
2.5 Aims and Objectives.....	38
2.5.1 Aims	38
2.5.2 Objectives.....	38

Chapter 3. Sporopollenin: Physical and Chemical Characteristics	39
3.1 Chemical Resistance	39
3.2 Thermal Resistance	44
3.3 The Elasticity of SECs	46
3.4 The Nature of SECs' Lipids.....	48
3.4.1 Raw Spores and Pollens	48
3.4.2 Acid Hydrolyzed SECs of Spores and Pollen	52
3.4.3 Dissolving the SECs Lipids	53
3.4.4 SECs and 'dry liquid' lipids	58
3.4.5 Determination the Chemical Structure of the 'dry liquid' Lipids of SECs.....	59
3.4.6 Attempted Determination of the Location of SEC 'dry liquid' lipids using Nile red staining and Fluorescence Microscopy	62
3.4.7 Adding Oleic acid to SECs after Removal of their Natural Lipids.....	63
3.4.8 Adding Oleic acid to SECs after Surface Modification	66
3.4.9 Covalent attachment of Oleic acid to SECs	69
3.4.10 Attempted PEGylation of SECs	72
Chapter 4. Encapsulation and Release of Vitamin D and Actives	77
4.1 SECs as a Solution Buffer.....	77
4.2 Encapsulation and Release of Vitamin D and the Role of pH.....	78
4.2.1 Vitamin D ₂ Release and the Role of pH.....	80
4.3 Other Drugs Encapsulation and Release (the role of pH).....	83
4.3.1 Diclofenac sodium salt	83
4.3.1.1 The Controlled Release of Diclofenac sodium.....	88

4.3.1.2 Comparison of Diclofenac Na Release with Different SECs species	90
4.3.1.3 Adsorption of Diclofenac sodium salt on SECs	92
4.3.2 Mesalamine	96
Chapter 5. Mucoadhesion Studies of SECs	100
5.1 Evaluation the Interaction between Mucin and SECs using Differential Scanning Calorimetry (DSC).....	101
5.2 <i>In vitro</i> Evaluation of Mucoadhesion Properties of SECs using Texture Analyzer	111
5.2.1 Powder form samples	113
5.2.2 Tablet form samples	116
Chapter 6. SECs' Morphology and Lipids role in their Mucoadhesivity	120
6.1 The Role of SECs' Morphology in their Mucoadhesivity	120
6.2 The Role of SECs' Lipids in their Mucoadhesivity	122
6.3 <i>Ex vivo</i> Evaluation of SECs' Morphology and Lipids in Mucoadhesion	124
6.4 Disintegration Test of SECs' Tablets	129
6.5 An attempt to Explain the Role of SECs Mucoadhesivity, the 'dry liquid' Lipids and the Controlled Release in Absorption Enhancement	136
Chapter 7. Conclusion	138
Chapter 8. Materials and Methods.....	141
8.1 Materials	141
8.1.1 Chemicals	141
8.1.2 Apparatus	142

8.1.2.1 Magic Angle Spinning solid-state proton Nuclear Magnetic Resonance (MAS SS- ¹ H-NMR)	142
8.1.2.2 Ultraviolet-Visual (UV-Vis) Spectroscopy	142
8.1.2.3 Scanning Electron Microscopy (SEM).....	142
8.1.2.4 Texture Analyzer	142
8.1.2.5 Differential Scanning Calorimetry (DSC).....	143
8.1.2.6 Elemental Composition Analysis	143
8.1.2.7 Inductively Coupled Plasma- Optical Emission Spectrometer (ICP-OES)	143
8.1.2.8 pH Testing	143
8.1.2.9 Gas Chromatography Mass Spectrometry (GC-MS).....	144
8.1.2.10 Disintegration Testing	144
8.2 Extraction of Sporopollenin exine capsules (SECs) from Raw spores.....	145
8.2.1 Protocol A: Extraction of <i>L. clavatum</i> SECs using Base Hydrolysis.....	145
8.2.2 Protocol B: Extraction of sporopollenin using Acid Hydrolysis.....	146
8.2.3 Protocol C: Treatment of Base hydrolyzed SECs of <i>L. clavatum</i> (BH-SECs) with acid	147
8.3 Chemical Resistance Study.....	147
8.4 Thermal Resistance Study.....	147
8.5 A study of <i>L. clavatum</i> SECs' Elasticity	148
8.6 A study of <i>L. clavatum</i> SECs' Lipids	148
8.6.1 An Attempt to Dissolve Raw SECs Lipids with Different Solvents.....	148
8.6.2 An Attempt to Dissolve AH-SECs Lipids with Different Solvents	149
8.6.3 An Attempt to Quantify the AH-SECs Lipids using MAS SS- ¹ H-NMR.....	149

8.6.4 Nile red Staining of SECs	149
8.6.5 An Attempt to Add C18 fatty acid to the Lipid-free AH-SECs Physically ..	150
8.6.6 Modifying the Surface of SECs with NaOH.....	150
8.6.7 An Attempt to Add C18 fatty acid to the Lipid-free AH-SECs Chemically.	150
8.6.8 Attempted PEGylation of SECs	151
8.7 A study AH-SECs and BH-SECs of <i>L. clavatum</i> Acting as a Buffer Particles...	152
8.8 Vitamin and Other Drugs Encapsulation and Release	152
8.8.1 Encapsulation of Vitamin D ₂ (ergocalciferol) into BH-AH-SECs of <i>L. clavatum</i>	152
8.8.2 Mixing DOPC with Vitamin D ₂	153
8.8.3 Mixing DOPC with Vitamin D ₂ encapsulated SECs	153
8.8.4 Diclofenac and Mesalamine Encapsulation and Release	153
8.8.4.1 Encapsulation of Diclofenac in AH-SECs of <i>L. clavatum</i>	153
8.8.4.2 Encapsulation of Mesalamine in AH-SECs of <i>L. clavatum</i>	154
8.8.4.3 Release of Encapsulated Drugs into Buffer Solutions.....	154
8.9 Drug Adsorption Study of Diclofenac sodium salt.....	154
8.10 Mucoadhesion Studies (<i>in vitro</i>).....	155
8.10.1 Preparation DSC samples.....	155
8.10.2 Preparing samples for Texture Analysis	156
8.11 Preparing the <i>ex vivo</i> Experiments of Mucoadhesion.....	156
8.12 Preparing Tablet Disintegration Experiments.....	157
<u>References</u>	158

Abbreviations

AH	Acid hydrolysis
AH-SECs	Acid hydrolyzed sporopollenin exine capsules
<i>A. trifida</i>	<i>Ambrosia trifida</i>
<i>A. artemisifolia</i>	<i>Ambrosia artemisifolia</i>
<i>A. niger</i>	<i>Aspergillus niger</i>
BH-SECs	Base hydrolyzed spores
°C	Degrees celsius
<i>C. vulgaris</i>	<i>Chlorella vulgaris</i>
BH-AH SECs	Base hydrolyzed, and then acid hydrolyzed SECs
DOPC	1,2-dioleoyl-sn-glycero-3-phosphocholine
DSC	Differential scanning calorimetry
D ₂ vitamin	Ergocalciferol
DMSO	Dimethyl sulfoxide
DCM	Dichloromethane
EPA	Eicosapentaenoic acid
FTIR	Fourier transform infrared spectroscopy
g	Gram
GIT	Gastrointestinal tract
GC	Gas Chromatography
GC-MS	Gas Chromatography Mass Spectrometry

Abbreviations

HPLC	High performance liquid chromatography
<i>H. annuus</i>	<i>Helianthus annuus</i>
h	hour
IR	Infrared
ICP-OES	Inductive coupled plasma optical emission spectrometer
J/g	Joule per gram
LC-MS	Liquid Chromatography Mass Spectrometry
L	Litre
<i>L. clavatum</i>	<i>Lycopodium clavatum</i>
mM	Millimolar
M	Molar
mN	Millinewton
mg	Milligram
ml	Milliliter
mm	Millimeter
min	Minute
MAS SS- ¹ H-NMR	Magic angle spinning solid-state proton nuclear magnetic resonance
MAS SS- ¹³ C-NMR	Magic angle spinning solid-state carbon nuclear magnetic resonance
MRI	Magnetic resonance imaging

Abbreviations

ng	Nanogram
NMR	Nuclear magnetic resonance
NSAID	non-steroidal anti-inflammatory drug
PEG	polyethylene glycol
psi	Per square inch
PBS	Phosphate buffered saline
<i>P. sylvestris</i>	<i>Pinus sylvestris</i>
ppm	Parts per million
SECs	Sporopollenin exine capsule
SEM	Scanning electron microscope
s	Second
<i>S. cereale</i>	<i>Secale cereale</i>
<i>T. angustifolia</i>	<i>Typha angustifolia</i>
Uv-Vis	Ultraviolet – Visible light
μL	Microlitre
% w/w	Weight to weight percentage
<i>Z. mays</i>	<i>Zea mays</i>

Abbreviations

C16 16 carbons

C18 18 carbons

List of Figures

Figure 1: General Illustration of spores and pollen anatomy [4].....	2
Figure 2: Common club moss plants, displays the feren-like stems (yellow) [1].....	4
Figure 3: <i>L. clavatum</i> spores SEM images and detailed illustration [2].....	6
Figure 4: <i>L. clavatum</i> spore cross-section showing the nanochannels [11].....	7
Figure 5: (A) <i>L. clavatum</i> exines before incubation in human plasma.....	10
Figure 6: Liquid ¹ H NMR spectrum of sporopollenin from <i>T. angustifolia</i> obtained at 400 MHz [29].....	15
Figure 7: MAS SS- ¹³ C-NMR spectrum of <i>L. clavatum</i> obtained at 100 Hz [40].....	16
Figure 8: MAS SS- ¹³ C-NMR full spectra of sporopollenin obtained at 37.8 MHz, showing (A) <i>C. vulgaris</i> ; (B) <i>L. clavatum</i> ; (C) <i>P. sylvestris</i> ; (D) <i>Triticum species</i> and (E) <i>A. trifida</i> [26].	19
Figure 9: Encapsulating cod fish oil in <i>L. clavatum</i> SECs	26
Figure 10: The bioavailability of EPA was enhanced when encapsulated by SECs, as shown by measuring EPA serum level over time [73].	28
Figure 11: Optical microscopy images.	30
Figure 12: SEM images of encapsulated yeast cells inside prepared <i>L. clavatum</i> SECs [76].....	31
Figure 13: (A) suspension of magnetic SECs with entrapped yeast cells; (B) The SECs are attracted to the external magnet due to the encapsulated magnetic nanoparticles as well as yeast cells [76].	31
Figure 14: Illustration of therapeutic active encapsulated in the SECs' cavity.	32

Figure 15: Structure of first generation mucoadhesive polymers. (A) poly(acrylic acid); (B) chitosan; (C) cellulose derivatives.....37

Figure 16: Summary of the acid hydrolysis (AH) method used to treat spores and pollens, to give empty shells of AH-SECs (Protocol B).....40

Figure 17: SEM images of raw spores of *L. clavatum*.....41

Figure 18: MAS SS-¹H-NMR spectra of AH-SECs of *L. clavatum*42

Figure 19: SEM images of AH-SECs of *L. clavatum* (A) before and (B) after incubation in oven at 200 °C for 24 h.....45

Figure 20: MAS SS-¹H-NMR spectra of AH-SECs of *L. clavatum* incubated for 3 h (A) and 24 h (B) at 200 °C, compared to raw spores (C).46

Figure 21: *L. clavatum* SECs return to its original shape after compression in just 40 seconds.47

Figure 22: (A) Attempted fragmentation of *L. clavatum* SECs by grinding with mortar and pestle using (70-110 μm) glass beads. (B) SECs outer shell deformity....48

Figure 23: MAS SS-¹H-NMR spectra of raw *L. clavatum* spores (a) following treatment with the different solvents namely, dodecane (b), chloroform (c), acetone (d) and ethanol (e).....50

Figure 24: MAS SS-¹H-NMR spectra of AH-SECs of *L. clavatum* and *P. sylvestris*. 55

Figure 25: MAS SS-¹H-NMR spectrum of AH-SECs of *L. clavatum* showing the lipids peaks,.....57

Figure 26: GC-MS show that SEC lipids are a mixture of mainly the mono- and di-unsaturated lipids60

Figure 27: MAS SS-¹H-NMR spectrum of ‘dry liquid’ lipids of *L. clavatum* SECs...61

Figure 28: Fluorescence microscopy of *L. clavatum* AH-SECs without stain (A), and after staining with Nile red (B).63

Figures

Figure 29: The MAS SS- ¹ H-NMR spectra illustrates dodecane-refluxed AH-SECs of <i>L. clavatum</i> after absorption of oleic acid.....	65
Figure 30: MAS SS- ¹ H-NMR of dodecane-treated AH-SECs of <i>P. sylvestris</i>	65
Figure 31: Modifying SECs' surface from acid and phenol to their salt forms.....	66
Figure 32: MAS SS- ¹ H-NMR spectra of surface-modified SECs from <i>L. clavatum</i> and <i>P. sylvestris</i>	67
Figure 33: Esterification of <i>L. clavatum</i> SECs using oleic acid (method A) and oleoyl chloride (method B).....	70
Figure 34: MAS SS- ¹ H-NMR spectra of esterified SECs of <i>L. clavatum</i> using oleic acid (A) and oleoyl chloride (B),	71
Figure 35: PEGylation of <i>L. clavatum</i> SECs using either K ₂ CO ₃ or NaH as base.....	73
Figure 36: MAS SS- ¹ H-NMR spectra of <i>L. clavatum</i> SECs showing (A) the lipid-free SECs, (B) the PEGylated SECs using the 1 st method and (C) the PEGylated SECs using the 2 nd method.	75
Figure 37: MAS SS- ¹ H-NMR spectra of PEGylated AH-SECs.....	76
Figure 38: Vitamin D ₂ (ergocalciferol) chemical structure.	79
Figure 39: SECs of <i>L. clavatum</i> after encapsulation of vitamin D ₂ with a loading of (0.3:1 w/w).....	80
Figure 40: MAS SS- ¹ H-NMR spectra of (a) DOPC and vitamin D ₂ interaction.....	82
Figure 41: Diclofenac sodium salt chemical structure.....	83
Figure 42: <i>L. clavatum</i> SECs after encapsulation of diclofenac sodium salt with a loading of (0.45:1 w/w).....	84
Figure 43: Release of diclofenac sodium salt from AH-SECs of <i>L. clavatum</i> into buffered solutions by time at different pH. <i>n</i> =3.....	85

Figures

Figure 44: Release of free acid (Dic) and salt (Dic-Na) form of diclofenac from AH-SECs of <i>L. clavatum</i> into buffered solutions by time at different pH. $n = 3$	88
Figure 45: Release of diclofenac Na form AH-SECs of <i>L. clavatum</i> into PBS (pH 7.4) over time.	90
Figure 46: SEM image of <i>H. annuus</i> AH-SECs showing their relatively large pore (yellow circle).	91
Figure 47: Release of diclofenac sodium salt form AH-SECs of <i>L. clavatum</i> (LC) and <i>H. annuus</i> (HA) into PBS pH 7.4 by time. $n = 3$	92
Figure 48: Showing the ability of SECs of <i>L. clavatum</i> to extract diclofenac sodium salt from a water solution.	94
Figure 49: The structure of mesalamine, showing the basic amino group and acidic carboxylic group that it possesses.	96
Figure 50: SEM images of <i>L. clavatum</i> AH-SECs after encapsulating mesalamine with a loading of (0.05:1 w/w).	97
Figure 51: Mesalamine release from AH-SECs of <i>L. clavatum</i>	98
Figure 52: A DSC thermogram of mucin as received.	103
Figure 53: A DSC thermogram of freeze-dried mucin	103
Figure 54: A DSC thermogram of AH-SECs of <i>A. artemisifolia</i>	104
Figure 55: A DSC thermogram of freeze-dried <i>A. artemisifolia</i>	105
Figure 56: A DSC thermogram of <i>A. artemisifolia</i> . SECs-mucin freeze-dried.	106
Figure 57: Overlay of the DSC thermograms of AH-SECs <i>A. artemisifolia</i> , SECs and mucin.	106
Figure 58: A DSC thermogram of AH-SECs of <i>L. clavatum</i>	108
Figure 59: A DSC thermogram of freeze-dried AH-SECs from <i>L. clavatum</i>	108
Figure 60: A DSC thermogram of AH-SECs of <i>L. clavatum</i> -mucin freeze dried.	109

Figures

Figure 61: Overlay DSC thermograms of AH-SECs of (a) <i>L. clavatum</i> freeze-dried, (b) mucin freeze-dried, (c) mucin powder as received and (d) mucin-SECs freeze-dried.	110
Figure 62: Schematic curve shows peak force and work of adhesion parameters that are measured by a texture analyzer.....	112
Figure 63: The detachment force of the four SEC samples and the two controls (all in powder form). $n = 3$	113
Figure 64: Work of adhesion of SECs in powder form, $n = 3$	115
Figure 65: Tablets of SECs show an increase in ‘detachment force’ for all types of SECs.....	117
Figure 66: ‘Work of adhesion’ vs different contact times for SEC tablets and controls. $n = 3$	118
Figure 67: SEM images of <i>H. annuus</i> SECs (A) showing their long spikes in comparison to <i>L. clavatum</i> (B).....	121
Figure 68: Peak force of tablet AH-SECs of <i>H. annuus</i> (HA), <i>L. clavatum</i> (LC) and controls (carbopol and chitosan). $n = 3$	122
Figure 69: Peak force of powder AH-SECs of <i>L. clavatum</i> (LC) with and without their lipids and the control polymers of chitosan and carbopol. $n = 3$	123
Figure 70: <i>Ex vivo</i> mucoadhesion experiment.	125
Figure 71: (A) AH-SECs of <i>L. clavatum</i> (lipids-free) spread over the cow cheek tissue, and (B) after shaking in water bath for 2 hours at 37 °C.	127
Figure 72: (A) AH-SECs of <i>L. clavatum</i> spread over the cow cheek tissue, and (B) after shaking in water bath for 2 hours at 37 °C.	127
Figure 73: (A) AH-SECs of <i>H. annuus</i> spread over the cow cheek tissue, and (B) after shaking in a water bath for 2 hours at 37 °C.	128

Figures

Figure 74: Tablet disintegration in upper GIT (stomach).....	130
Figure 75: Disintegration apparatus used to study SECs tablets	131
Figure 76: AH-SECs of <i>H. annuus</i> tablets after 2 hours in disintegrator instrument.	132
Figure 77: AH-SECs of <i>H. annuus</i> tablets preserved their structure after subjecting to the disintegration for 2 hours	133
Figure 78: AH-SECs of <i>L. clavatum</i> tablets after disintegration for 2 hours..	134
Figure 79: BH-SECs of <i>L. clavatum</i> tablets before disintegration.	135
Figure 80: Role of SECs in absorption enhancement..	137

List of Tables

Table 1: Diameters of different spores/pollen grains [4].	3
Table 2: The chemical composition of sporopollenin from different species that was shown in MAS SS- ¹³ C-NMR.	17
Table 3: Interpretation of the four main peaks in the 140-200 ppm region of sporopollenin from different species using MAS SS- ¹³ C-NMR spectra.	17
Table 4: Summary of bioadhesion theories [86, 88-89].	35
Table 5: Chemical bonds that contribute in mucoadhesion [85, 90].	36
Table 6: Mass recovered after treating 1.000 g of raw spores/pollen with different solvents (1g SEC/ 10 ml solvent). <i>n</i> = 3.	49
Table 7: Mass recovered after treating 0.200 g of ethanol and acetone refluxed-spores and pollen with dodecane at 60 °C for 4 hours. <i>n</i> = 3.	51
Table 8: Mass recovered after hydrolyzing 5 g of spores and pollens with 9 M HCl for 1 h. <i>n</i> = 3.	52
Table 9: Elemental analysis of extracted <i>L. clavatum</i> SECs. The elemental analysis was run in triplicate. <i>n</i> = 3.	53
Table 10: Mass recovered of HCl-extracted spores/pollen (1 g) after treatment them with dodecane for 4 h at 60 °C. <i>n</i> = 3.	56
Table 11: Elemental analysis for <i>L. clavatum</i> AH-SECs after removal of lipids by dissolution in dodecane. <i>n</i> = 3.	58
Table 12: AH-SECs from <i>L. clavatum</i> and <i>P. sylvestris</i> , after treatment with dodecane, are able to sequester oleic acid from an oil-water emulsion. The results show the mass gain after oil sequestration. The mass of oil that can be sequestered by the SECs is similar the oil that they lose after initial dodecane washing. <i>n</i> = 3.	64

Tables

Table 13: Mass gain of SECs after sequestration of oleic acid by salt form of AH-SECs from <i>L. clavatum</i> and <i>P. sylvestris</i> . $n = 3$	68
Table 14: Elemental analysis for PEGylated SECs from <i>L. clavatum</i> using NaH. $n = 3$	74
Table 15: pH of pure water (20 ml) after addition of 200 mg of AH and BH SECs of <i>L. clavatum</i> at different incubation times. The pH measurements were run in triplicate for each type of SECs. $n = 3$	78
Table 16: Diclofenac sodium salt release from SECs in solutions of different pH. $n = 3$	86
Table 17: Illustrates the amount of diclofenac adsorbed by one sample of <i>L. clavatum</i> AH-SECs (10 mg) from five 1 ml aliquots of a diclofenac sodium salt (5 $\mu\text{g}/\text{ml}$). $n = 3$	95
Table 18: Mesalamine release % from AH-SECs of <i>L. clavatum</i> (10 mg of SECs contains 500 μg of mesalamine) into 1 ml buffer solution by time at different pHs. $n = 3$	99
Table 19: Summary of Peak force of powder AH-SECs of <i>L. clavatum</i> (LC) with and without their lipids and the control polymers of chitosan and carbopol. $n = 3$	124
Table 20: <i>Ex vivo</i> experiments of mucoadhesion of different SECs. $n = 3$	126
Table 21: Elemental analysis of BH-SECs <i>L. clavatum</i> . The elemental analysis was run in triplicate. $n = 3$	146

Chapter 1. Sporopollenin: Definitions, Properties and Structure

1.1 Spores and Pollen

In general terms, the spore is part of the reproductive system of plants and they are typically micron sized transportable particles [1]. They composed of one or two sporoplasms (small cells that contain different types of lipids, carbohydrates and proteins). Spores are formed inside the internal cavity (loculus) of the sexual organs of plant, which is known as the sporangia. The loculus is lined by a tissue of cells called tapetum where the spores originate. When the spores mature in the tapetum, they cluster into a tetrad unit (four spores grouped together).

The main role of spores is to spread away the half of the genetic materials of their own plants, i.e. haploid nuclei, in order to reproduce [2]. Therefore, spores have complicated morphology and spreading mechanisms due to their role in the mobile sexual cycle

Basically, the spore wall has a complex, two layer structure and its main role is to protect the spore content from any harsh environmental conditions [3]. The layers of the spore wall are divided into an internal layer, called the intine, and an external layer called the exine (see Figure 1). The intine is mainly comprised of cellulose and other polysaccharides and the exine is composed of sporopollenin [4].

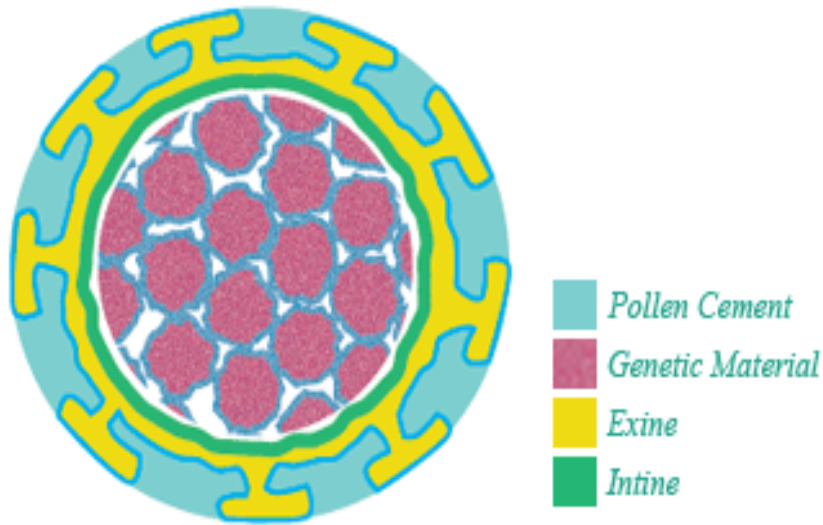


Figure 1: General Illustration of spores and pollen anatomy [4].

Pollen grains, or just pollen, are the most mature phase of spermatophytes in seed bearing plants. The main difference between spores and pollens is that spores are the mature phase which when they fall in soil they can grow to a full plant, while the pollens are in need of reaching a female gametophyte, ovule, in order to make seeds which give a full plant [1,5]. The size of spores is usually measured by their diameter, and they range typically from 1-25 μm (see Table 1), though some may be larger.

Spore/ Pollen	Diameter size
<i>Myosotis</i> (“forget-me-not”)	2.4 – 5 μm
<i>Aspergillus niger</i>	4 μm
<i>Penicillium</i>	3 – 5 μm
<i>Cantharellus minor</i>	4 – 6 μm
<i>Ganoderma</i>	5 – 6.5 μm
<i>Chlorella vulgaris</i>	8 - 10 μm
Oilseed rape	10 - 12 μm
<i>Agrocybe</i>	10 – 14 μm
<i>Urtica dioica</i> (common nettle)	10 – 12 μm
<i>Periconia</i>	16 – 18 μm
<i>Epicoccum</i>	20 μm
<i>Lolium perenne</i> (ryegrass)	21 μm
<i>Phleum pratense</i> (Timothy grass)	22 μm
<i>Secale cereale</i> (rye)	22 μm
<i>Lycopodium clavatum</i> (club moss)	25 μm

Table 1: Diameters of different spores/pollen grains [4].

1.1.1 Spores from *Lycopodium clavatum*

Spores from *Lycopodium clavatum* (*L. clavatum*, the common club moss) were used in this study. Club moss can be found worldwide. Generally, it grows near the ground with fern-like stems up to half-meter long (see Figure 2). In the last two centuries [1], *L. clavatum* spores have been used as a combustible powder for blossoming of fireworks because of their cheap price. In addition, they have been used in old traditional medicine and in new advanced pharmaceutical application as a drying agent [6].



Figure 2: Common club moss plants, displays the feren-like stems (yellow) [1].

1.2 Sporopollenin

The origin of the term sporopollenin comes from two words. In 1814, John described the difficulty of modifying the exines of tulips and their lack of chemical responses compared to the rest of the pollen layers, and then gave the name 'pollenin' to define the contents of this material [7]. Later on, Zetzsche gave the name 'sporonin' to define the highly resistant materials that made the exines of *L. clavatum* [8]. Experiments began on the examination of the membranes of pollen and spores, and in particular the sporopollenin structure. Sporopollenin was isolated from various pollen grains, spores and even fossil material in order to identify their composition. By the end of 1931, Zetzsche adopted the term 'sporopollenin' indicating that the resistant materials in spores' exines and pollen walls have the same chemical structure.

As it was mentioned earlier (in Section 1.1), *L. clavatum* spores have two layers. The inner layer, intine, which is composed mainly of cellulose and the outer layer, exine, consists mostly from sporopollenin. The intine surrounds and protects the cytoplasm (which contains nitrogenous genetic materials, fats and some proteins) [2]. Since the intine consists of cellulose, it can be cleaved by acetolysis (acetic anhydride and sulfuric acid) and removed. On the other hand, the exine is resistant to strong acid and base and can resist many chemical, physical and biological factors [9].

Hence, sporopollenin has been defined as "the most resistant non-soluble materials left after acetolysis" [3]. However, the precise chemical structure of sporopollenin is still unclear.

1.3 Morphology of *L. clavatum* spores

There are two types of decorations visible from the outside: the tectal elements and the apertures [2]. Figure 3 illustrates some tectal elements and apertures present in *L. clavatum* spores used in this study and compare them to the scanning electron microscopy (SEM) images.

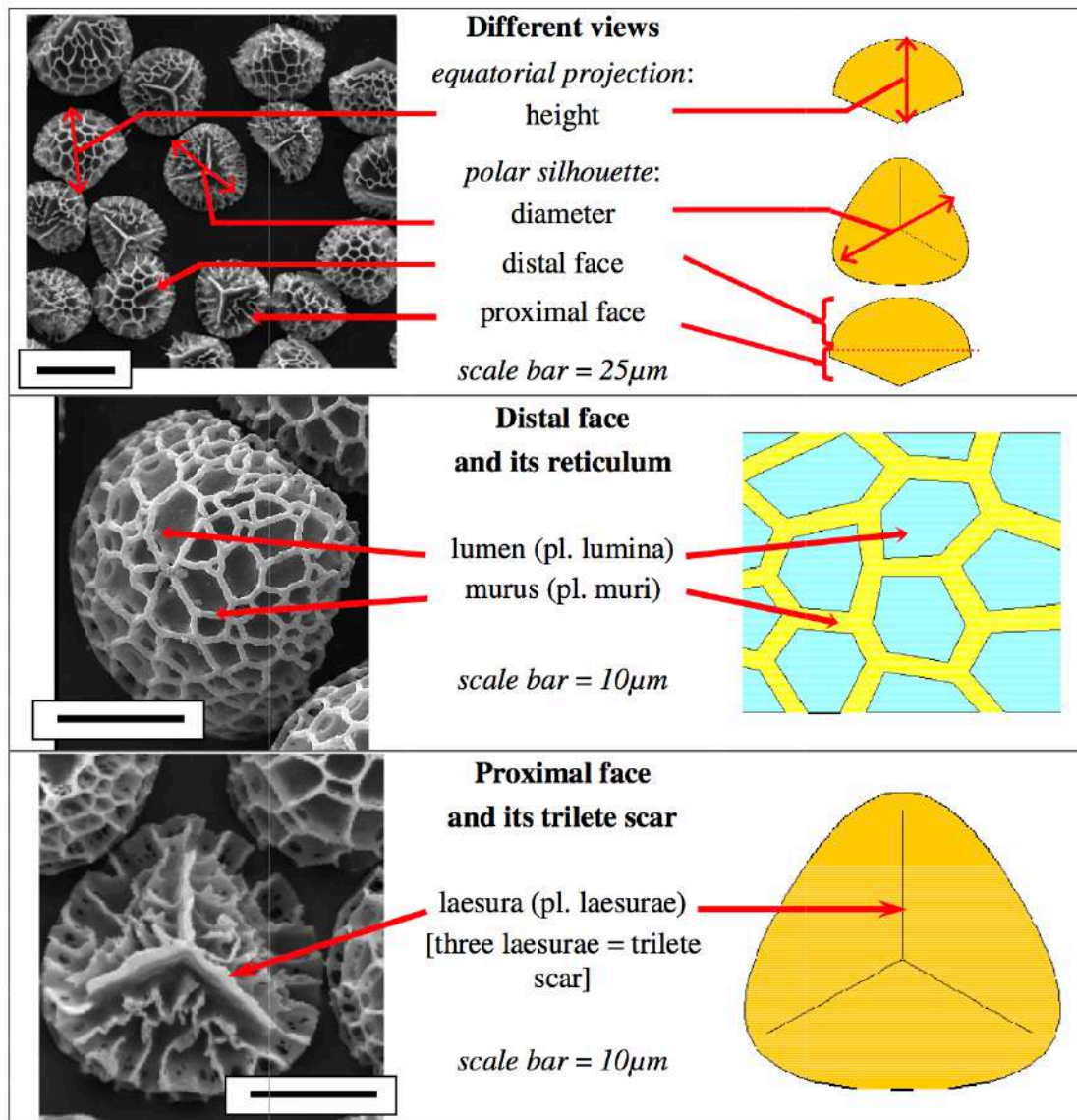


Figure 3: *L. clavatum* spores SEM images and detailed illustration [2].

Tectal elements are little embossments spread around the spore or pollen and are dependent on the plant species [2]. For example, *Lycopodium clavatum* spores are decorated with a honeycomb-like structure

Apertures are areas of different thickness in the exine layers [2]. An example of these apertures is the *laesurae*, which are scars of the grouped growth of spores. The *laesurae* can form *monolete* (a single line) or *trilete* marks (three lines united to form a Y-shape).

1.3.1 Nanochannels of *L. clavatum* spores

The exine layer “is not a barrier to penetration”, as Pettitt wrote. [10] It is indeed crossed by nanochannels. A more recent work described those nanochannels as being around 25 nm in diameter in mature pollen (but can reach 40 nm in the developing stage of spore) [11]. Also, it has been found that these nanochannels not only cross the exine but also the intine [10,11]. Figure 4 shows the nanochannels in exine and intine wall.

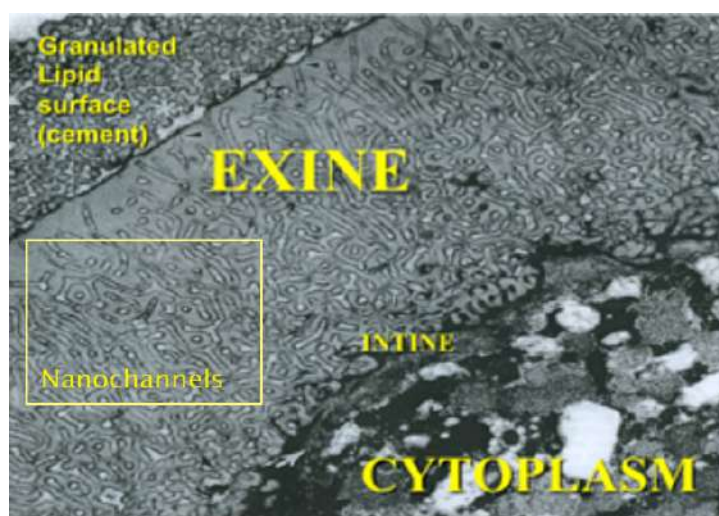


Figure 4: *L. clavatum* spore cross-section showing the nanochannels [11].

1.4 Physical Characteristics of Sporopollenin

Sporopollenin is “one of the most extraordinary resistant materials known in the organic world” [4]. Also, Brooks wrote “sporopollenins are probably the most resistant organic materials of direct biological origin found in nature and geological samples” [12]. Moreover, exines were been found in the sedimentary rocks laid down 500 million years ago and they were intact and had survived the harsh environments. Although the intine and cytoplasmic materials had decayed, the exines were unchanged [13]. In this section, the chemical, thermal and biological resistance of sporopollenin will be reviewed.

1.4.1 Chemical Resistance

Many methods have been used to extract the sporopollenin and exines from *L. clavatum*. These methods were extremely harsh and give an indication of the extraordinary resistant nature of such biomolecular materials. For example, spore exines have strong resistance to acids such as, phosphoric acid, hydrofluoric acid and sulfuric acid. Also, strong alkali such as sodium or potassium hydroxide will not outwardly affect the exine structures [8].

However, with Erdtman’s acetolysis (acetic anhydride and sulfuric acid) the structure of some exines could be changed due to cross-linking, but the sporopollenin was never to be degraded [14]. In contrast, oxidizing chemicals such as chromic acid, nitric acid, ozone and potassium permanganate were found to have the ability to degrade sporopollenin [15].

1.4.2 Thermal Resistance

Sporopollenin can resist temperatures up to 400 °C, a really high temperature for a biomolecular material to normally resist. It has been noticed that increasing heat on sporopollenin could lead to color changes and these changes are related to carbonization and water loss from sporopollenin [16]. For instance, below 100 °C there is no noticeable change, whereas above 180 °C it seems the sporopollenin begins to lose water and carbon dioxide. Over 220 °C, sporopollenin shows an immediate darkening and released hydrocarbons [12].

1.4.3 Biological Resistance

Sporopollenin has the ability to resist decay for more than 500 million years [13], as evidenced by their identification in some sedimentary rocks. Furthermore, Wiermann *et al.* [17] showed the capability of sporopollenin to survive many types of enzymes e.g. amylases, celluloses, lipase and proteases. However, sporopollenin as a natural material must be a biodegradable to allow the spores to germinate and continue their life cycle. All natural materials should have some enzymes that could break them down [18].

Studies have shown that under certain circumstances, pH for example, some kinds of bacteria have the ability to degrade the sporopollenin [18,19]. In addition, it was found that intestine by itself can secrete some types of enzymes to rupture the exine following pollination [19]. Moreover, some studies displayed the ability of human plasma enzymes to destroy the sporopollenin in bloodstream [20]; however, the exact

enzymes responsible for sporopollenin degradation have not been recognized yet (see Figure 5). These findings indicate that sporopollenin exines are biodegradable.

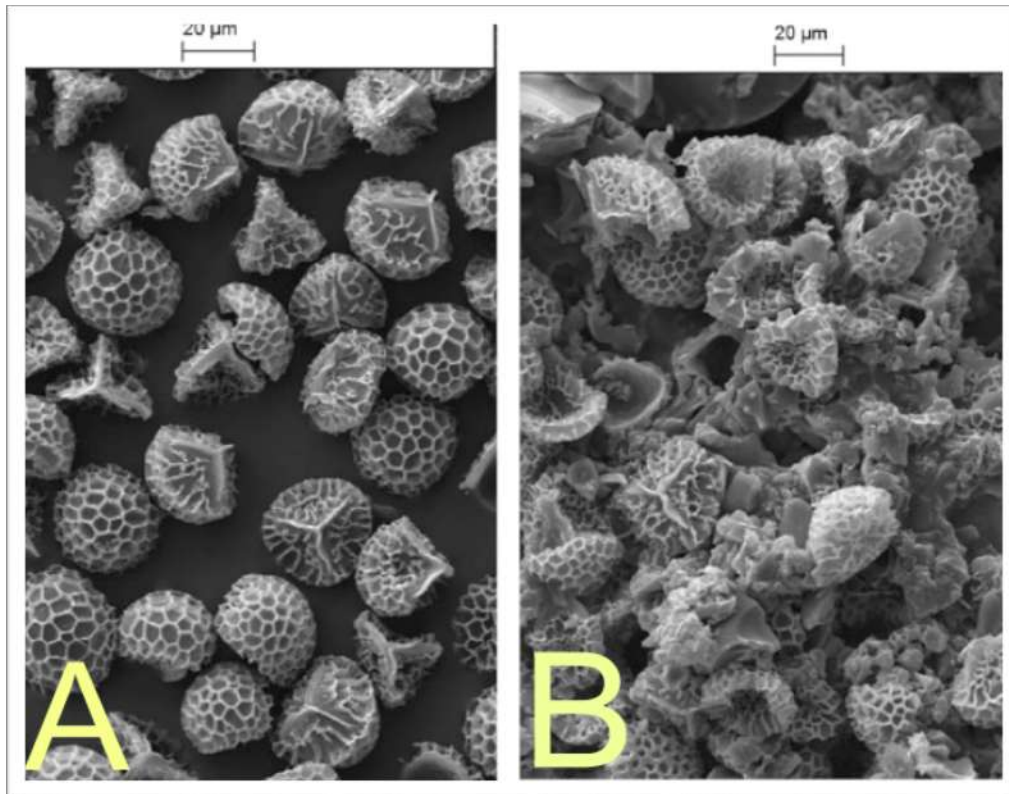


Figure 5: (A) *L. clavatum* exines before incubation in human plasma. (B) Sporopollenin after incubation in human plasma for 30 min. SEM. [21].

1.5 Extraction of Sporopollenin from Raw spores and pollen grains

There are different methods that describe the extraction of sporopollenin from fresh spores and pollen grains. Some involve using harsh treatments with strong acids and bases, however, it has been suggested that harsh conditions may bring changes to the structure of the sporopollenin, e.g. the hydrolysis of ester groups [20]. Extraction of

sporopollenin exines leaves an empty shell with relatively large cavity, which are referred to as sporopollenin exine capsules (SECs) in this thesis. The main methods for extraction that can be found in literature are detailed below.

1.5.1 Treatment with Alkali and Phosphoric acid

Zetzsche *et al.* [8] explained a method by treatment the spores or pollen grains with organic solvents followed by a hot alkali and then finally with hot 80 % ortho-phosphoric acid for 6 days. However, Shaw *et al.* [20], found that ortho-phosphoric acid did not remove the intine completely and an extra treatment with 80 % H₂SO₄ (after treating with the hot 80 % ortho-phosphoric) was necessary to remove the cellulose of intine completely.

1.5.2 Acetolysis

Erdtman introduced acetolysis method for spores and pollen gains extraction [14]. In this method; he treated the spores and pollen grains with a mixture of acetic anhydride and concentrated H₂SO₄ with 9:1 ratio.

1.5.3 Anhydrous Hydrofluoric acid

Dominguez *et al.* developed a method of extraction [22], which involved using anhydrous hydrofluoric acid in pyridine at 40 °C for 5 hours for extraction.

1.5.4 Enzymes

Different enzymes (amylase, cellulases, hemicellulose, lipase, protease and pectinase) have been used to extract raw spores and pollens instead of using a strong acid, removing their genetic material in addition to their inner layer (mainly cellulose). Washing with hot methanol produced empty shell from *Corylus avellana* and *Pinus mugo* pollens [17].

1.5.5 4-Methylmorpholine-*N*-oxide

In this method, 4-methylmorpholine-*N*-oxide monohydrate (4-MMNO.H₂O) was used to extract spores and pollen grains [23, 24]. Spores or pollen grains were suspended in molten 4-MMNO.H₂O at 75 °C to release sporoplasts (pollen contents), and both sporoplasts and sporopollenin were recovered by using this treatment.

1.5.6 Hydrochloric acid

In this method, raw spores were treated with 6 M hydrochloric acid (HCl) at 110 °C for 24 hours to produce empty shell of spores [80-82]. This process can be used for the extraction of shells from different types of spores and pollens including *L. clavatum*, *P. sylvestris*, *A. trifida*, *A. artemisifolia*, *H. annuus*, *S. cereale* and *Z. mays*.

1.6 Overview of Sporopollenin Chemical Structure

SECs are composed of carbon, hydrogen and oxygen only [15], and they are nitrogen free when extracted. Although resistance and stability of sporopollenin have preserved the morphology of the ancient pollen and spores for millions years [25], this stability make it very difficult to have a clear picture of the chemical structure of sporopollenin. Over the last two decades, it has been thought that sporopollenin is a polymer made of a combination of fatty acids and phenolic compounds [26, 27]. However, ozonolysis of spores and pollen from *L. clavatum* and *P. sylvestris*, showed large amounts of straight and branched chain of monocarboxylic acids (breakdown products of fatty acids) supporting that fatty acids are main component of sporopollenin structure [28].

Recently, enhanced degradation and purification techniques joined with various analytical methods [e.g. magic angle spinning solid-state carbon and proton nuclear magnetic resonance (MAS SS-¹³C-NMR; MAS SS-¹H-NMR) spectroscopy and Fourier transform infrared (FTIR) spectroscopy] have illustrated that sporopollenin consists, mainly, of poly-hydroxylated unbranched aliphatic units, phenylpropanoids and small amounts of oxygenated aromatic rings [26, 29-31]. Other studies showed that inhibiting the chain elongating steps (one of the long-chain fatty acids synthesis steps) using thiocarbamate herbicide and then using radioactive tracers, lipid metabolism is an essential part of sporopollenin biosynthesis [32, 33].

In addition, sporopollenin NMR and infrared (IR) analysis has confirmed carbonyl, carboxyl and ether functional groups in sporopollenin structure [34]. Also, phenols

represented essential parts of sporopollenin, as it has large amount of *p*-coumaric acid as an end product [35, 36]. Moreover, aromatic functional groups were confirmed to be part of sporopollenin components using pyrolysis gas chromatography (GC) [37, 38].

MAS SS-¹³C-NMR showed that sporopollenin has aliphatic groups such as methyls, carboxylic, olefinic, aromatic unsaturated functions, esters [20, 26, 39-41] and phenols [17]. Moreover, recent researches suggest that sporopollenin is a polymer composed of different cinnamic acids crossed by ether-links, and large amounts of hydroxy fatty acids that cross-linked by ether groups [30, 9, 42-47].

1.6.1 NMR Spectroscopy of Sporopollenin

1.6.1.1 Liquid-state ¹H-NMR

Ahler *et al.* tried to explore the chemical structure of sporopollenin from *Typha angustifolia* (*T. angustifolia*) using liquid-state ¹H-NMR [29]. They found it is difficult to have a full structure of sporopollenin using liquid ¹H-NMR due to the fact that the sporopollenin is insoluble in water. In this case they claimed that they were able to dissolve the sporopollenin in deuterated 2-aminoethanol-water solution in order to analyze the sporopollenin [48]. The sporopollenin was heated at 100 °C for 1 h in 2-aminoethanol and so reaction with the solvent may have occurred. However, they found it is still difficult to interpret the data due to contaminations from the solvent as peaks from the pure solvent overlapped with the sporopollenin signals (see

Figure 6).

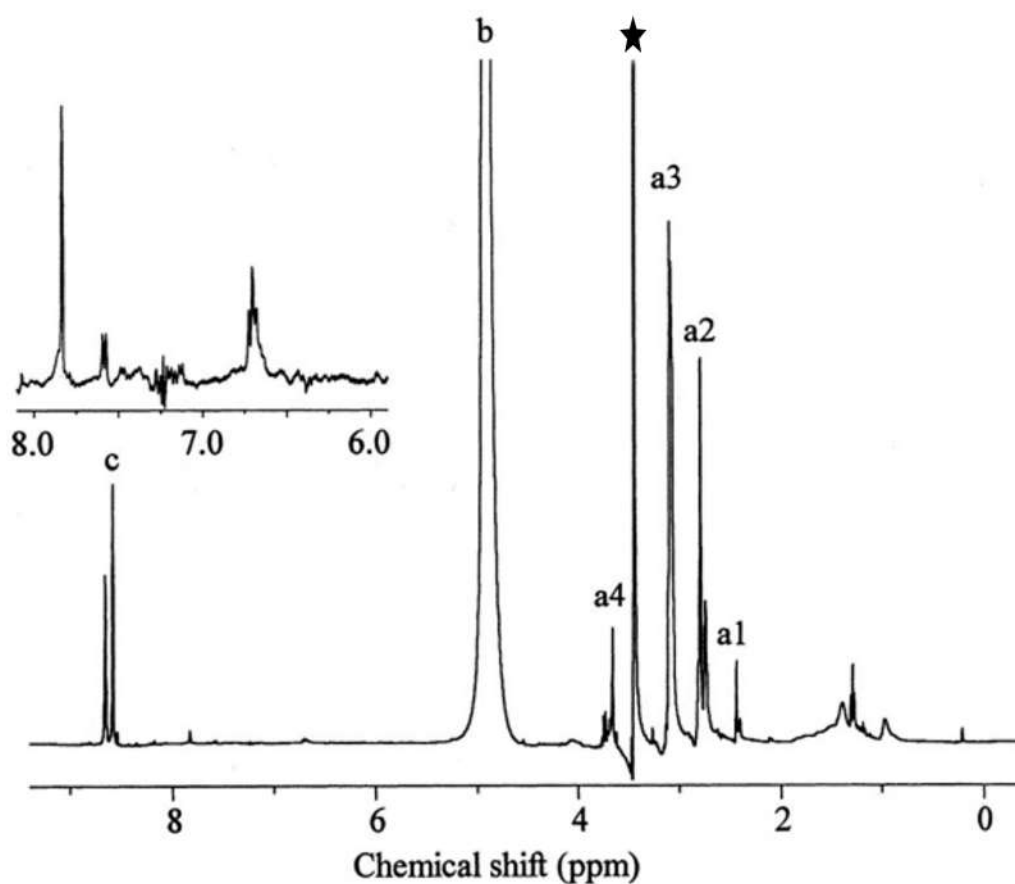


Figure 6: Liquid ^1H NMR spectrum of sporopollenin from *T. angustifolia* obtained at 400 MHz [29].

It was not possible to interpret the whole spectrum, except for the aromatic area from 6.5 ppm to 8.0 ppm and the peak around 3.43 ppm. The peaks (a1, a2, a3, a4 and c in Figure 6) were not obtained from the sporopollenin, because they appear in a blank spectrum. The peak at 4.9 ppm (b) is related to the deuterium and the transferable H^+ of 2-aminoethanol. The peaks (from 0.8 to 1.6) indicate polymers with various aliphatic protons; however, no interpretation is possible due to the suspicion of contamination from the solvent. The peak around 3.43 ppm (* shape) represent methyl group that is related to methanol residues from the sporopollenin treatment.

1.6.1.2 MAS SS-¹³C-NMR

The MAS SS-¹³C-NMR of sporopollenin from *L. clavatum*, (see Figure 7), displays a spectrum that is typical of a sporopollenin that was found by Guilford *et al.* [26] and Hemsley *et al.* [40]. The peaks in the MAS SS-¹³C-NMR are assigned according to spectral area. The area between 0 to 50 ppm indicates aliphatic hydrocarbon; from 50 to 105 ppm indicates oxygenated aliphatic groups; from 110 to 160 ppm indicates unsaturated carbons (olefins/aromatics); from 160 to 180 ppm indicates carboxylate groups (acids/esters).

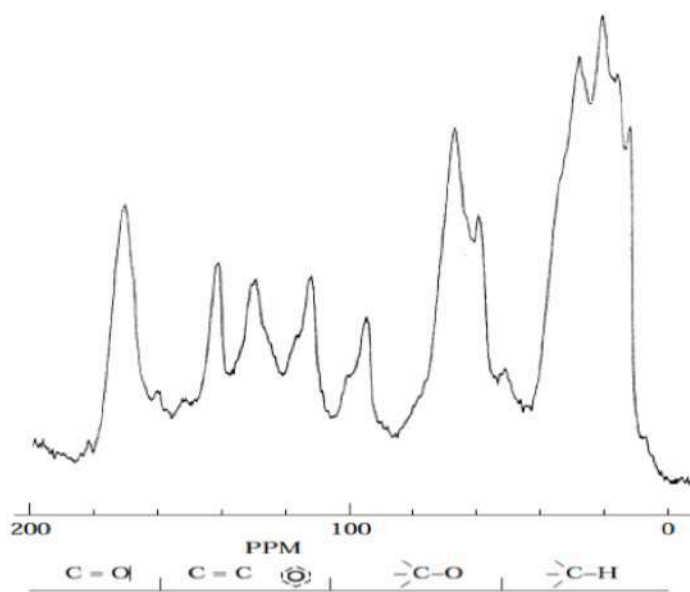


Figure 7: MAS SS-¹³C-NMR spectrum of *L. clavatum* obtained at 100 Hz [40].

Further studies were carried to determine the chemical nature of sporopollenin using MAS SS-¹³C-NMR of different sporopollenin from different plant species, such as *L.*

clavatum, *P. sylvestris*, *A. trifida* and *T. angustifolia*, it gave clear signals about the chemical composition of sporopollenin (see Table 2) [31, 34].

¹³ C signals ppm	Chemical nature or group
15-20	C-CH ₃
29-30	C-CH ₂ -C
60-70	C-O
120-130	olefinic and aromatic C
170	COOH

Table 2: The chemical composition of sporopollenin from different species that was shown in MAS SS-¹³C-NMR.

Wilmesmeier *et al* [34], assigned the multiple peaks in the 140-200 ppm region into four main regions that can be interpreted as described in Table 3

¹³ C signals ppm	Chemical nature or group
145	Weak quaternary aromatic C
165	Ester
175	Acid
200	Ketone

Table 3: Interpretation of the four main peaks in the 140-200 ppm region of sporopollenin from different species using MAS SS-¹³C-NMR spectra.

An earlier study of sporopollenin chemical structure of different plant taxa using MAS SS-¹³C-NMR was carried by William *et al* [26]. They found that carbon resonances occur mainly in four distinct areas. However, they are varying in peak strength and shape (Figure 8, A-E). For instance, the spectrum of sporopollenin from the algae *C. vulgaris*, (Figure 8. A) shows the presence of aliphatic carbons (strong resonance at 20-40 ppm), by a weak resonance at 70 ppm (indicates carbon bearing oxygen), olefinic character at 130 ppm, and carbonyl groups at 170 ppm originating from esters or carboxylic acids. Nevertheless, the spectrum of sporopollenin from *L. clavatum* spores showed type of peaks at 206 ppm in addition to the previous four kinds of MAS SS-¹³C-NMR signals indicating the presence of ketone carbonyl carbons (Figure 12. B). The spectrum of sporopollenin from *L. clavatum*, also, showed it to be unsaturated more than any other sample examined. However, the spectrum of *P. sylvestris* sporopollenin (Figure 8. C) showed less intense carbonyl resonances than any other sporopollenin. Moreover, the spectrum of *P. sylvestris* sporopollenin showed that they are different in structure from sporopollenin from *L. clavatum* or *C. vulgaris* in the quantity of oxygen present. This was noted by increasing the resonance at 70 ppm in addition to the shoulder (at 40 ppm) on the aliphatic carbon resonance. The 40 ppm resonance indicates carbon neighboring to an oxygen-bearing carbon. The 40 ppm resonance indicates carbon neighboring to an oxygen-bearing carbon. Spectra from *A. trifida* and *Triticum* species (Figure 8. D and E), show that they are similar to each other. They have the previous five resonance types; however, they have different associated intensities than the sporopollenin from other plant species.

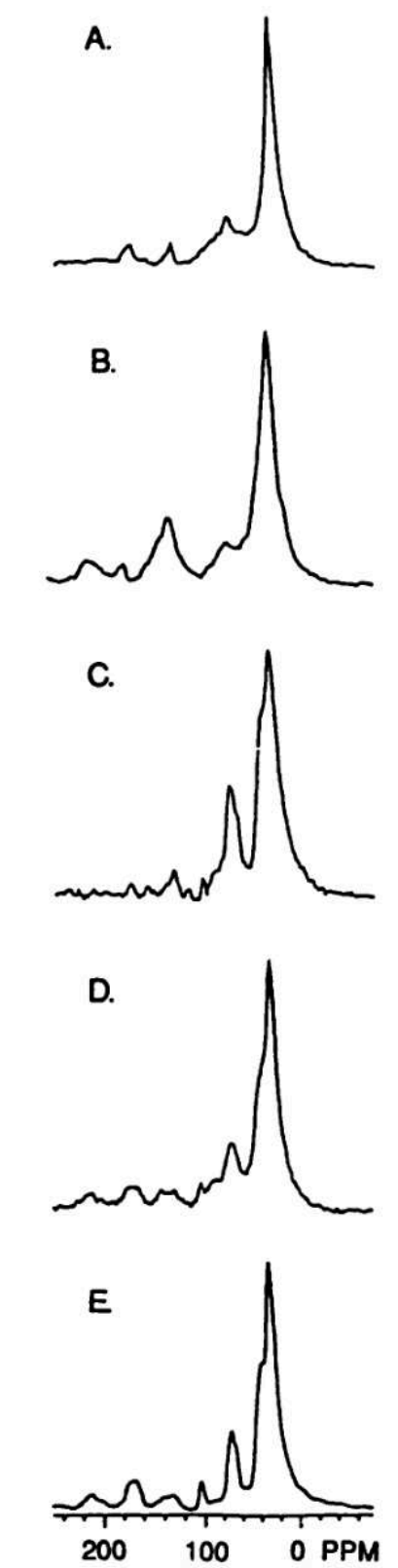


Figure 8: MAS SS-¹³C-NMR full spectra of sporopollenin obtained at 37.8 MHz, showing (A) *C. vulgaris*; (B) *L. clavatum*; (C) *P. sylvestris*; (D) *Triticum species* and (E) *A. trifida* [26].

In conclusion, MAS SS-¹³C-NMR spectra of the SECs from different plant sources reveal that these substances are all distinct. Therefore, sporopollenin can be defined as a class of biopolymers instead of a single, homogeneous macromolecule. These studies using the MAS SS-¹³C-NMR spectra supports the idea that fatty acids are the precursor of sporopollenin (the long saturated aliphatic chains and the low olefinic intensity), even though, it showed less features that similar to a carotenoid precursor (significant quaternary olefinic intensity and methyl intensity). In fact, the spectra of *L. clavatum* spores showed it was the only species that contains a substantial similarity to polymerized β-carotene ones.

Chapter 2. Sporopollenin: Ingestion, Toxicology and Applications

2.1 Ingestion and Absorption of Sporopollenin

Ingestion of different types of sporopollenin has been studied. For example, Volkheimer *et al.* studied the ingestion of *L. clavatum* spores in rats, and they found that the spores were absorbed and migrated into rats' blood-stream [49]. Later, he termed this phenomenon as persorption and defined it as "the passage of large solid, non-deformable food particles in the micron size range through the epithelial cell layer of the intestinal tract" [50], and reported the persorption of particles ranging from 5-150 μm in diameter. Therefore, it was clear that sporopollenin has the ability to resist the mechanical, chemical and immunological defense of gastrointestinal tract (GIT), and reach the blood stream.

It was thought that the persorption would take place *via* a paracellular route (between epithelial cells of the small intestine), however, Weiner later wrote that "it is doubtful that 30 μm particles gain entry via this route" and explained that the tight junctions between cells form an effective barrier to large particles that are above the 0.005 μm range [51].

2.2 Digestion of Sporopollenin

Sporopollenin has to face pH and enzymatic attack whilst it is migrating from the oral cavity until it reaches the small intestine where the absorption process has been proposed to take place [51-54]. For example, there is amylase enzyme in the oral cavity with a neutral pH, pepsin enzyme in the stomach with a strong acidic pH (1-2),

and different types of digestive enzymes in the basic pH (7-8) small intestines. The mechanism of digestion of sporopollenin is still unclear. Nevertheless, some studies [55] showed that sporopollenin could be degraded in whole blood and in plasma (containing white blood cells and clotting factors), but not serum (plasma without clotting factors). Therefore, the clotting cascade enzymes may participate in this enzymatic degradation of sporopollenin.

2.3 Toxicology of Sporopollenin

Spores and pollen grains have been studied for a long time for their usage in food and medicine. Thus, it was important to study the toxicity of sporopollenin in the human body. Generally, sporopollenin was found in human food sources, e.g. bee honey and some fungi [56]. Also, it has been used in an anti-allergy preparation made from pollen tablets [57]. Moreover, sporopollenin from other species (*C. vulgaris*) showed that they were harmless when rubbed on skin, swallowed and injected into bloodstream. Furthermore, a study showed that anti-bodies can track sporopollenin and bind to them in blood [58]. Therefore, they can be removed easily by the immune system (*via* macrophages).

2.4 Applications of Sporopollenin SECs

The extraordinary stability of SECs and their uniform size [59], offers an extensive range of applications that extend over many other naturally occurring or synthetic materials, such as chitosan and acrylic resins, respectively. It can be extracted easily from pollens or spores using low-priced, non-toxic reagents that are used daily in the

food industry. Also, spores and pollens are natural materials that are commercially available in large quantities and are relatively cheap [4]. SECs are monodispersed particles and if they are taken from one species, they will show uniformity in morphology, size and even in chemical composition [60]. Achieving such uniformity in synthetic products is difficult and expensive especially producing large cavity microcapsules that have the ability to be filled with a diverse range of polar and non-polar materials. Hence, SECs can replace the conventional encapsulants that have been used previously for macromolecules (see Section 2.4.1.1), which are more expensive and often with low loading ability [60].

Moreover, SECs have been used as solid support materials for several biological applications, due to their biocompatibility and non-toxicity. Recently, this type of solid-support material has been used in medicine, encapsulation and enzyme immobilization [61, 62]. Furthermore, SECs has been used as anion [63-65] and cation exchange resin to remove heavy metal ions from aqueous medium [66, 67]. For instance, carboxyl, glyoxime and epoxy derivatives of sporopollenin have been investigated to be used as ligand exchangers, and they used at high temperatures or in the presence of strong acids [68-70].

2.4.1 Microencapsulation

Microencapsulation can be defined as the process of filling a microscopic size shell with small particles, or coating active materials for protection or controlled release [122]. The reasons for microencapsulation can be summarized in the following points:

- Active protection: avoid the degradation of encapsulants by environmental factors (such as light, heat, water and oxygen), or from body conditions (such as low pH and enzymes attack in the GIT), which resulting in the prolonged shelf life of the encapsulated actives.
- Odour, taste and colour masking: regarding some drugs that have unpleasant taste, smell or colour such as fish oil.
- Drug delivery control: regulate the drug delivery and release in the site of absorption.

2.4.1.1 Currently available drug delivery system

A number of synthetic and natural polymers have been investigated for their use in drug delivery. Many synthetically designed microcapsules have been developed to deliver drugs orally [136], but lack consistency in their size and morphology. Examples of biodegradable, synthetic polymers include polymers of lactic acid (PLA), glycolic acid (PGA) and their co-polymers (PLGA). Limitations with such microspheres as drug delivery vehicles are the low encapsulation efficiency (typically 61-65% for PLGA microspheres) [137]. In addition, there have been many attempts to manufacture microcapsules from 'natural' materials. some of these are detailed below:

❖ Liposomes

Liposomes are formed from concentric spherical phospholipid bilayers with an inner compartment [138] that has been used for encapsulating drugs [139]. Applications of

liposomes are limited by their instability and poor permeability to polar molecules [140].

❖ **Chitosan**

Chitosan widely used as a drug delivery vehicle [141]. Examples of its use include the development of chitin/PLGA blend microspheres to deliver anti-cancer drugs [142] and hydrogels composed of a biodegradable chitosan backbone [143].

Chitosan is soluble in dilute acidic solutions [144]; this would be a major disadvantage for the use of chitosan as a drug delivery vehicle, since it would simply degrade when exposed to the harsh environment of the GI tract.

2.4.2 SECs in Taste Masking

The unpleasant taste of some valuable food supplements, such as cod liver oil, raise the need to find a safe and healthy method to mask these undesirable tastes. Cod liver oil contains polyunsaturated fatty acids that are very important vitamins for human health (vitamin A and D) but which have an unpleasant fish flavour. This repugnant taste is due to the oxidized by-products of a chemical reaction that takes place when ingesting the oil. However, SECs have displayed a taste masking ability by encapsulating the cod fish oil within and protecting the fatty acids and vitamins of cod fish oil from oxidation, light and water (see Figure 9) [71].

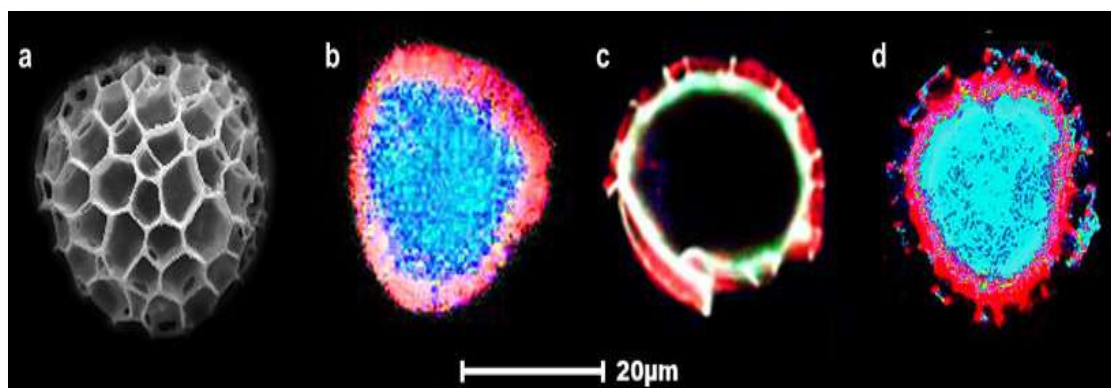


Figure 9: Encapsulating cod fish oil in *L. clavatum* SECs: (a) an SEM image of the SECs, (b) Laser scanning confocal microscopy (LCSM) images of inner genetic material (*blue*) and the SEC shell (*red*). (c) LCSM images of the empty SEC cavity with the SEC layer (*red* and *white*). (d) LCSM images of the SEC filled with the oil (*blue*) [71].

Mackenzie *et al.* [71] examined the ability of SECs in taste masking by eliminating all the inner components of spores (intine and cytoplasmic material), and leaving the outer shell (SEC) only. Then, the SEC was filled with different ratios of oil/sporopollenin (ranging from 0.5:1 to 4:1 w/w). Results showed a successful taste masking with a ratio of 1:1 g/g, however, any higher ratio than that led in taste tests to the recognizable fishy flavour. That could be due to the excess oil residue on the coating of the SEC. This work suggested that a double encapsulation (e.g. with wax) could be used to increase the taste masking of the encapsulated material.

2.4.3 SECs as Absorption Enhancers

Absorption enhancer is a functional excipient that used to enhance the absorption of an active therapeutics. Poor therapeutic agents' bioavailability can be caused by early degradation in the GIT, for orally ingested drugs, or poor membrane permeability when the target area of absorption is reached. Compounds with large molecular weight, such as proteins, or hydrophilic compound with low molecular weight have poor bioavailability, and they usually need an absorption enhancer [72].

A functional excipient for absorption enhancement must have two main criteria [72]:

1. The ability to prevent the encapsulated therapeutic from degradation and early metabolism.
2. The ability to enhance membrane permeability, e.g. disruption of membrane bilayer of transcellular route or tight junctions of paracellular route.

SECs showed that they can act as a bioavailability enhancer in studies carried out by Wakil *et al* [73]. The studies showed an improvement in the bioavailability of eicosapentaenoic acid (EPA) (omega-3 fatty acid) after encapsulation in the SECs (see Figure 10).

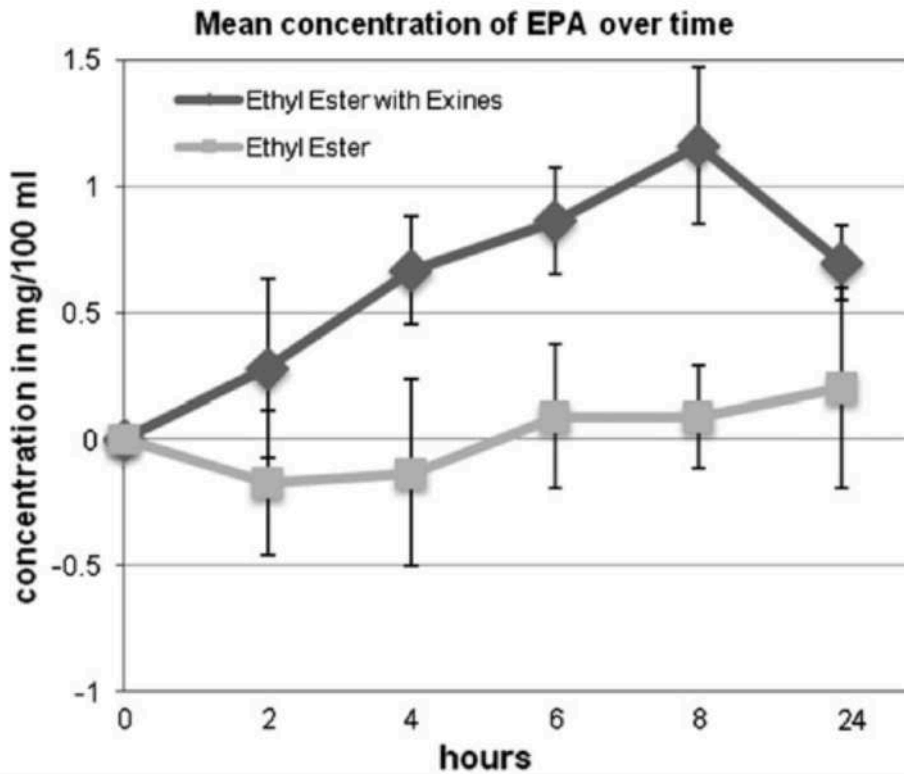


Figure 10: The bioavailability of EPA was enhanced when encapsulated by SECs, as shown by measuring EPA serum level over time [73].

This reason for the improvement in the bioavailability of EPA by SECs is unclear, but it could be in part due to the resistance of SECs to various biological and chemical factors as they remain intact until they reach the targeted area (i.e. blood) in addition to their antioxidant properties which protected EPA from aerial oxidation [73].

Enhancing the bioavailability of EPA when encapsulated into SECs indicates that the SECs may have the ability to enhance the small intestine membrane permeability, in addition to protect it from early degradation by the GIT. The reasons behind the bioavailability enhancement of SECs will be investigated and discussed later as part of this thesis (Section 6.5).

2.4.4 SECs as Sequestrators

Removing oil from a solution or emulsion is a sequestration process. The unique characteristics of sporopollenin, such as lipophilicity, their ionizable peripheral groups and fine porosity, gave the SECs the ability to sequester oil from oil-water emulsions. Recently, Mackenzie *et al.* [74] used SECs to remove edible oil from oil-in-water emulsions, and they showed the ability to recover the oil from the SECs. The amount of oil sequestered varied depending on size of the SEC's cavity. For instance, a 4:1 oil/SEC ratio can be obtained using *L. clavatum* SECs due to their larger inner cavity; on the other hand, *C. vulgaris* SECs can take a ratio of 1:1 oil/SEC. Moreover, functionalizing sporopollenin SECs with acetylated and methylated groups increased the SEC's lipophilicity. To further improve the efficiency, the hydroxyl groups on the SEC surface were modified into salts (Na^+ and K^+), acetates and methyl esters [74].

2.4.5 Micro-reactors and Bio-reactors

The SECs of *L. clavatum* were used as a "micro-reactor" in the research carried out by Paunov *et al* [75]. It is a very simple process where there is an *in situ* synthesis with either inorganic or organic nanoparticles. The end products can form nanoparticles with average diameter greater than the SEC's pore size (nanochannels diameter 25 nm) and that traps the particles inside, whilst the SECs are still permeable to the solvent. This experiment could be applied potentially to drug delivery by preparing magnetite nanoparticles (Fe_3O_4) *in situ*, in addition to adding drug or food supplements, and then delivery may be directed by an external magnetic field.

Later studies from the Hamad *et al.*, showed the ability of SECs to act as a bioreactor by encapsulating living cells [76]. They claim to have encapsulated yeast cells in a suitable environment. Figure 11 and 12 show the yeast cells after encapsulation into SECs. Also, the same group suggested that these cells can grow inside the SECs if they were placed into culture medium whereby nutrients pass through the SECs nanopores. Encapsulating living cells in SECs can be used in food industry for probiotics protection and pharmaceutical purposes.

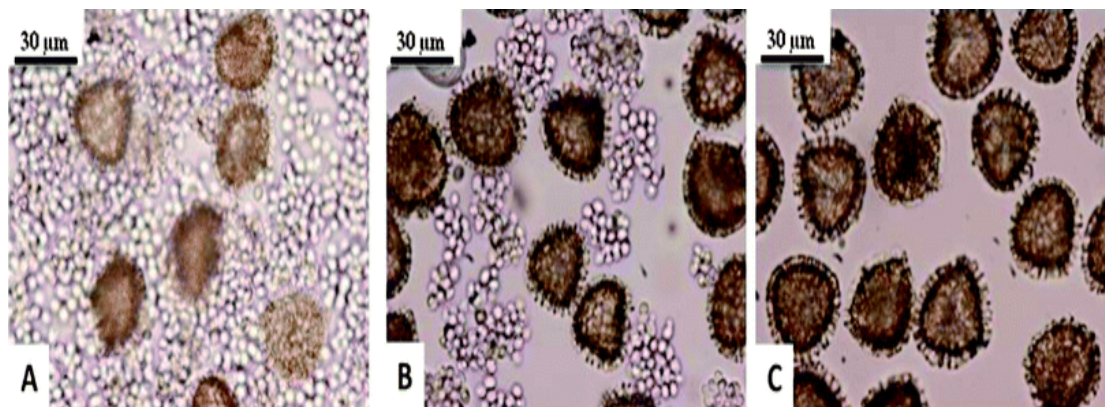


Figure 11: Optical microscopy images shows A) a mixture of non-encapsulated yeast cells and *L. clavatum* SECs loaded with yeast cells before washing, (B) after washing three times, and (C) after washing ten times [76].

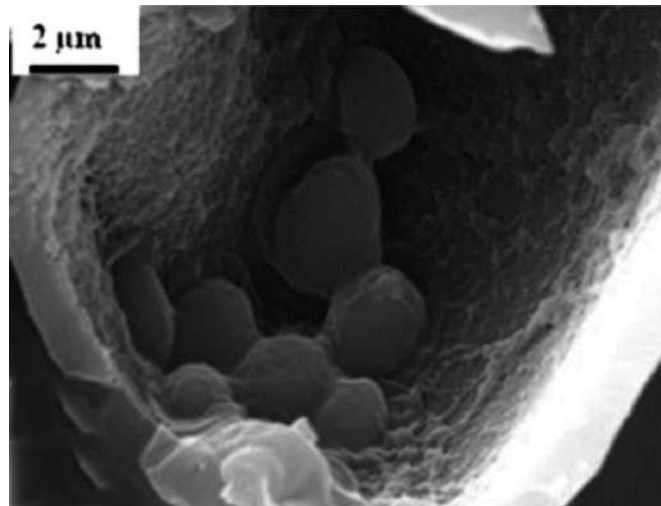


Figure 12: SEM images of encapsulated yeast cells inside prepared *L. clavatum* SECs [76].

Another study suggested that encapsulating magnetic nanoparticles with living cells in SECs can help in manipulation of SECs [76] and directing them to the required target (see Figure 13).

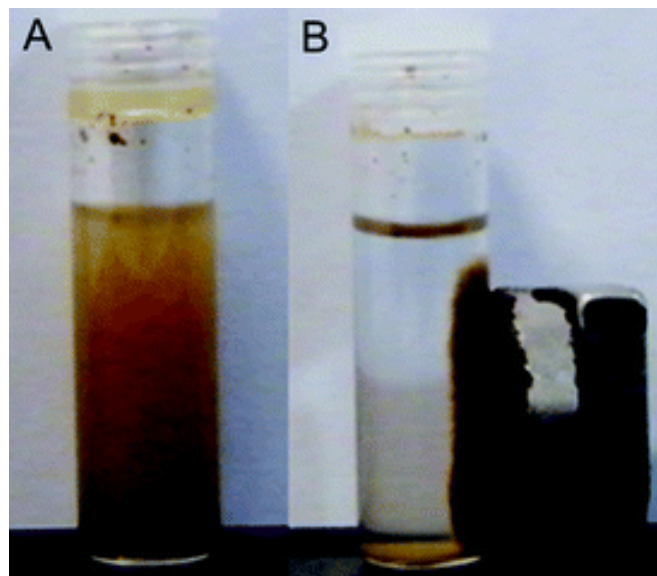


Figure 13: (A) suspension of magnetic SECs with entrapped yeast cells; (B) The SECs are attracted to the external magnet due to the encapsulated magnetic nanoparticles as well as yeast cells [76].

2.4.6 SECs in Drug Delivery

Sporopollenin and its unique characteristics have inspired many scientists to use sporopollenin capsules in many applications, especially in drug delivery [77]. Due to the significant chemical and biological properties (such as polycationic properties, and biodegradability), sporopollenin has been investigated as a carrier for controlled drug delivery [78]. They have also been used as a micro-capsule to encapsulate many medical substances and then release them into blood-stream. Furthermore, much research has been done to deliver medical macromolecules to their targeted organs using SECs because they can be used as a non-invasive drug carrier [79]. Figure 14 shows an illustration of therapeutic active encapsulant.

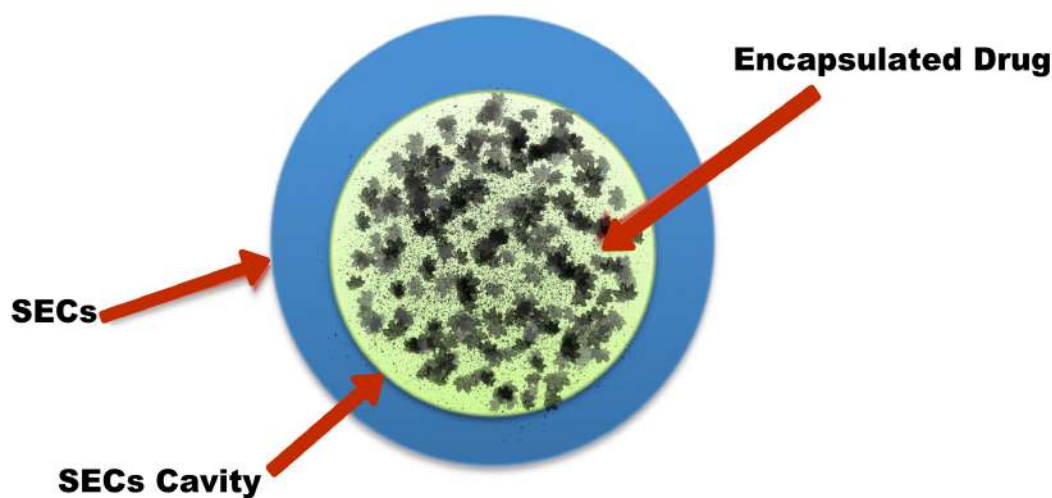


Figure 14: Illustration of therapeutic active encapsulated in the SECs' cavity.

Using empty SECs as a micro-capsulation for drug delivery is not a new theory as many patents have been granted [80-82]. Also, Lorch *et al* [21] have shown how

sporopollenin SECs can be used to encapsulate a magnetic resonance imaging (MRI) contrast agent, and control its release into the human blood plasma. Conventional administration of MRI contrast agents can be replaced using cheap and available SECs and can be administered orally or intravenously.

It is worthy of mentioning that SECs from different spore and pollen species can be used in different applications depending on the size that is needed in relation to the area which is targeted. For instance, the SECs from *A. niger* (4 μm diameter) could be used to reach the small vessels of the lung alveoli and deliver treatment for respiratory problems after extracting their allergenic content [83]. It is relevant to note that the spores from *A. niger* can cause the fungal lung disease known as aspergillosis by this inhalation route.

The search for a new approach to drug delivery must always be related with the enhanced bioavailability of the drug compared to an existing carrier system or usual pharmaceutical form. SECs were known to enhance bioavailability of EPA as discussed earlier (in Section 2.4.3). Maintaining intimate contact with the mucosa of the GIT can enhance bioavailability, and for that reason mucoadhesive polymers have been of interest in the last three decades [84]. Therefore, it is important to understand the physiology of mucosa and their role in absorption in addition to the mucoadhesion mechanism and investigate if SECs have some kind of mucoadhesivity that may give them the absorption enhancing capability.

2.4.6.1 Mucoadhesion

Mucoadhesion is the event in which a material is held in contact with mucus membrane, or mucosa, for an extended period of time by interfacial forces [85]. Mucosa is a tissue composed of epithelial cells layers that lines internal body cavities such as GIT. A watery layer known as mucus covers these epithelial layers. Mucus consists mainly of water (95%) and mucin glycoproteins (5%) in addition to traces of lipids. The glycoproteins give the structure of mucin and are responsible for its bioadhesivity. Mucus acts as protector and lubricant for the epithelial cells in addition to its role in facilitating the transports between the body cavities and the epithelial cells [85].

2.4.6.1.1 Mucoadhesion Mechanism

Mucoadhesion mechanism composed of three different stages. The first stage is the contact between the mucoadhesive polymer and the mucus. The second stage starts when a physical entangled occurs between the mucus and polymer chains (by the interpenetration of the chains of both). The last stage starts when a secondary interaction is formed between the mucus and the mucoadhesive polymer via non-covalent bonds e.g. H bonds [86, 87].

There are different theories that can explain the mechanism of bioadhesion between the mucus and mucoadhesive polymers. Table 4 summarizes all the bioadhesive theories, which all of them contribute to explain the formation of mucoadhesive bonds [84, 86, 88]. Chemical bonds are essential to keep the bioadhesive polymer adhered for a longer period of time to the surface of mucosa. Table 5 shows these chemical bonds that contribute to mucoadhesion [90].

Theory	Mechanism of Adhesion	Characteristics
Electronic	Due to differences in electronic structure in the surfaces, attractive forces occur between the adhesive polymer and mucus glycoprotein network	Electron transfer occurs, forming an electrical double layer
Adsorption	Chemical bonds formation	Strong primary forces: covalent bonds Weak secondary forces: ionic bonds, hydrogen bonds and van der Waal's forces
Wetting	The adhesive polymer has the ability of spread over the mucus membrane, developing an intimate contact	More applicable to liquids adhesive systems
Diffusion	The polymer chains of the polymer diffuse into the mucus network and vice versa	Formation of a physical entanglement by interpenetration of mucin strands and polymer chains
Fracture	Relates the difficulty of separation of two surfaces after adhesion, and this strength is regarded as being equal to adhesive strength	Mainly used for calculation of adhesive bonds for rigid formulations, with lack flexible chains

Table 4: Summary of bioadhesion theories [86, 88-89].

Type of Force	Characteristics
Ionic bonds	Attraction of two oppositely charged ions via electrostatic interactions to form a strong bond.
Covalent bonds	Electrons are shared, in pairs, between the bonded atoms to form strong bonds.
Hydrogen bonds	Hydrogen covalent bonded to electronegative atoms carries a slight positively charged and can be attracted to other electronegative atom. The bond formed is generally weaker than ionic or covalent bonds.
Van-der-Waals bonds	Interaction between dipole–dipole and dipole-induced dipole attractions of polar molecules. One of the weakest forms of interaction.
Hydrophobic bonds	Indirect bonds that occur when non-polar groups are present in an aqueous solution.

Table 5: Chemical bonds that contribute in mucoadhesion [85, 90].

2.4.6.1.2 Mucoadhesive Polymers

Mucoadhesive polymers have been used as drug delivery system due to their ability to retain the dosage form of drug at the site of action for longer period of time, which will enhance the drug bioavailability [84, 87]. Figure 15 shows examples of the first generation of mucoadhesive polymers that were used in denture fixative powders such as carbomers, chitosan, sodium alginate and the cellulose [85]. These polymers have hydroxyl, carboxyl or amine groups that can form bonds to support the mucoadhesion.

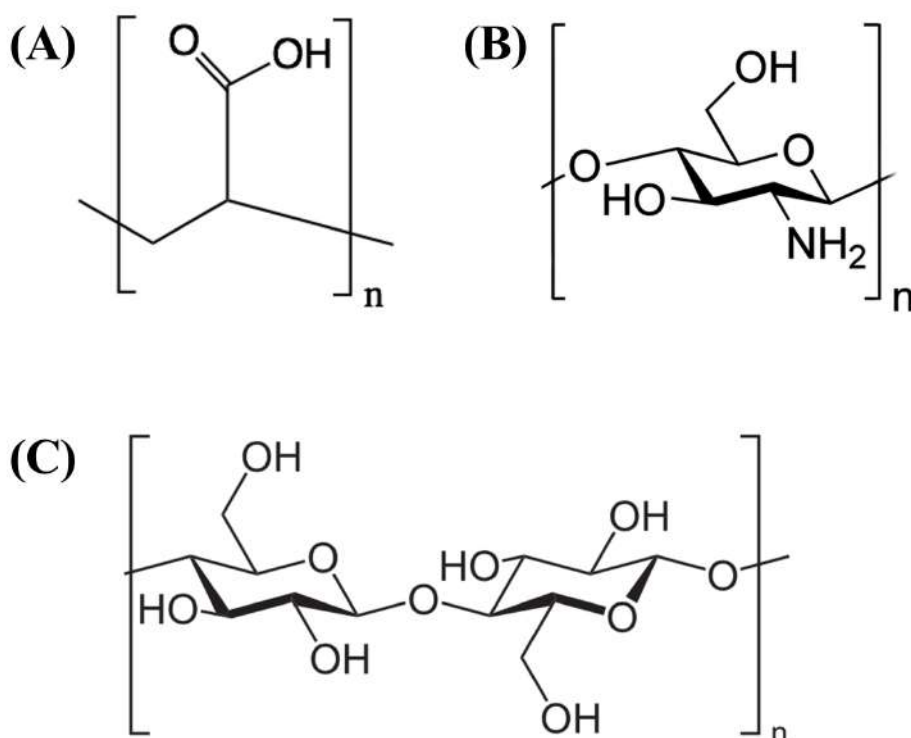


Figure 15: Structure of first generation mucoadhesive polymers. (A) poly(acrylic acid); (B) chitosan; (C) cellulose derivatives.

2.5 Aims and Objectives

2.5.1 Aims

The aim of this project was to explore capability of sporopollenin exines capsules (SECs) in drug encapsulation, protection and controlled release. Also, exploring the chemical structure of SECs would help in understanding the mechanism of drug adsorption and release. Furthermore, investigating the mucoadhesivity of SECs would help to explain the absorption enhancement of EPA by SECs, as revealed in the literature review above.

2.5.2 Objectives

The overall objective could be achieved through the following detailed objectives:

- Choose the best SEC extraction method for each application.
- Encapsulate actives (such as vitamin D and diclofenac Na) and study their release in different pH according to spores' species.
- Study the adsorption capacity of SECs toward the released drug.
- Study the bioadhesive properties of SECs.
- Explain the mechanism of drug absorption enhancement.
- To analyze the research outcomes and suggest the future work.

Chapter 3. Sporopollenin: Physical and Chemical Characteristics

As preliminary work, spores of *L. clavatum* were extracted following base hydrolysis method (BH) (Protocol A) and acid hydrolysis method (AH) (Protocol B) (see Section 8.2 for more details), in order to reveal the unique characteristics of this kind of biological material. MAS SS-¹H-NMR spectroscopy and SEM were used to observe any chemical or structural changes, respectively, in the SECs of *L. clavatum* after refluxing them in strong acid (9 M HCl) and base (1.5 M NaOH) for 24 hours, and after keeping them at the relatively high temperature (200 °C) for 24 hours. Also, their resistance to pressure was investigated, as discussed in Section 3.3.

3.1 Chemical Resistance

To obtain an empty shell of SECs with a large cavity for micro-encapsulation, the spores and pollen grains can be treated with either strong base (Protocol A), (to remove the nitrogenous material inside the intine) [134], or strong acid (Protocol B) (to remove the whole intine with its nitrogenous materials contained therein) [80-82], (see experimental Sections 8.2 and 8.3 for more details). Figure 16 shows schematically the main method that was used to extract the SECs in these studies.

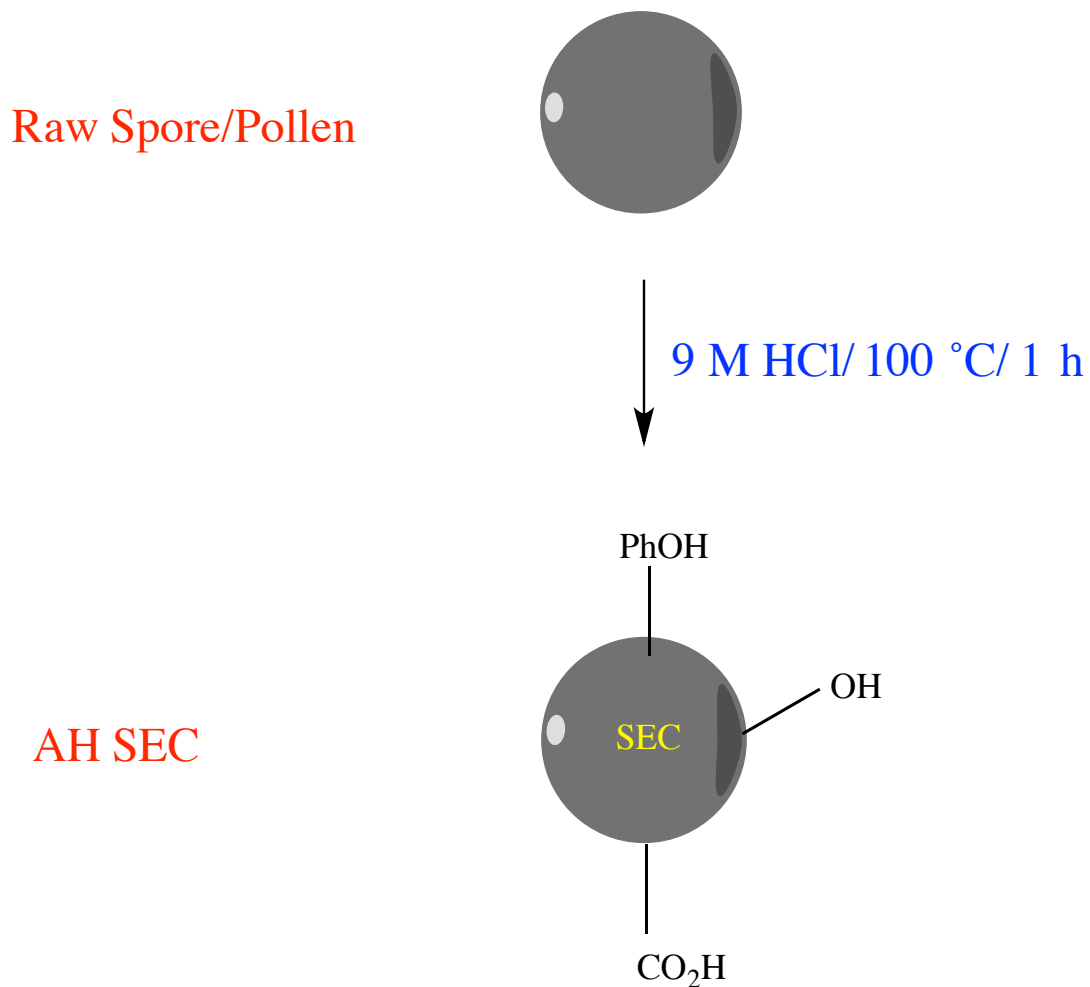


Figure 16: Summary of the acid hydrolysis (AH) method used to treat spores and pollens, to give empty shells of AH-SECs (Protocol B).

Figure 17 shows the SEM images of the *L. clavatum* spores before and after extraction with a harsh treatment using a strong acid (9 M HCl), and the changes in the outer shell which result.

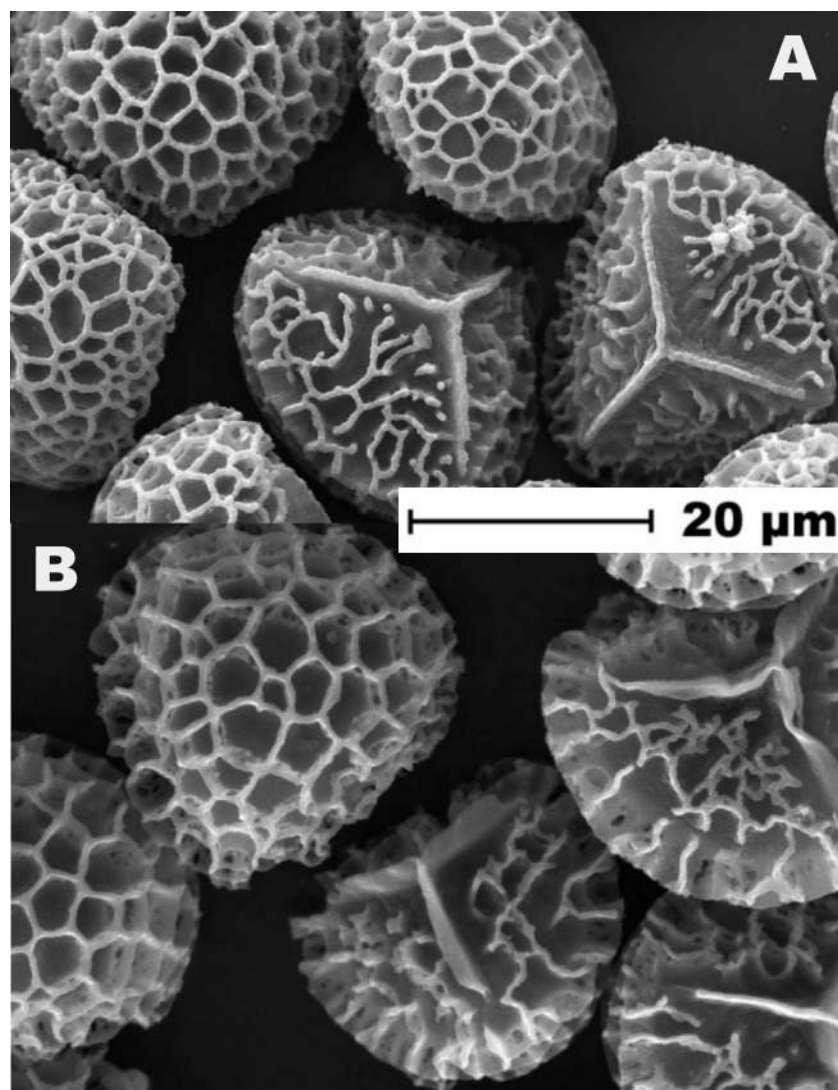


Figure 17: SEM images of raw spores of *L. clavatum* before extraction (A) showing the thick coating of pollen cement (wax and fats), and after acid extraction ‘AH-SECs’ with 9 M HCl for 1 h. (B).

Also, MAS SS-¹H-NMR was used to observe the chemical resistance of SECs following treatment of *L. clavatum* spores with strong acid over different refluxing times (See Figure 18.A, 18.B).

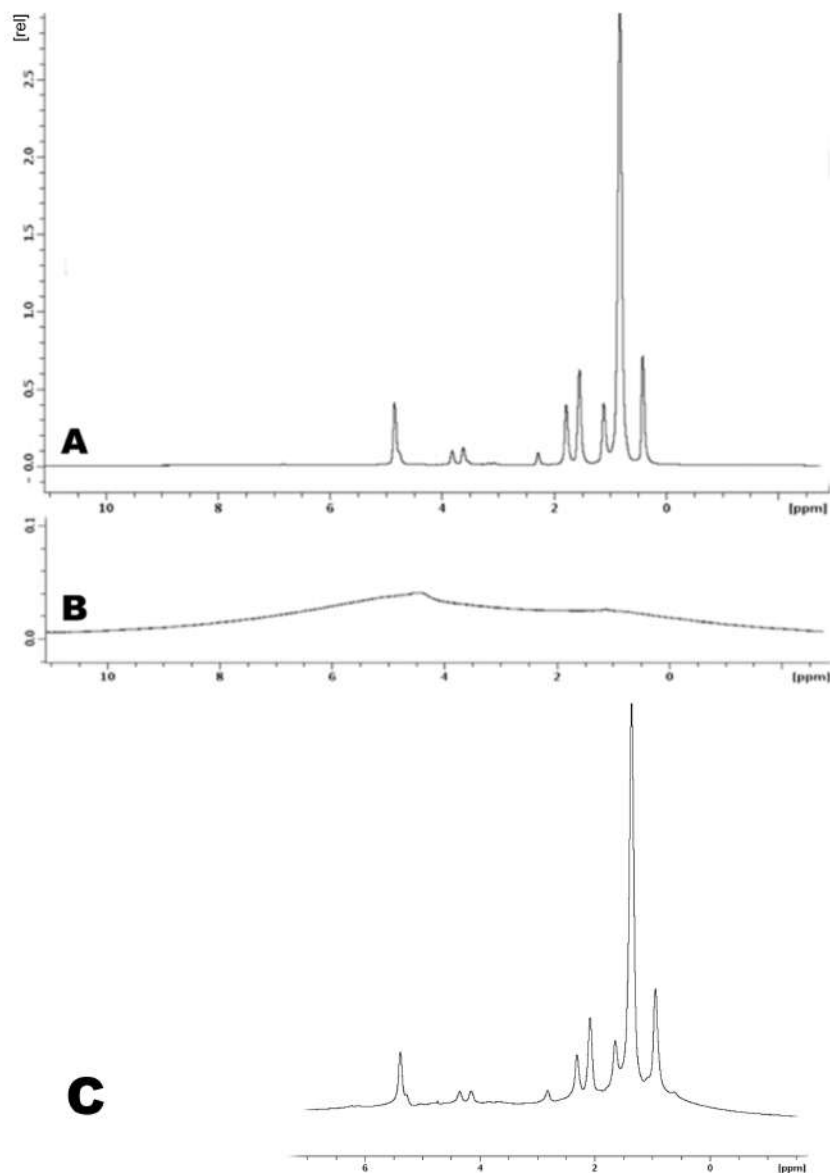


Figure 18: MAS SS-¹H-NMR spectra of AH-SECs of *L. clavatum* obtained at 500 MHz show the chemical resistance of SECs to strong acid (9 M HCl) (A): refluxed for 1h where the sharp peaks still exist. (B): refluxed for 24 h where the peaks disappeared, and (C) raw spores with their peaks.

Extracting SECs using Protocol B (9 M HCl) showed that the SECs have the feasibility to resist this strong acid for more than one hour as they still have their

sharp peaks. However, refluxing the same SECs for 24 hours showed no peaks in the NMR spectrum, which indicated the direct effect of refluxing time on chemical resistance of SECs.

The chemical resistance of *L. clavatum* SECs was expected as it was discussed previously (in Section 1.4.1); however, the MAS SS-¹H-NMR spectrum of *L. clavatum* SECs showed peaks that were similar to the peak found in raw spores (Figure 18.C), and they appeared to be fatty acids when compared to the spectrum of reference fatty acids in addition to the literature [135]. This was unusual as it was thought that extracting the raw spores and pollen should remove the whole waxes, fats, polysaccharides and the proteins of the raw spores.

Moreover, these lipids look like as they are in a liquid state as they showed sharp peaks in the MAS SS-¹H-NMR (which are similar to those collected on phospholipids in fluid phase spectra [135]), instead showing broad spectrum as would be expected behaviour for a solid material. Nevertheless, the SECs were dry and in solid form during the analysis, which indicates that it is just the lipids that were in liquid state to show these sharp peaks. This finding was of interest to study further (in Section 3.4), after the discussion of the physical properties of sporopollenin.

3.2 Thermal Resistance

SEM micrographs were obtained to observe any changes in size and morphology of SECs of *L. clavatum* following treatment in an oven in air at 200 °C for 24 hours (see experimental Section 8.4). As it is clear from the SEM images (Figure 19), that the SECs were still intact and had resisted the high temperature; however, some of them were bent from outside to the inside (deflated in the center of the trilete), though this could be due to the high vacuum used in SEM when the images were taken.

The MAS SS-¹H-NMR was used firstly, to examine the effect of high temperature on the SECs after incubation for three hours, and then after for 24 hours. Figure 20 shows that incubating the SECs for three hours showed no change in the spectrum associated with the peaks expected for the SECs (lipids peaks that are shown, also, in the raw spores as discussed earlier in Section 3.1). It appears that the SECs have high resistance to heating at 200 °C for this time period.

However, incubation of the same batch of SECs for another 24 hours showed a dramatic change in the MAS SS-¹H-NMR spectrum which could be due to the break down of such as the linkages ether of these fatty acids on the SECs [26-28], (discussed later in Section 3.4).

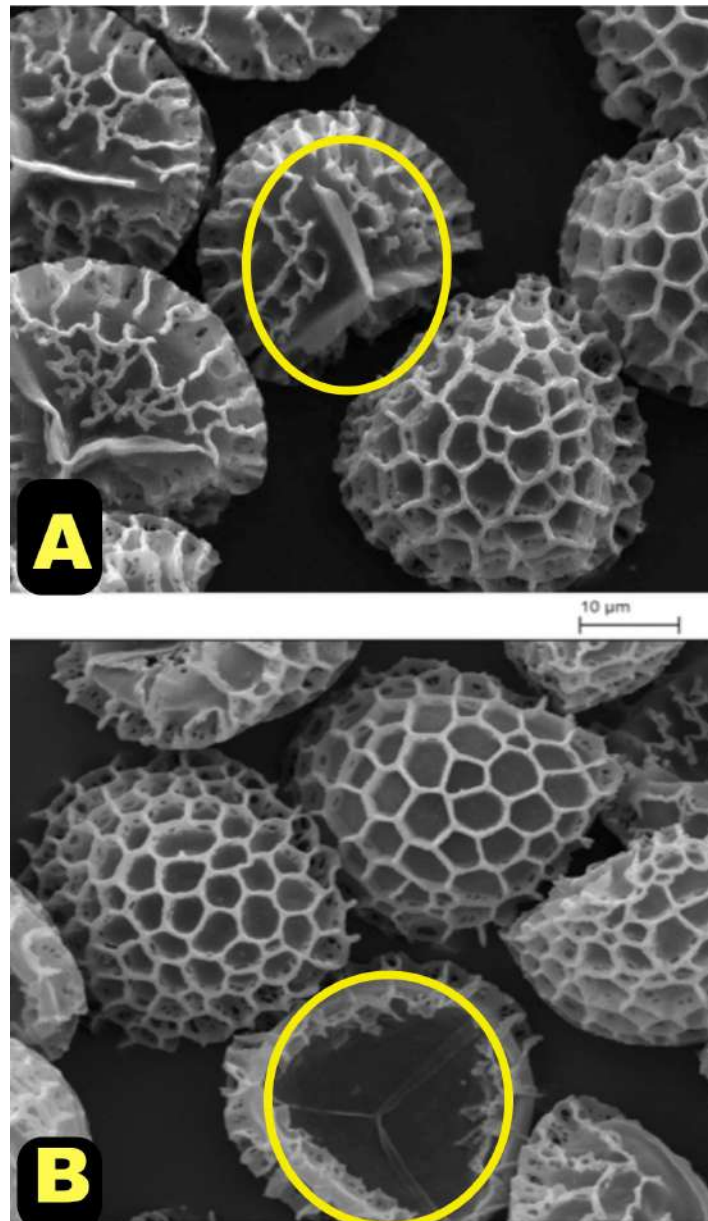


Figure 19: SEM images of AH-SECs of *L. clavatum* (A) before and (B) after incubation in oven at 200 °C for 24 h. The SECs were still intact and had resisted the high temperature, however, some of them were bent from outside to the inside (deflated) in the center of the trilete (in yellow circles).

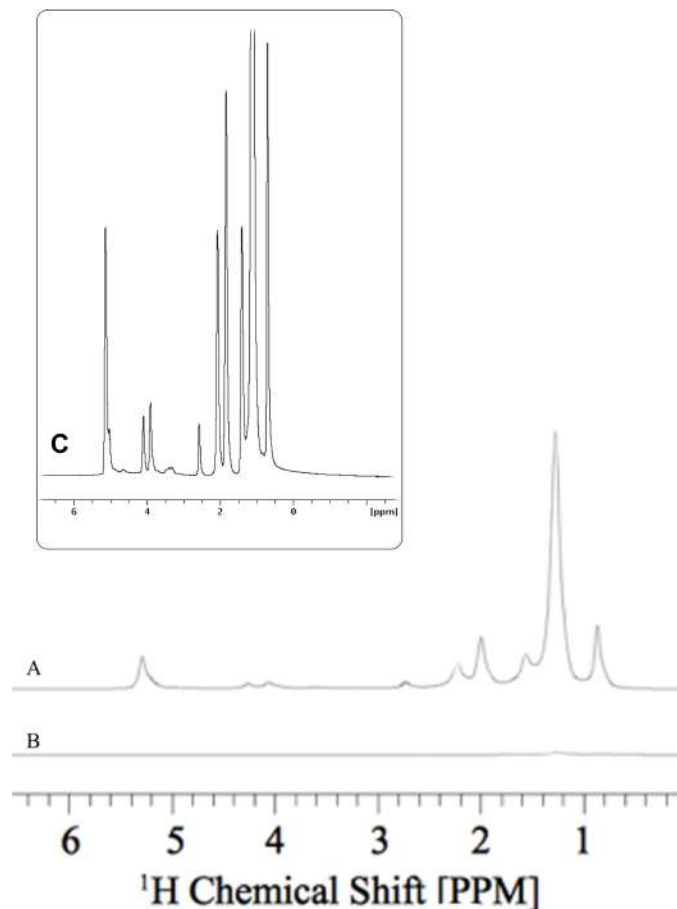


Figure 20: MAS SS-¹H-NMR spectra of AH-SECs of *L. clavatum* incubated for 3 h (A) and 24 h (B) at 200 °C, compared to raw spores (C). The spectra were obtained at 500 MHz.

3.3 The Elasticity of SECs

One of the characteristics that makes SECs a potential drug carrier and microencapsulating material is their elasticity, as when they passing through the GIT the peristaltic movement of GIT can apply pressure on the SECs and squeeze them to release their contents of encapsulated actives. When the SECs are compressed, for example, they are able to retain their original shape in just few seconds. This elasticity, gives the SECs more ability to resist mechanical stress. Co-workers

observed how quickly the SECs can, after compression using an IR KBR disc maker (compressor), return to their regular shape in few seconds after addition of a few drops of ethanol [91] (shown in Figure 21).

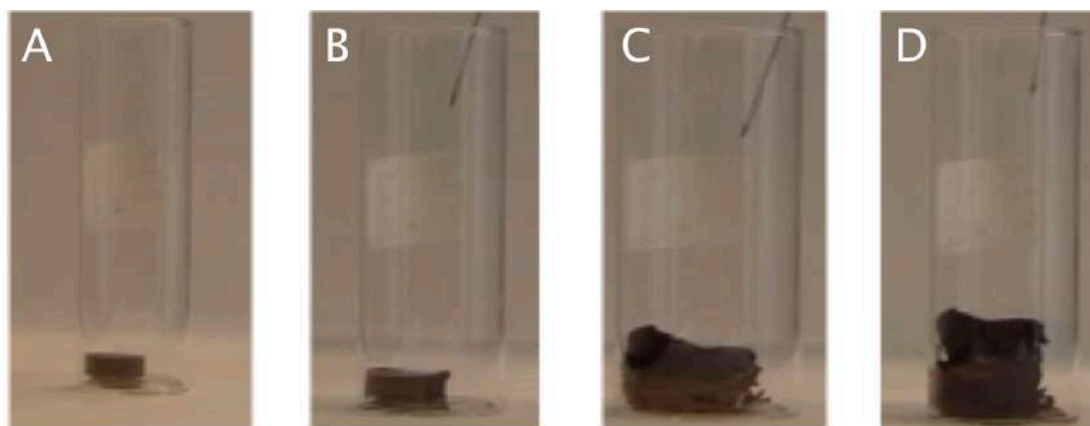


Figure 21: *L. clavatum* SECs return to its original shape after compression in just 40 seconds. (A) 200 mg of SECs compressed at 10 tons/cm², (B) after 5 s of ethanol drops being added, (C) after 20 s ethanol being added, and (D) after 40 s ethanol being added (2 ml total of ethanol being consumed during the 40 s) [91].

Another harsh method was used to examine the robustness of the SECs by attempting to break them grinding with a hard object, namely 70-110 μm glass beads (see experimental Section 8.5). The SECs and the glass beads were mixed together and ground using pestle and mortar manually for 5 minutes. Then, SEM images were taken of the mixture of the resulting fine powder of the SECs and the glass beads. Although the morphology of the SECs was changed, they resisted well and did not fragment. Figure 22 shows the SECs after they were smashed by the glass beads. The outer shell of the SECs was deformed, but they did not break.

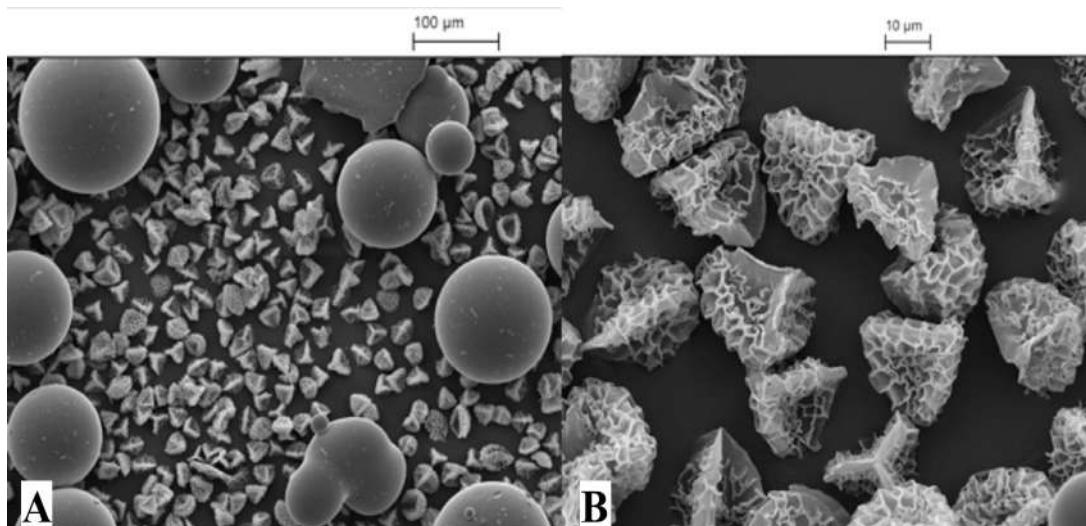


Figure 22: (A) Attempted fragmentation of *L. clavatum* SECs by grinding with mortar and pestle using (70-110 μm) glass beads. (B) SECs outer shell deformity.

3.4 The Nature of SECs' Lipids

Heating *L. clavatum* SECs at reflux in 9 M HCl for 24 hours removed the lipids from the SECs, but as discussed earlier, refluxing for 1 hour was insufficient to remove these lipids (in Section 3.1). In this section, the nature of these lipids was studied in order to identify how they are attached to SECs, i.e. if they are covalently attached to the framework or physically entrapped within the sporopollenin matrix of the SECs' outer shell.

3.4.1 Raw Spores and Pollens

Samples of raw *L. clavatum* and *P. sylvestris* were treated individually with acetone, ethanol, dodecane and chloroform (10 mg of spores/pollens refluxed in 10 ml of the previous solvents for 24 h), (see experimental Section 8.6.1). These common

Results and Discussion

solvents are well known to dissolve a range of lipids. Table 6 shows that after these treatments, there was a weight loss (10-40 %). Surprisingly ethanol and acetone dissolve the spore/pollen lipids more than chloroform, where is last one is a well-known strong lipid dissolver.

As it was said previously, there was weigh loss from the spore/pollen after treating with the lipid dissolver solvent, however, lipid peaks were still evident in the MAS SS-¹H-NMR spectra (Figure 23) of the recovered SECs. Spectra from *L. clavatum* SECs were similar to the spectrum for *P. sylvestris*. A comparable set of experiments were then conducted with the acid hydrolyzed spores and pollens (AH-SECs) (shown in the next section 3.4.2), which made a significant difference in removing the lipids or the ability of the lipids to dissolve in the solvents.

	Ethanol	Acetone	Chloroform
	Mass of recovered spore/pollen (g)	Mass of recovered spore/pollen (g)	Mass of recovered spore/pollen (g)
<i>L. clavatum</i>	0.600 ±0.005	0.640 ±0.003	0.800 ±0.007
<i>P. sylvestris</i>	0.780 ±0.002	0.890 ±0.004	0.910 ±0.010

Table 6: Mass recovered after treating 1.000 g of raw spores/pollen with different solvents (1g SEC/ 10 ml solvent). *n* = 3.

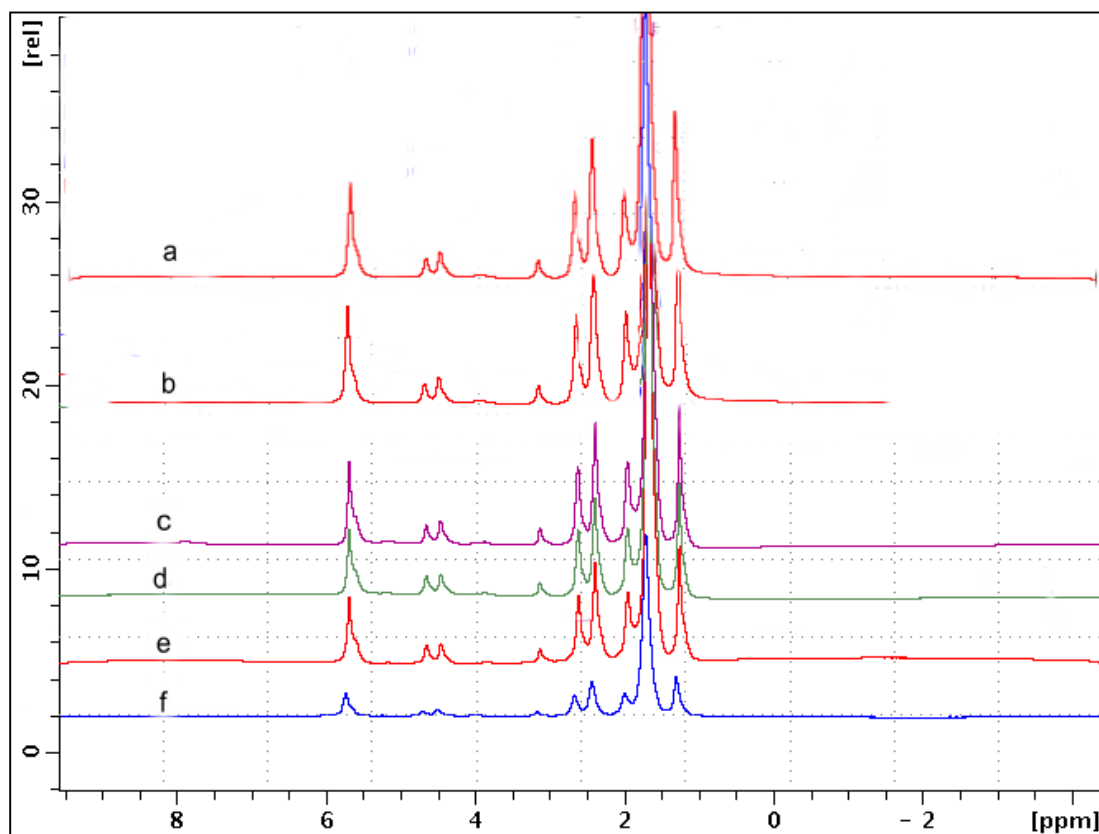


Figure 23: MAS SS-¹H-NMR spectra of raw *L. clavatum* spores (a) following treatment with the different solvents namely, dodecane (b), chloroform (c), acetone (d) and ethanol (e). Comparing MAS SS-¹H-NMR spectra with that from AH-SECs (f), show that even with the observed weight loss, lipid peaks are not significantly diminished just by treatment with a polar or non-polar solvent. The spectra were obtained at 500 MHz.

As seen from Table 6, ethanol and acetone were more efficient at removing lipids than chloroform. The ethanol and acetone-treated spores and pollen were then treated a second time with dodecane to observe any further changes in the weight loss or MAS SS-¹H-NMR spectral characteristics. Table 7 shows that there was indeed further mass loss of *L. clavatum* spores and *P. sylvestris* pollens after heating in acetone, ethanol with dodecane respectively at 60 °C for 4 hours; however, the MAS

Results and Discussion

SS-¹H-NMR spectra did not show any distinguishable differences. Interestingly, dodecane can dissolve these lipids from the AH-SECs but not the raw spores (see Section 3.4.2). This indicates that lipids on the SECs might be attached covalently to the SECs surface or trapped inside the sporopollenin matrix of the SECs, such that they need to be hydrolyzed by strong acid such as 9 M HCl to break down the covalent bonds to dissolve the lipids easily.

	Ethanol-dodecane	Acetone-dodecane
	Mass of recovered spore/pollen after heating with dodecane (g)	Mass of recovered spore/pollen after heating with dodecane (g)
<i>L. clavatum</i>	0.100 ±0.002	0.100 ±0.001
<i>P. sylvestris</i>	0.100 ±0.003	0.090 ±0.002

Table 7: Mass recovered after treating 0.200 g of ethanol and acetone refluxed-spores and pollen with dodecane at 60 °C for 4 hours. $n = 3$.

The dodecane filtrates from the acetone and ethanol treated raw spores were collected analyzed by gas chromatography mass spectroscopy (GC-MS), and the results showed there was no lipids in the filtrate. This indicates that mass loss was not from the SECs lipids. The mass loss could be from losing some material that coating the raw spores' wall, such as wax.

3.4.2 Acid Hydrolyzed SECs of Spores and Pollen

As described previously in (Section 3.1), hydrolyzing raw spores and pollens with 9 M HCl can remove the polysaccharide intine and the genetic material. In addition, a small percentage of the total SECs lipids mass is removed if refluxed in 9 M HCl for 1 hour reflux, and most if not all is removed after refluxing for 24 hours in 9 M HCl. In this section, the same lipid dissolving solvents that were used to investigate the raw spores and pollen (in Section 3.4.1), were used to treat the AH-SECs from *L. clavatum* and *P. sylvestris* in order to explore the nature of the lipids present and determine how they can be cleaved from the raw spores/pollens. Table 8 shows that a large mass loss was observed in the AH-SECs of spore/pollen (around 38 % of total mass for *L. clavatum* and 52 % for *P. sylvestris*). This mass loss is related to removing the wax, fats, nitrogenous genetic material and the polysaccharide intine present in the spores and pollen.

Extraction solvent HCl (9 M)	
Mass of recovered SECs (g)	
<i>L. clavatum</i>	3.100 ±0.010
<i>P. sylvestris</i>	2.400 ±0.008

Table 8: Mass recovered after hydrolyzing 5 g of spores and pollens with 9 M HCl for 1 h. $n = 3$.

The elemental analysis for acid extracted *L. clavatum* SECs is shown in Table 9 below.

Element	% Found
C	68.200 ±3.000
H	9.790 ±1.300
N	0.000 ±0.000

Table 9: Elemental analysis of extracted *L. clavatum* SECs. The elemental analysis was run in triplicate. $n = 3$.

The combustion elemental analysis data showed that carbon and hydrogen were found in extracted SECs, whilst there was no trace of nitrogen. The removal of nitrogen indicates the removal of proteins in the empty microcapsules. The removal of these contents provided a relatively large cavity ready to be used for such as drug encapsulation.

3.4.3 Dissolving the SECs Lipids

All of the previous lipid-dissolving solvents used, resulted in a small mass loss from the raw spore/pollen (in sections 3.4.1 and 3.4.2); however, they could not remove the material which gave rise to the peaks that appeared in MAS SS-¹H-NMR spectrum, even after refluxing the raw spores/pollens with dodecane. As stated above in (Section 3.4.1), it was concluded that the lipids were covalently attached to the spores/pollens and need to be hydrolyzed first with acid or base before being

extracted with these solvents. It was found that these solvents (acetone, ethanol, dodecane and chloroform) were able to dissolve part of the lipids from the AH-SECs, and dodecane was able to dissolve the hydrolyzed lipids from *L. clavatum* SECs completely (see experimental Section 8.6.2). However not all of the lipids from the AH-SECs of *P. sylvestris* could be extracted using dodecane using same temperature and reflux time (see Figure 24). The reason behind the different behavior of AH-SECs of *L. clavatum* and *P. sylvestris* towards dodecane extraction is not clear. Both *L. clavatum* and *P. sylvestris* seem to have the same lipid structures in their SECs as was shown in the MAS SS-¹H-NMR spectra (Figure 24). The dodecane filtrates from AH-SECs of both *L. clavatum* and *P. sylvestris* were collected and analyzed by GC-MS. The results showed that there were no lipids in dodecane filtrate of AH-SECs of *P. sylvestris*; however, the dodecane filtrate of *L. clavatum* AH-SECs showed traces amount of lipids. Increasing the reaction time and temperature (80 °C for 6 h) of the extraction was sufficient to extract some lipids from the pine, which were then analyzed by GC-MS (see Section 3.4.5). The reason behind this difference could be a steric reason and difficulty of solvent penetration with the *P. sylvestris* SECs.

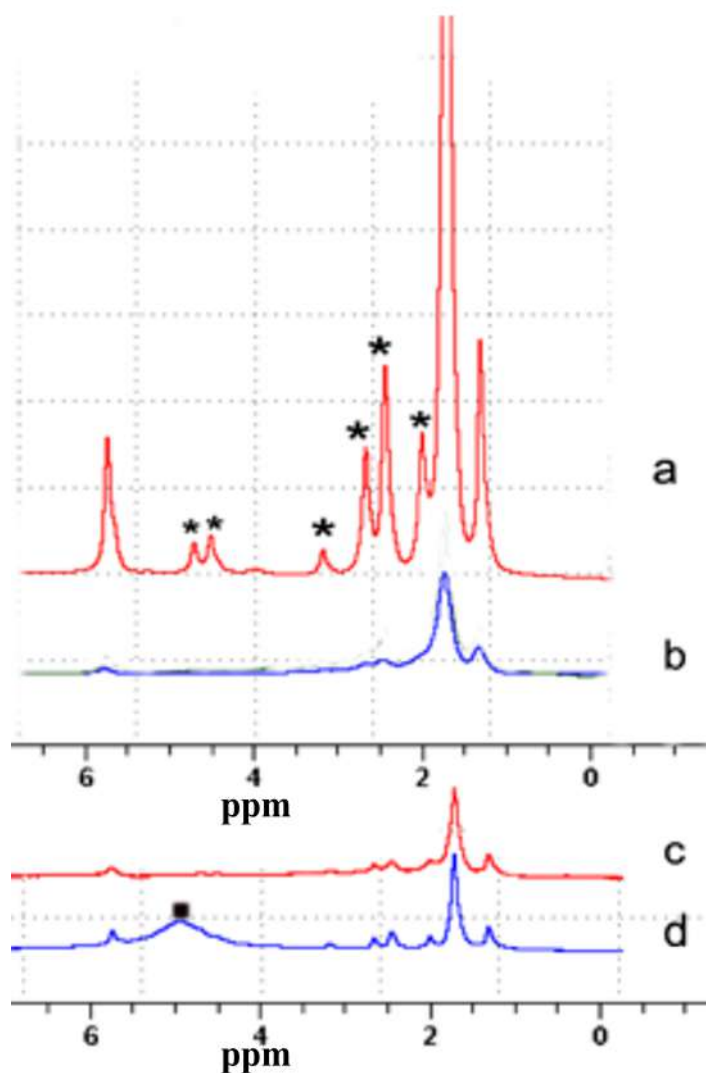


Figure 24: MAS SS-¹H-NMR spectra of AH-SECs of *L. clavatum* (**top**): (a) with black stars indicating the lipid peaks that disappear (b) after treatment with dodecane for 4 h at 60 °C. AH-SECs of *P. sylvestris* (**Bottom**): (c) after treatment with dodecane for 4 h at 60 °C, showing that dodecane did not dissolve (d) the lipids of AH-SECs of *P. sylvestris*. The broad peak at 5 ppm (indicated by a black square) is related to water contamination from washing the NMR rotor. The spectra were obtained at 500 MHz.

Results and Discussion

Table 10 shows the mass loss after refluxing AH-SECs with dodecane, indicating that lipids form 14 ± 1 % of *L. clavatum* and 12 ± 3 % of *P. sylvestris* SECs (% w/w).

Dodecane	
Mass of recovered AH-SECs after dodecane extract (g)	
<i>L. clavatum</i>	0.86 ± 0.010
<i>P. sylvestris</i>	0.87 ± 0.020

Table 10: Mass recovered of HCl-extracted spores/pollen (1 g) after treatment them with dodecane for 4 h at 60 °C. $n=3$.

In addition to the above technique, to determine the SECs lipids component by mass loss, another quantification method was carried out (see experimental Section 8.6.3). In this method water (5 mg) was added to an accurately weighed SECs sample, to compare the lipid peaks in relation to the water peak (which appears at 4.5 ppm) (Figure 25). This spectrum showed a ratio of 1:3 (water/lipid). Therefore, it could be estimated that the percentage of the lipids of *L. clavatum* SECs is nearly 20 %, i.e. roughly 15 mg of lipids in 75 mg of AH-SECs.

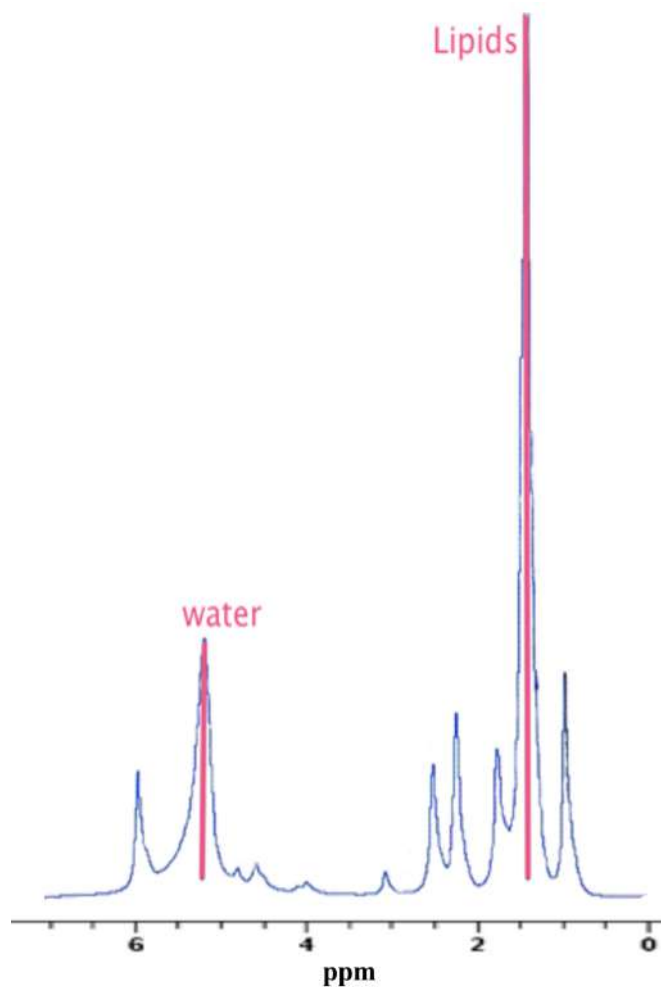


Figure 25: MAS SS- ^1H -NMR spectrum of AH-SECs of *L. clavatum* showing the lipids peaks, compared to 5 mg of water. This shows a ratio of 1:3 (water: lipids). The lines are indicating relative area under peak integration. The spectra were obtained at 500 MHz.

The elemental analysis of the AH- SECs after removal of their lipids with dodecane is shown in Table 11 below.

Element	% Found (before dodecane treatment)	% Found (after dodecane treatment)
C	68.200 ±3.000	62.77 ±1.000
H	9.790 ±1.300	8.34 ±0.700
N	0.000 ±0.000	0.000 ±0.000

Table 11: Elemental analysis for *L. clavatum* AH-SECs after removal of lipids by dissolution in dodecane. $n = 3$.

The elemental analysis data shows that there was a slight decrease in the amounts of C and H in AH-SECs after washing with dodecane due to the removing of part of the original lipid component.

3.4.4 SECs and ‘dry liquid’ lipids

The SEC lipids that were left after extraction showed interesting behavior. The lipids resisted the harsh acid treatment and remained in / on the SECs after “normal” washing, and needed another treatment with a lipid-dissolving solvent, such as dodecane, to remove them (Section 3.4.3). The sharp signals in the MAS SS-¹H-NMR spectrum (Figure 24 (a 1-5 ppm), in Section 3.4.3) indicate the H atoms of the lipid’s aliphatic chains have freedom to move, a behavior that is similar to a mobile liquid sample as opposed to a solid. The indication is therefore that these lipids are in a liquid-like state even though the samples appear to be solids. These types of materials are often known as “dry liquids” [15]. At the time of writing this thesis, no one has described the dry liquid behavior of SECs lipids (lipids that are not readily

removed after the extraction of SECs), nor of such “dry liquids” in a naturally occurring system. This behaviour of SECs toward their natural lipids should be investigated further as it could be useful to explain how they are able to preserve lipids from oxidation [73].

3.4.5 Determination the Chemical Structure of the ‘dry liquid’

Lipids of SECs

In this section, the chemical structure of the natural SECs lipids that are not readily removed after SEC extraction with acid or base treatment (referred to as the ‘dry liquid’ lipids) will be proposed. The dodecane extract from AH-SECs of *L. clavatum* and *P. sylvestris* were each collected and analyzed using GC-MS and results showed that the SECs “dry liquid” lipids composed of C16 and C18 fatty acids (see Figure 26.A). Also, the GC-MS showed that the SEC lipids were a mixture of mono- and polyunsaturated fatty acids, with a large proportion of palmitoleic acid (C16), oleic and linoleic acids (C18). Furthermore, reference samples of oleic and linoleic acid were analyzed by GC-MS and compared to the lipids found in the SECs, and shown to give identical spectra (see Figure 26.B and C). Figure 27 shows the MAS SS-¹H-NMR spectrum of these lipids and their proton assignments (Figure 27.A and 27.B), and a proposed structure of the ‘dry liquid’ lipids of SECs that could not be removed during the extraction with 9 M HCl for 1 h (Figure 27.C).

Results and Discussion

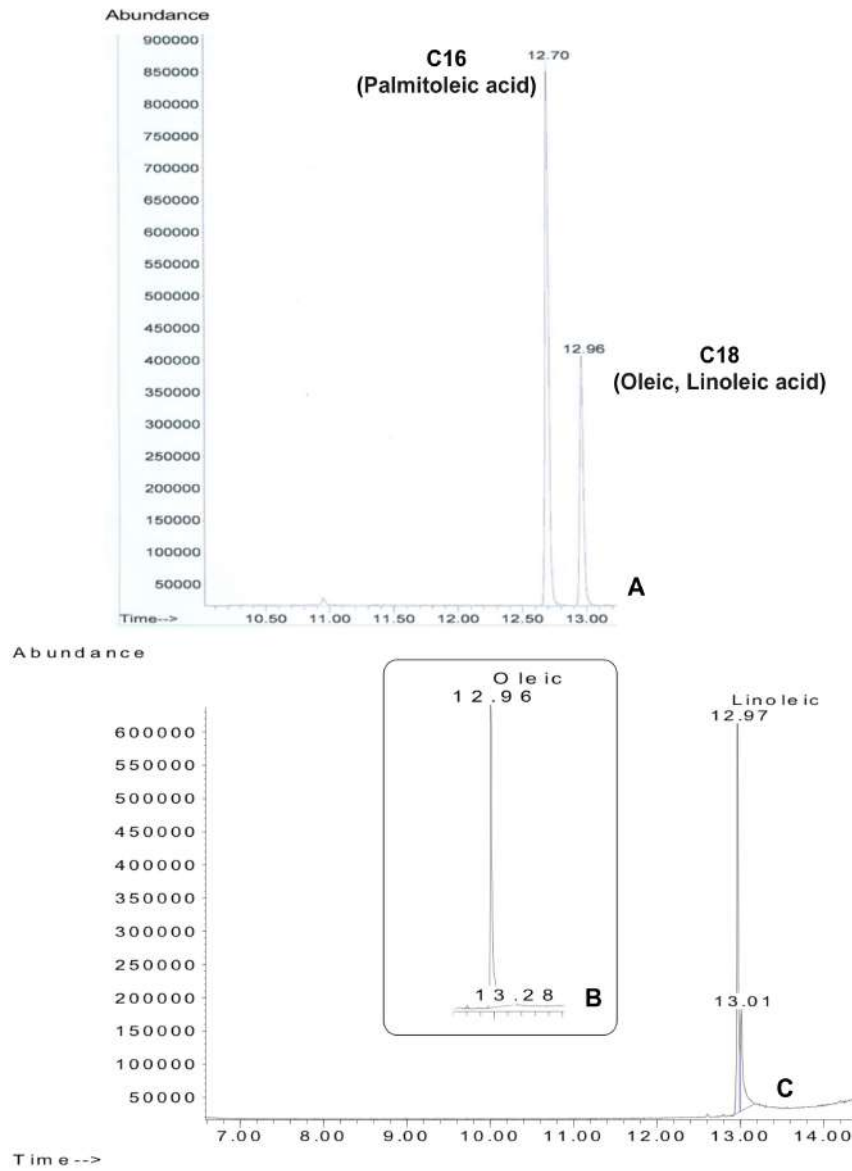


Figure 26: GC-MS show that SEC lipids are a mixture of mainly the mono- and di-unsaturated lipids (A). GC-MS trace of reference oleic acid (B) and linoleic acid (C).

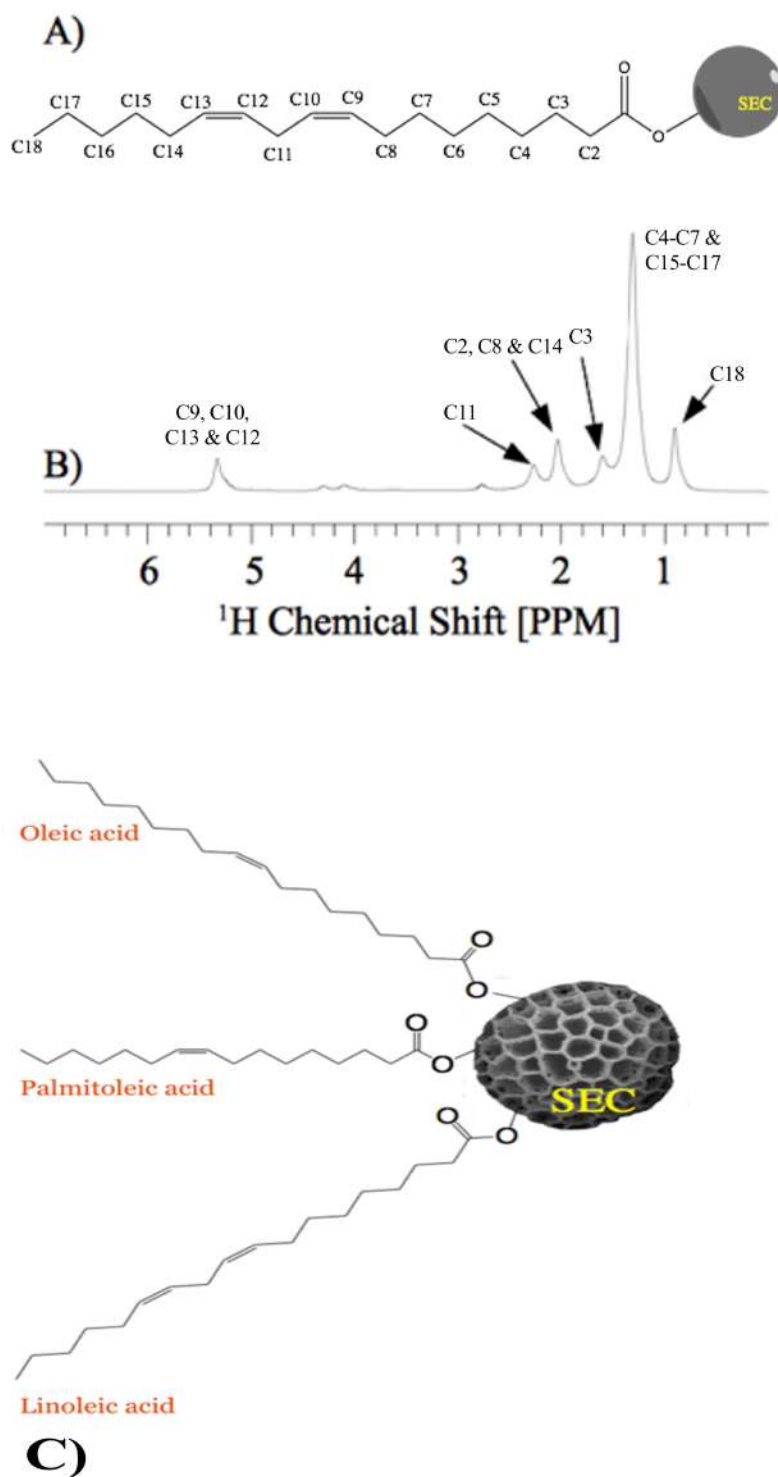


Figure 27: MAS SS- ^1H -NMR spectrum of ‘dry liquid’ lipids of *L. clavatum* SECs and assignment of the signals (A, B), spectrum was obtained at 500 MHz.. The proposed structure of *L. clavatum* SEC ‘dry liquid’ lipids (C).

3.4.6 Attempted Determination of the Location of SEC ‘dry liquid’ lipids using Nile red staining and Fluorescence Microscopy

The SECs show that they still have their own lipids even after extraction with concentrated acid or base, and these lipids are composed of a mixture of mono- and di-unsaturated C16 and C18 fatty acids, which were found to be palmitoleic, oleic and linoleic acids using GC-MS (Section 3.4.5). Here, it was attempted to use Nile red dye to stain the SEC lipids and see if the lipids are on the surface of the exines or actually trapped inside the sporopollenin matrix. Nile red is a lipophilic fluorescent stain that is used commonly to stain lipids for visualization using fluorescence microscopy [92].

To stain the AH-SECs of *L. clavatum*, an excess (1 ml) of 31.41 mM Nile red stain/acetone solution (1 mg/ml) was added to SECs in acetone (1 g/ml). The mixture was left in orbital shaker at 240 rpm for 20 minutes at room temperature, filtered, washed with PBS and then vacuum dried overnight (see experimental Section 8.6.4).

Figure 28 shows the fluorescence microscopy images of stained and un-stained SECs. The fluorescence images show no difference between the stained and unstained SECs, and that is due to the fact the SECs are autofluorescent microparticles and they absorb and scatter light even without the stain [93,94]. That made it difficult to proceed with the next step of this experiment, where the plan was to stain the AH-SECs of *L. clavatum* and the ‘lipid free’ SECs to check if the lipids are attached to the surface of the SECs or trapped inside the sporopollenin matrix. If these ‘dry liquid’ lipids were attached to the surface, the fluorescence intensity would decrease when the lipids were removed.

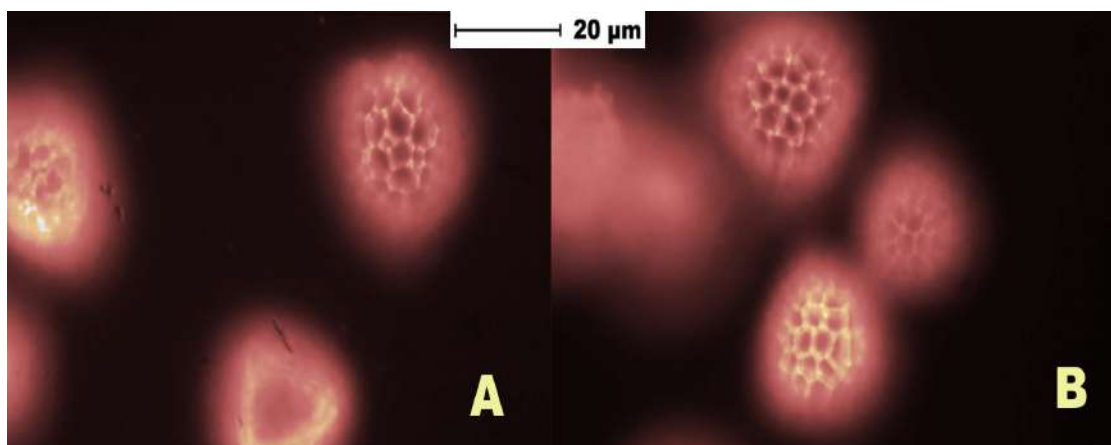


Figure 28: Fluorescence microscopy of *L. clavatum* AH-SECs without stain (A), and after staining with Nile red (B).

3.4.7 Adding Oleic acid to SECs after Removal of their Natural Lipids

After the successful attempts to remove lipids from AH-SECs of *L. clavatum* and *P. sylvestris* (in Section 3.4.3), a further investigation was made to see if the removed lipids could be re-added, and if they would still show the ‘dry liquid’ behaviour. Also, it was envisaged that the lipid added could be varied to tune the properties of the SECs for some of the applications in drug adsorption and release (see Chapter 4). Oleic acid was chosen as the lipid to add after removing SECs lipids, and this was done by adding oleic acid to the AH-SECs after removal of their own lipids by dodecane.

An emulsion of oleic acid in water was made (400 mg of oleic acid was added to 7 ml of water followed by agitation of the mixture for 20 minutes in orbital shaker at 900 rpm) and then AH-SECs (200 mg) from *L. clavatum* or *P. sylvestris* were added to the (202.28 mM) emulsion which was then further shaken manually for 1 minute.

After being left at room temperature for 4 h, the emulsion was filtered and the AH-SECs carefully washed with hexane (10 ml x 3), filtered and dried thoroughly (see experimental Chapter 8, in Section 8.6.5). The mass results are shown in Table 12.

	Mass of lipid-stripped AH-SECs (g)	Mass of lipid-stripped AH-SECs after sequestering oil (g)
<i>L. clavatum</i>	0.200	0.221 ±0.004
<i>P. sylvestris</i>	0.200	0.235 ±0.002

Table 12: AH-SECs from *L. clavatum* and *P. sylvestris*, after treatment with dodecane, are able to sequester oleic acid from an oil-water emulsion. The results show the mass gain after oil sequestration. The mass of oil that can be sequestered by the SECs is similar the oil that they lose after initial dodecane washing. $n = 3$.

The maximum amount of oleic acid that the AH-SECs of *L. clavatum* were able to absorb was 10 ± 2.5 % w/w (see Table 12). As discussed before (in Section 3.4.3), dodecane could not remove the lipids from AH-SECs of *P. sylvestris* using the same reflux time and temperature as used for AH-SECs of *L. clavatum*; nevertheless, they were still able to absorb oleic acid (17 ± 1.5 % of their mass). Figure 29 shows the MAS SS- ^1H -NMR spectrum of *L. clavatum* SECs, after removal of their natural lipids and after subsequent absorption of oleic acid. Figure 30 shows the MAS SS- ^1H -NMR spectrum indicating that the AH-SECs of *P. sylvestris* retain their own lipids after treatment with dodecane and were still able to absorb oleic acid.

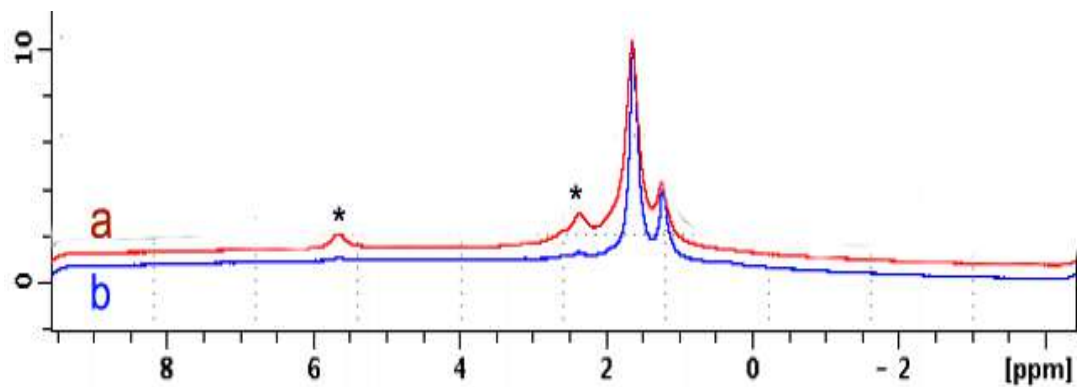


Figure 29: The MAS SS-¹H-NMR spectra illustrates dodecane-refluxed AH-SECs of *L. clavatum* after absorption of oleic acid. The stars shows the lipid peaks that appear again in the spectrum (a); (b) the lipid-stripped SECs before sequestration of oleic acid. The spectra were obtained at 500 MHz.

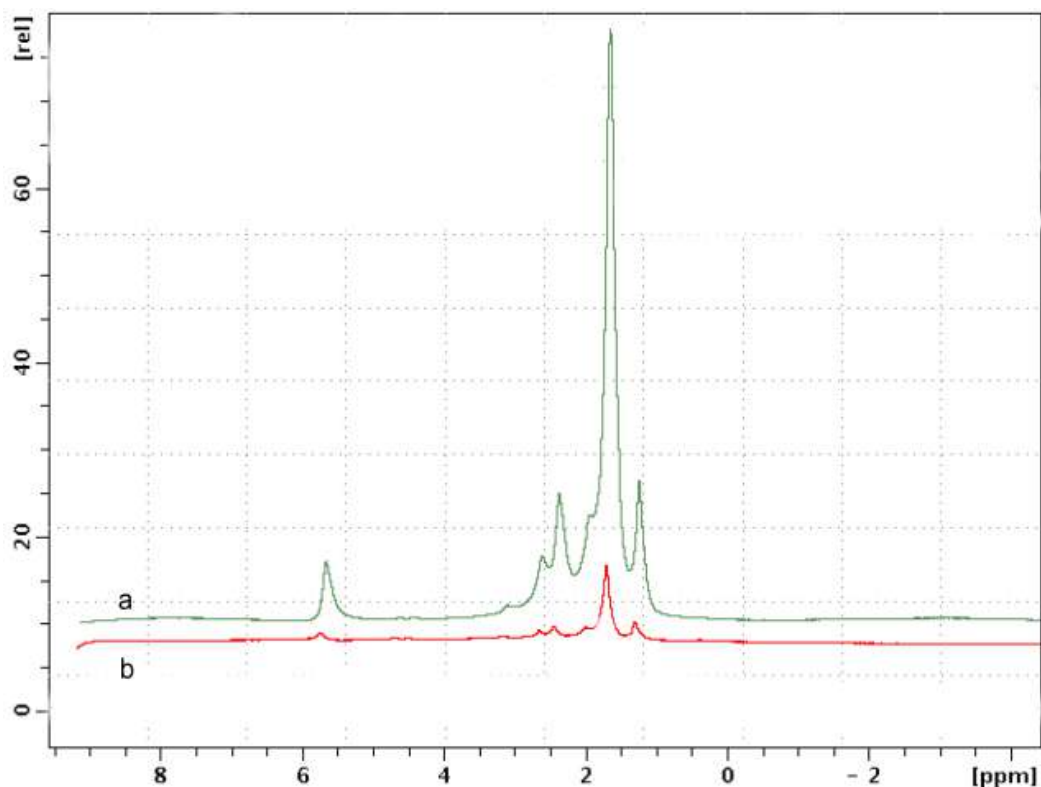


Figure 30: MAS SS-¹H-NMR spectra of dodecane-treated AH-SECs of *P. sylvestris*. The dodecane-treated AH-SECs were able to (a) absorb oleic acid (17% of their mass), in comparison to (b) dodecane-treated AH-SECs of *P. sylvestris*. The spectra were obtained at 500 MHz.

3.4.8 Adding Oleic acid to SECs after Surface Modification

Modifying the functional groups on the SECs' surface from acid (carboxylic) and phenol to their salt form (sodium carboxylate and sodium phenoxide) was expected to decrease the lipophilicity of the SECs such that they release their own lipids more readily. Therefore, the AH-SECs of *P. sylvestris* and *L. clavatum* were treated with base (NaOH) to form sodium salts of the surface functional groups (see Section 8.6.6). Figure 31 shows schematically the expected SECs' surface after modification.

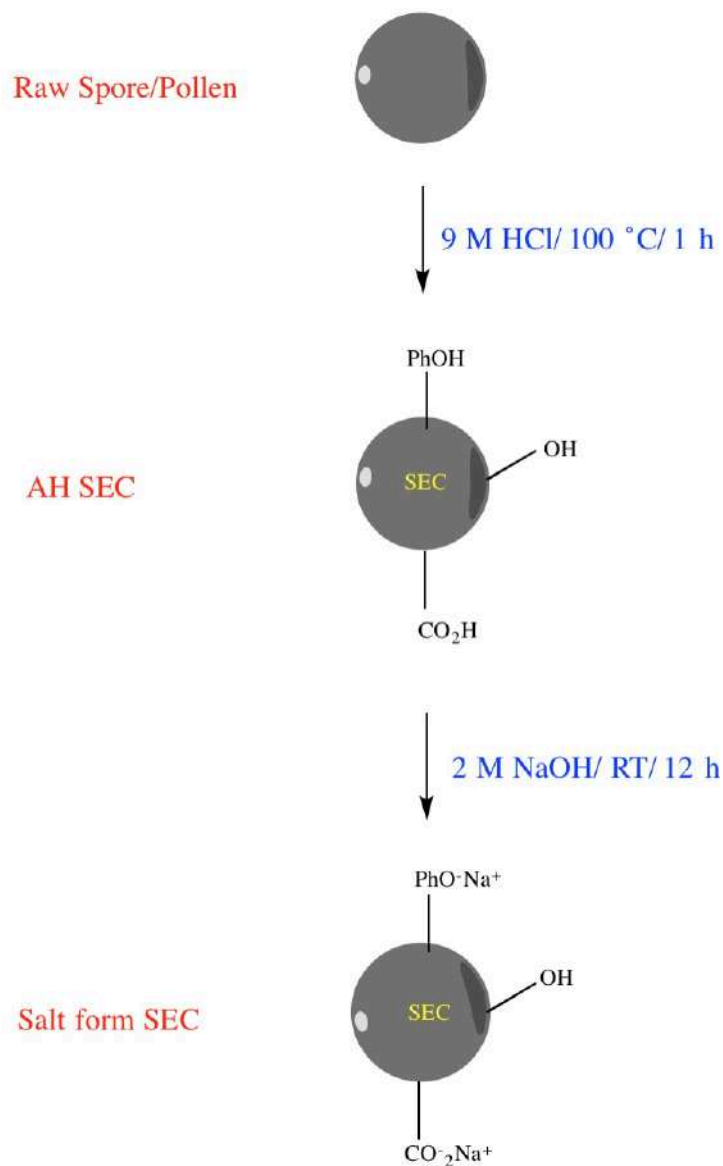


Figure 31: Modifying SECs' surface from acid and phenol to their salt forms.

Results and Discussion

These modified SECs were analyzed using the MAS SS- ^1H -NMR, and the spectrum showed there were no longer any peaks assigned to lipids in both *L. clavatum* and *P. sylvestris* SECs. These findings were very helpful in reattaching the oleic acid to the SECs that have no detectable lipids. Figure 32 and Table 13, represent the surface-modified SECs before and after sequestering oleic acid from the oil-water emulsion.

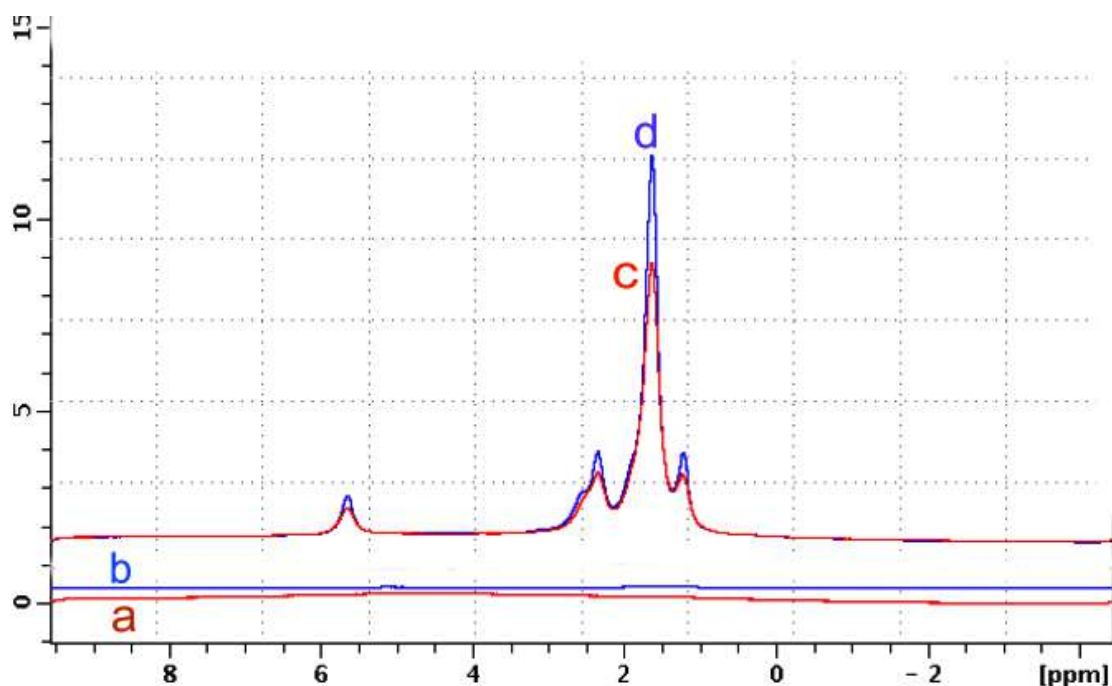


Figure 32: MAS SS- ^1H -NMR spectra of surface-modified SECs from *L. clavatum* and *P. sylvestris*. The spectra were obtained at 500 MHz.

L. clavatum The spectrum shows no lipids after treating AH-SECs with 2 M NaOH for 10 h at room temperature (**a**), in comparison to the SECs after sequestering oleic acid (**c**).

P. sylvestris: The spectrum indicates an absence of lipids after treating AH-SECs with 2 M NaOH for 10 h at room temperature (**b**), in comparison to the SECs after sequestering oleic acid (**d**).

Results and Discussion

	Mass of Na-Salt SECs g	Mass of Na-Salt SECs after sequestering oil g
<i>L. clavatum</i>	0.200	0.254 ±0.002
<i>P. sylvestris</i>	0.200	0.260 ±0.001

Table 13: Mass gain of SECs after sequestration of oleic acid by salt form of AH-SECs from *L. clavatum* and *P. sylvestris*. $n=3$.

The salt form of AH-SECs from *L. clavatum* were able to sequester 27 ± 1 % (w/w) of oleic acid, and the salt form of AH-SECs of *P. sylvestris* sequestered 30 ± 0.5 % (w/w) oleic acid. By comparing these percentages to the acid form SECs (Table 12, section 3.4.7), it appears that the capacity of the salt form of AH-SECs to sequester oleic acid was double the capacity of the acid form. The acid form of the *L. clavatum* SECs were able to soak up 10%, and the *P. sylvestris* SECs soaked up 17% (% w/w).

This change in oil sequestering capacity between the AH-SECs and the salt form of the AH-SECs is presumed to be due to the total removal lipids in the salt form, whilst the AH-SECs still retained some natural lipids adsorbed / attached, even after refluxing in dodecane. The removal of the lipids had presumably facilitated their being dissolved under aqueous conditions through their conversion to the fatty acid carboxylates. It was envisioned that this could be beneficial when considering the encapsulation (and release) of different drugs, as some drugs might prefer to be in hydrophobic carrier while others a hydrophilic one. Therefore, by removing the lipids from the AH-SECs, or re-attaching them, two forms of microcapsules can be created, namely in hydrophilic, and hydrophobic forms respectively.

3.4.9 Covalent attachment of Oleic acid to SECs

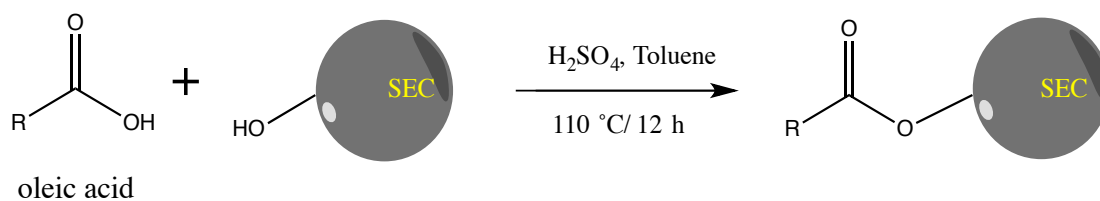
In the last two sections (Section 3.4.7 and 3.4.8) it was reported that oleic acid could be adsorbed successfully by the SECs, simply by mixing with a water/oil emulsion. This prompted attempting to attach oleic acid covalently to SECs and studying the behaviour of these lipids to see if they still display the mobile phase of the natural SEC's lipids or the oleic acid that was adsorbed.

The first method (A) to esterify the 'lipid-free' AH-SECs was done by adding oleic acid to the SECs in toluene and adding 5 drops of concentrated sulfuric acid, then refluxing at 110 °C overnight. The mixture was filtered, washed thoroughly with hexane and dried in a desiccator to a constant weight. The second method (B) to covalently attach the oleic acid to the 'lipid-free' SECs was done by suspending the SECs in dry dichloromethane (DCM) and then adding triethylamine (Et₃N) and oleoyl chloride to the SECs-DCM suspension at 0 °C. The mixture was stirred for 4 hours at room temperature, then filtered, washed with 2 M HCl, pure water until neutral, ethanol and acetone respectively and vacuum dried overnight to constant weight. These two methods are shown schematically in Figure 33.

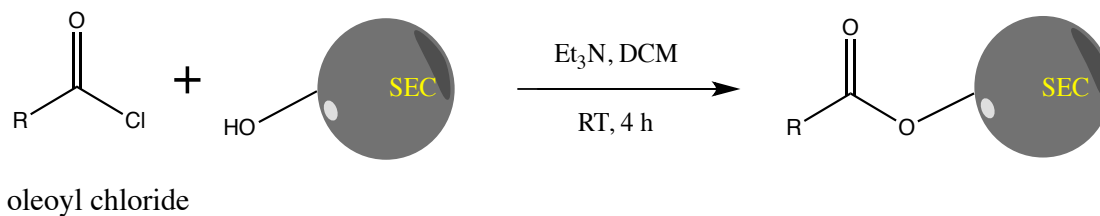
The MAS SS-¹H-NMR spectra (in Figure 34) confirmed the esterification of the SECs that was prepared using methods A and B as the peaks of the original lipids of SECs appeared again; however, the spectra showed that method B (using oleoyl chloride) was more effective than method A (oleic acid / H₂SO₄). Also, the MAS SS-¹H-NMR results of the covalently attached oleic acid showed similar mobility behavior of the original SECs lipids that has been removed (signals from C2-C18). The behavior of SECs having 'dry liquid' lipids of their own natural lipids and the

SECs with similar added lipids C18, such as oleic need to be investigated further. This would help to explain how they are able to preserve lipids from oxidation [73].

A



B



R= 17

Figure 33: Esterification of *L. clavatum* SECs using oleic acid (method A) and oleoyl chloride (method B).

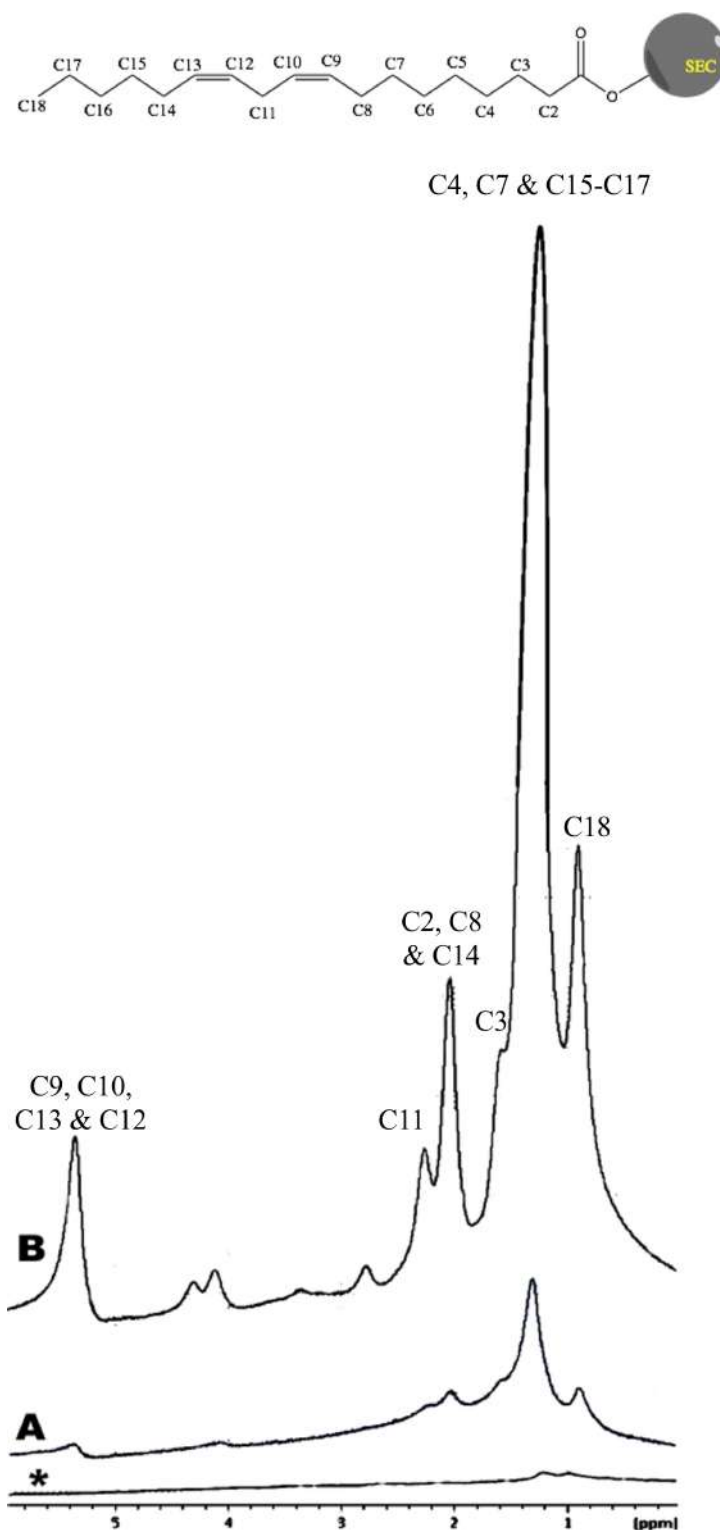


Figure 34: MAS SS-¹H-NMR spectra of esterified SECs of *L. clavatum* using oleic acid (A) and oleoyl chloride (B), compared to lipid-free SECs (*). The spectra were obtained at 500 MHz.

3.4.10 Attempted PEGylation of SECs

The last three sections above, (Section 3.4.7, 3.4.8 and 3.4.9), describe how a lipid (oleic acid) was added to SECs physically and covalently as a replacement of the natural lipid mixture found on the SECs. An interesting idea was to follow this up by trying to add a synthetic “modifier” instead of a natural lipid. In this experiment, it was envisaged that the SECs could be modified with a low molecular weight polyethylene glycol (PEG) chain.

AH-SECs (1 g) of *L. clavatum* were stirred in dimethyl sulfoxide (DMSO) (20 ml) for 5 minutes in room temperature, and then anhydrous potassium carbonate (K_2CO_3) (1 g) (126.08 mM) was added to the SECs-DMSO mixture with a catalytic amount of potassium iodide (0.05 g) (33.53 mM). mPEG-tylosate (av. MW = 1,000) (0.5 g) was added in portion over 10 minutes at room temperature to give final concentration of (0.025 mM). After that the mixture was left for 4 h at 170 °C to complete the reaction, then filtered, washed thoroughly with water and then ethanol before drying overnight in a desiccator.

The second method used the same steps and chemical components of the first method except replacing anhydrous K_2CO_3 with sodium hydride (NaH) (1 g) (2083.53 mM) (see experimental Section 8.6.8). The reaction is shown schematically in Figure 35 and the elemental analysis for the PEGylated SECs is given in Table 14 below.

SEC

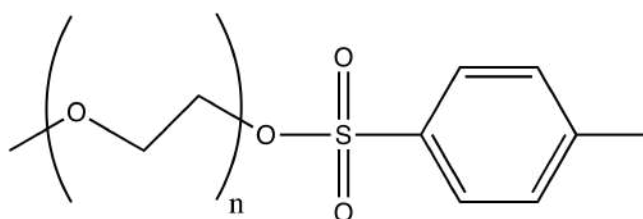


First method: stirred in DMSO, K_2CO_3 , KI/ RT/ 10 min

Second method: stirred in DMSO, NaH , KI/ RT/ 10 min

+

PEG



170 °C/ 4 h

PEGylated SEC

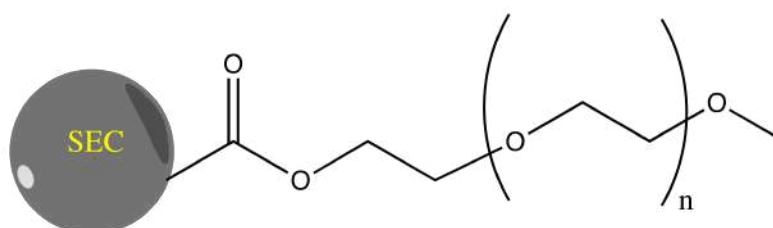


Figure 35: PEGylation of *L. clavatum* SECs using either K_2CO_3 or NaH as base.

Results and Discussion

Element	% Found (Before SECs PEGylated)	% Found (After SECs PEGylated)
C	62.770 ±1.000	62.930 ±1.200
H	8.340 ±0.700	7.560 ±0.300
N	0.000	0.000

Table 14: Elemental analysis for PEGylated SECs from *L. clavatum* using NaH. $n = 3$.

The elemental analysis shows there are no significant changes in C and H content in SECs before and after PEGylation. Therefore, the MAS SS-¹H-NMR spectroscopy was used to see any difference in the SECs peaks before and after. The MAS SS-¹H-NMR results of the PEGylated SECs show that the second method (using NaH) was more effective than the first method (using K₂CO₃) in the PEGylation reaction, (see Figure 36), as the PEGylated SECs showed increase intensity of lipids peaks at 1ppm (which represent methylene groups that were added to the C4-C7 and C15-C17 parts of the SECs' natural lipids), however, we were looking for the CH₂O groups of PEG.

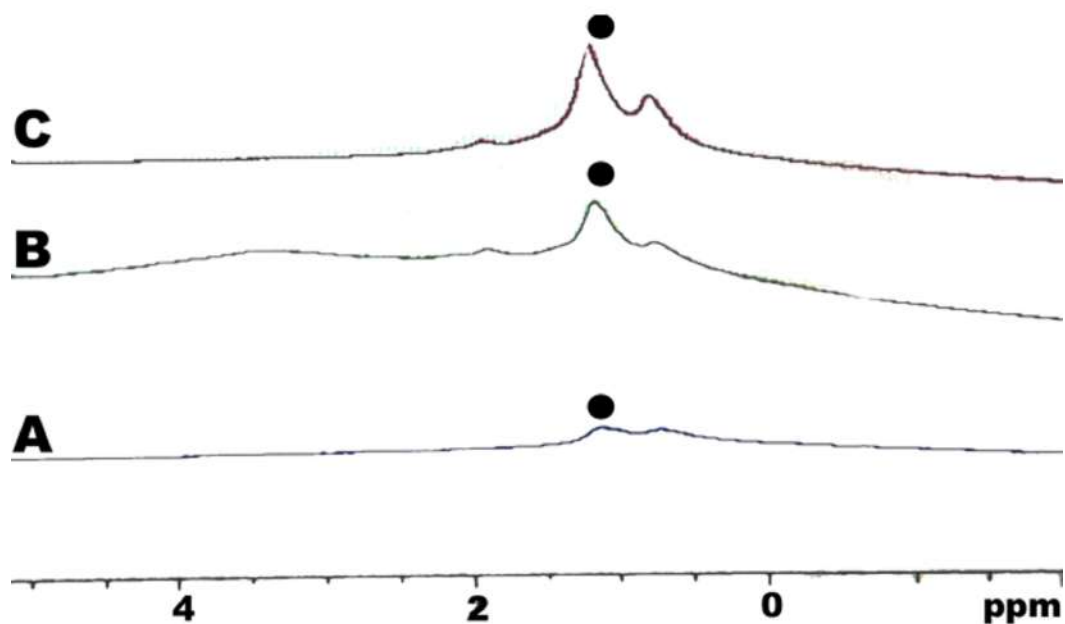


Figure 36: MAS SS-¹H-NMR spectra of *L. clavatum* SECs showing (A) the lipid-free SECs, (B) the PEGylated SECs using the 1st method and (C) the PEGylated SECs using the 2nd method. The 2nd method shows sharper peak (black dots) than the 1st method, which represent methylene groups that were added to the C4-C7 and C15-C17 of the SECs' lipids parts. The spectra were obtained at 500 MHz.

It was anticipated that the low molecular weight PEG chain, if mobile, would show a clear signal between 3.6 and 3.8 ppm due to the CH₂O groups. Even though the mPEG-tysolate was in liquid state at 33 °C, when added to the reaction mixture, the resulting PEGylated SECs showed a broad peak between 3.5 and 4.5 ppm, and the peak became more pronounced when the temperature was increased to 60 °C (see Figure 37).

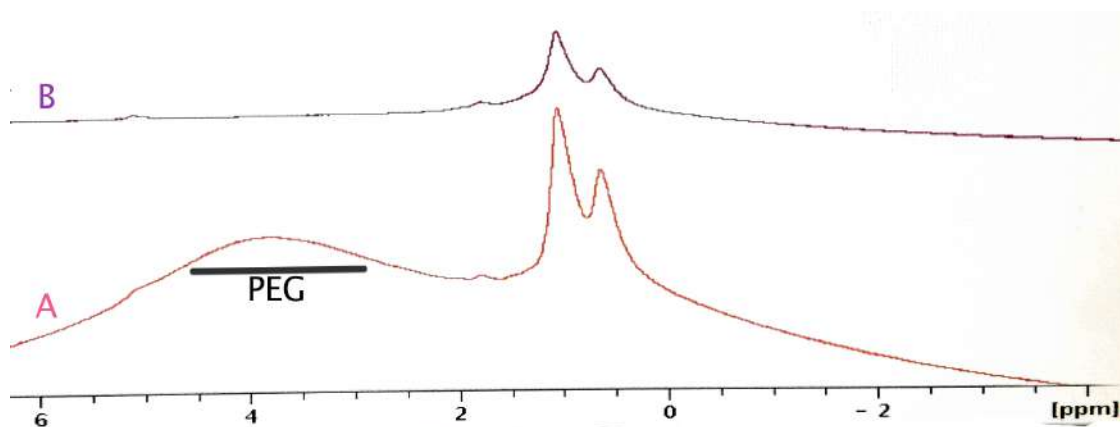


Figure 37: MAS SS-¹H-NMR spectra of PEGylated AH-SECs at 60 °C (A) showing the broad peak in the PEG region (3.5 – 4.5 ppm), compared to AH-SECs (B) where there is no detectable peak in this region. The spectra were obtained at 500 MHz.

To confirm the presence of PEG in this sample, 50 mg of PEGylated SECs and non PEGylated one (control sample) were sent to inductively coupled plasma optical emission spectrometer (ICP-OES) analysis to determine Na loading. It was anticipated that if the Na in the PEGylated sample was more than the control sample, this would indicate the presence of PEG group, because the Na ions from the NaH would attach to the core of PEG. The ICP-OES analysis result of Na/SECs was 2.7% w/w for the PEGylated sample and was 0.7% for the control sample. The Na that was found in the PEGylated sample was 4 times greater than the control sample, which indicated the presence of PEGs in the SEC sample.

The broad peak in the MAS SS-¹H-NMR spectrum indicated that the PEG group present in the SECs was in a “solid state” and did not have the same ‘dry liquid’ properties of the SEC’s natural lipids.

Chapter 4. Encapsulation and Release of Vitamin D and Actives

4.1 SECs as a Solution Buffer

Using the SECs for drug encapsulation and release needs an understanding of the behaviour of SECs towards the watery fluid of human GIT at its natural pH 7 [55]. This is because some active molecules are more readily dissolved in acidic pH, whereas the others prefer to be dissolved in a basic condition, often linked to their pK_a [95]. As all solids carry a charge (zeta potential), even if there are no ionizable groups on their surface, it was of interest to investigate the effect of different types of SECs on the pH of deionized water (neutral pH).

AH-SECs and BH-SECs of *L. clavatum* (200 mg) were added to deionized water (100 ml) and left for a period of time (1 h, 6 h and 24 h) in an orbital shaker at 120 rpm, and then the SECs-water mixture was filtered and the water pH was measured (see experimental Section 8.7).

Interestingly, the SECs of *L. clavatum* showed characteristics of a buffering agent when added to water. For example, the AH-SECs decreased the pH of deionized water from 6.80 to 5.38 when added to it after 24 hours of incubation (make the solution more acidic due to their peripheral functional groups COOH). On the other hand, when the BH-SECs were added to the water it increased the pH of the water from 6.80 to 8.15 after 24 hours of incubation. This behavior of SECs toward the deionized water indicated the need for an externally buffered solution to study the drug release for each active material in this study. Using deionized water of a given pH would mean that the SECs themselves could affect the desired pH. It should be

noted that all of the SECs (AH or BH) in this study, when first extracted, were thoroughly washed until the filtrates were neutral. The reasons behind their activity in changing the pH of a medium seems due to the weakly acidic or basic groups that the SECs possess, which makes them a natural solid buffer biomaterial. Table 15, shows the change in pH after adding AH and BH SECs to purified water as a function of time.

SECs Type	pH of pure water	pH of water after 1 h of adding SECs	After 6 h	After 24 h
AH	6.80 ±0.05	6.52 ±0.09	5.62 ±0.20	5.38 ±0.10
BH	6.80 ±0.05	6.98 ±0.04	7.63 ±0.10	8.15 ±0.11

Table 15: pH of pure water (20 ml) after addition of 200 mg of AH and BH SECs of *L. clavatum* at different incubation times. The pH measurements were run in triplicate for each type of SECs. $n = 3$.

4.2 Encapsulation and Release of Vitamin D and the Role of pH

Vitamin D₂, or ergocalciferol, is a fat-soluble vitamin that is naturally present in very few foods, added to others, and available as a dietary supplement. It is also produced endogenously when ultraviolet rays from sunlight strike the skin and trigger vitamin D₂ synthesis [96]. Vitamin D₂ promotes calcium absorption in the gut and maintains adequate serum calcium and phosphate concentrations to enable normal mineralization of bone and to prevent hypocalcemic tetany. It is also needed for bone growth and bone remodeling by osteoblasts and osteoclasts [96, 97]. Figure 38 shows the chemical structure of vitamin D₂.

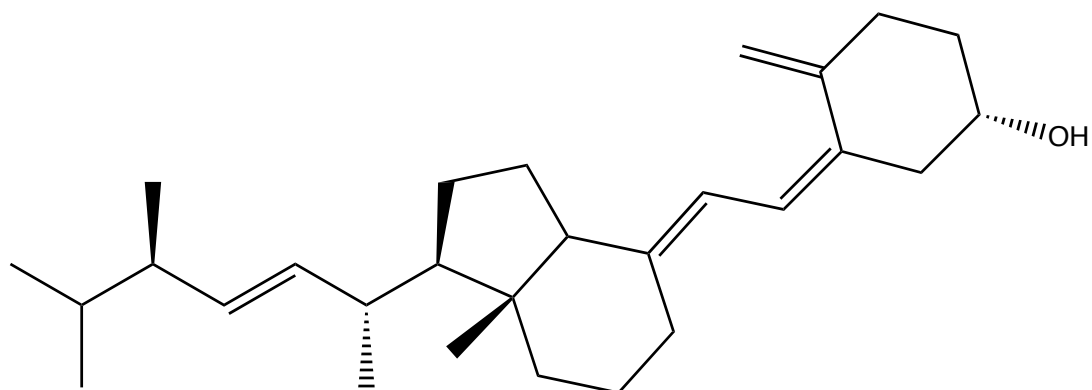


Figure 38: Vitamin D₂ (ergocalciferol) chemical structure.

Here vitamin D₂ was encapsulated in BH-AH-SECs of *L. clavatum* in order to test the SECs ability to encapsulate vitamin D₂, protect it from an acidic environment and then release it into a basic environment to mimic the various pH points of the GIT. It is important here to mention that the SECs that were used in this experiment were extracted using Protocol C (BH-AH SECs). It was envisaged that the encapsulated vitamin D₂ peaks could be analyzed by MAS SS-¹H-NMR, but this would have been an issue if they overlapped with the fatty acid chains of the SECs' own lipids. Therefore, This method (Protocol C) was chosen to avoid overlapping of SECs' lipids with vitamin D₂ lipids when using MAS SS-¹H-NMR.

Vitamin D₂ (ergocalciferol) (300 mg) was suspended in 1 ml of absolute ethanol to give final concentration of 756.33 mM, and then mixed in ultrasonic bath for two minutes until the vitamin D₂ had dissolved. The solution was added to 1 g of BHS-AHS SECs, and then mixed manually for a few minutes to ensure equal distribution. The final mixture (vitamin D₂ encapsulated SECs) was covered with kitchen foil to

protect vitamin D₂ from exposure to light, and left under vacuum overnight to evaporate the ethanol (see Section 8.8.1).

The SEM image of AH-SECs (Figure 39) shows SECs of *L. clavatum* after encapsulation of vitamin D₂ revealed it had a clean surface and there was no residue of the vitamin D around or on the surface of the SECs, i.e. most of the vitamin was encapsulated.

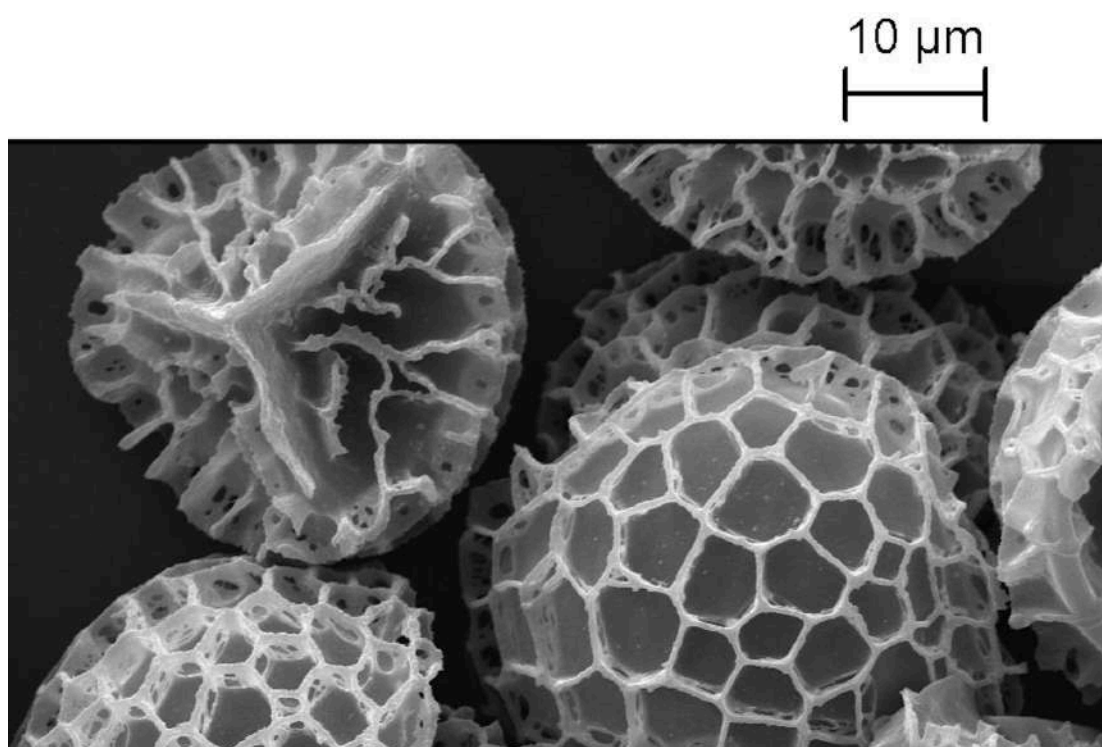


Figure 39: SECs of *L. clavatum* after encapsulation of vitamin D₂ with a loading of (0.3:1 w/w).

4.2.1 Vitamin D₂ Release and the Role of pH

After the successful encapsulation of vitamin D₂, MAS SS-¹H-NMR was used to study its release at different pHs using a cell-membrane phospholipid model based on 1,2-dioleoyl-*sn*-glycero-3-phosphocholine (DOPC). DOPC is a phosphatidylcholine that is a derivative of a phospholipid, and which is found in cell

membranes [98]. In order for any molecules to enter the bloodstream and reach their targeted organ, they need to pass-through the cell membrane and therefore they need to interact with the lipid bilayer, which acts as a natural barrier protecting the cells. [99].

The MAS SS-¹H-NMR was performed with 8 KHz speed spinning rate at 283 Kelvin temperature, $\pi/2$ pulse length and 2 seconds of relaxation delay. The spectra were collected using 16 scans for measuring the DOPC and vitamin D. For the encapsulated vitamin D₂ SECs and DOPC, the temperature was optimized to meet the normal human body temperature 37 °C, i.e. 310 K.

Firstly, DOPC (10 mg) was mixed with 10 mg of vitamin D₂ and 10 μ l of deuterium oxide (D₂O), (see experimental Section 8.8.2), and analyzed using the MAS SS-¹H-NMR, which showed a peak between 6.0-6.5 ppm (See Figure 40.a). That peak was evidence to the interaction between the DOPC and vitamin D₂, as it appeared in the vitamin D₂ and DOPC mixture spectrum, but not in the DOPC only or vitamin D₂ only spectrum. This peak was used as the reference for the next experiment of encapsulated vitamin D₂. The vitamin D₂ encapsulated SECs (10 mg) were mixed with DOPC (10 mg) in D₂O (10 μ l), (see Section 8.8.3). The MAS SS-¹H-NMR spectrum did not show any sign of the interaction between DOPC and vitamin D₂ (See Figure 40.b). At this point, the SEC suspension was tested for pH, as it was known previously (in Section 4.1) that SECs had the capability of buffering solutions. We also wanted to optimize the pH to the normal level of the small intestine where the absorption process would take place [53, 54]. It was found that the BHS-AHS SECs changed the pH of the D₂O from neutral to acidic (from 7.4 to

4.2). After that, 0.01 mM phosphate buffer powder (9.7 ml) was added to D₂O (10 ml) in order to rebalance the pH to 7.4 and that was confirmed using the pH meter.

The encapsulated vitamin D₂ SECs (10 mg) were mixed again with DOPC (10 mg) in the new pH 7.4 buffered D₂O solution (10 μl), and the MAS SS-¹H-NMR spectrum was collected. This spectrum now showed the same peaks at the same chemical shift (6.0-6.5 ppm) revealing the interaction between DOPC and vitamin D₂ (See Figure 40.c). Therefore, this experiment confirmed the release of vitamin D₂ from the SECs interior to the NMR rotor and mixed with DOPC.

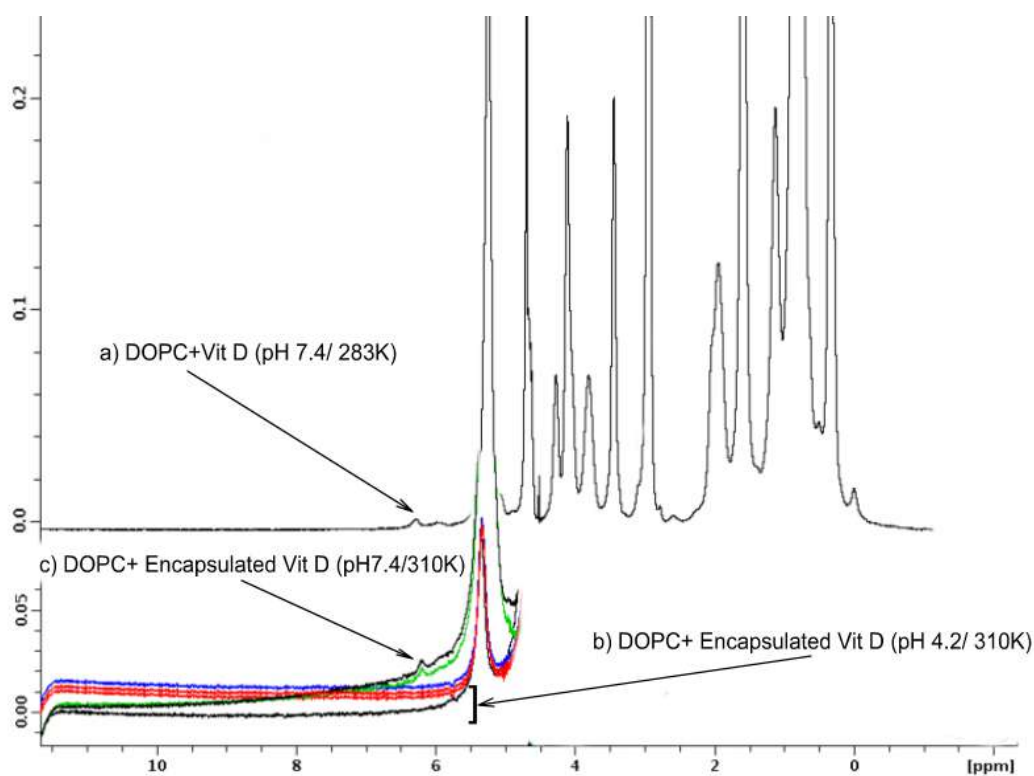


Figure 40: MAS SS-¹H-NMR spectra of (a) DOPC and vitamin D₂ interaction shown in 6.0-6.5 ppm. (b) Vitamin D₂ encapsulated SECs did not release vitamin D₂ and there was no sign of interaction between vitamin D₂ and DOPC. (c) Vitamin D₂ encapsulated SECs released vitamin D₂ and interacted with DOPC shown between 6.0-6.5 ppm. The spectra were obtained at 500 MHz.

Fascinatingly, it was clear from this experiment the direct effect of pH on the release of the SECs' contents. Moreover, this was an interesting point, especially, for protecting the encapsulated vitamin D₂ from the harsh acidic environment of stomach (pH 1-2). Thus, the encapsulated vitamin could reach the small intestine and released in the relatively basic environment of small intestine (pH 6-8).

4.3 Other Drugs Encapsulation and Release (the role of pH)

4.3.1 Diclofenac sodium salt

Diclofenac is a well-known non-steroidal anti-inflammatory drug (NSAID) with anti-inflammatory, analgesic and antipyretic properties, comparable or superior to other NSAIDs [100, 101]. The sodium salt of diclofenac is mainly used in the treatment of osteoarthritis and rheumatoid arthritis. [102,103]. Figure 41 shows the chemical structure of diclofenac sodium salt.

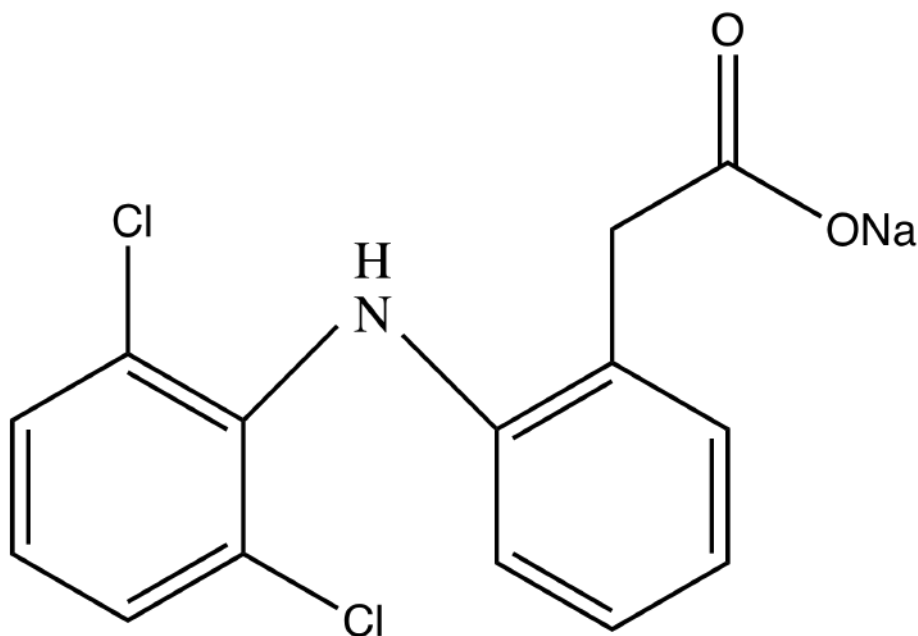


Figure 41: Diclofenac sodium salt chemical structure.

Results and Discussion

Diclofenac sodium salt was encapsulated by SECs of *L. clavatum* as described in (Section 8.8.4.1). Briefly, diclofenac sodium salt (450 mg) was added to ethanol (1 ml) to give 1414.51 mM final concentration. The diclofenac solution was added to 1 g of AH-SECs and mixed manually with a spatula for 1 minute to obtain a homogenous mixture. The mixture was dried in a vacuum desiccator overnight until constant weight.

Figure 42 shows the AH-SECs of *L. clavatum* after diclofenac sodium salt encapsulation and as can be seen the surface of the SECs shows no drug crystals around or on the surface of the SECs. This indicates that the drug was encapsulated successfully inside the SECs.

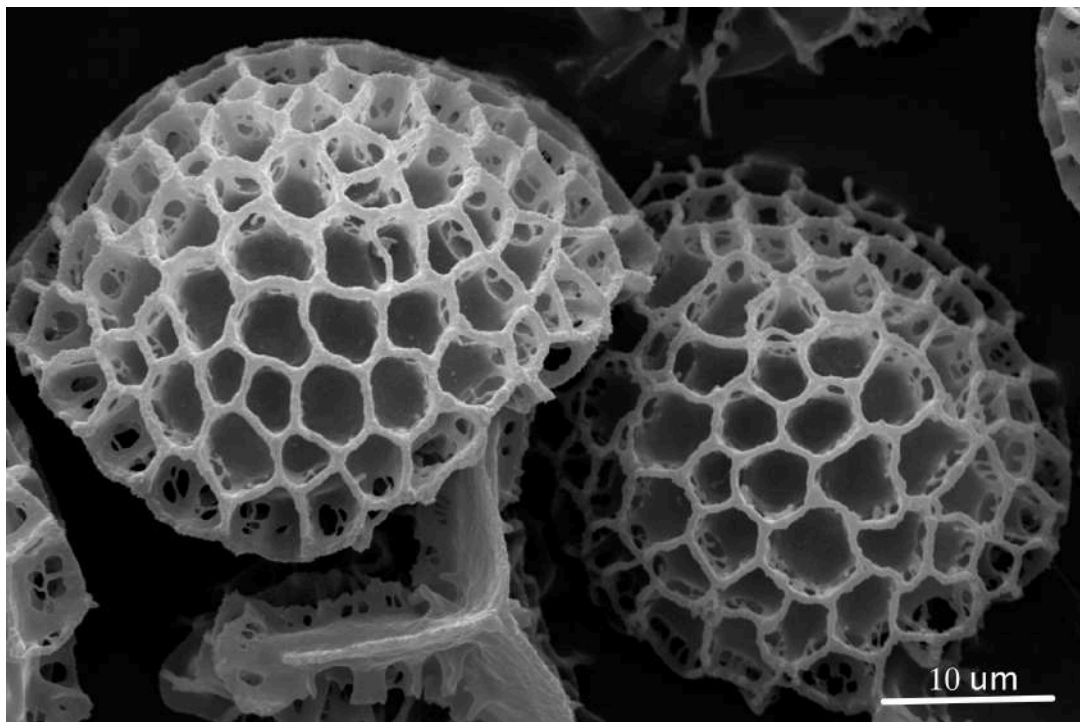


Figure 42: *L. clavatum* SECs after encapsulation of diclofenac sodium salt with a loading of (0.45:1 w/w).

Results and Discussion

After the encapsulation of diclofenac sodium salt, the next aim was to study the release of the drug into a range of buffered solutions at different pHs. It was thought that the easiest way to do this was to filter the SEC suspensions at different times, collect the filtrate and then assay the drug by UV-Vis analysis using a standard calibration curve. Thus, the filled SECs (10 mg containing 3 mg of active) were left for a period of time agitated in a buffered solution (6 ml) of different pH (pH 1.5 to mimic stomach gastric fluid, pH 7.4 to mimic intestinal fluid and pH 9 to compare the release in higher pH at room temperature (see Section 8.8.4.3). Figure 43 shows the percentage of diclofenac released in these buffered solutions.

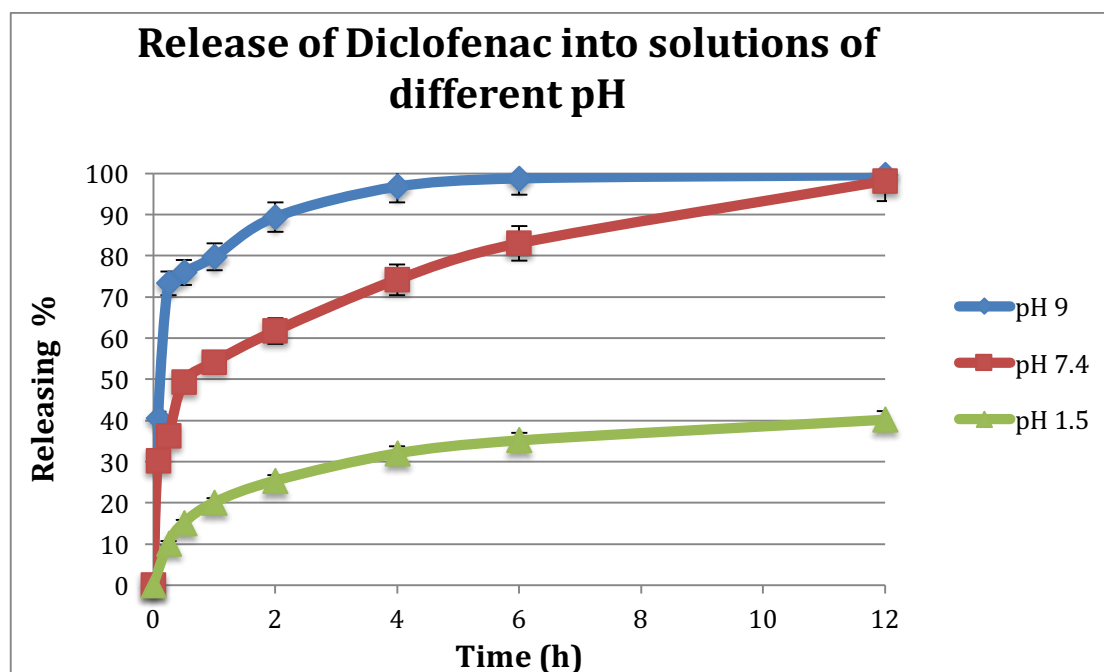


Figure 43: Release of diclofenac sodium salt from AH-SECs of *L. clavatum* into buffered solutions by time at different pH. $n = 3$.

Results and Discussion

At pH 1.5, 40 % of the diclofenac sodium was released into the buffer solution over 12 hours. However, when the pH of the solution was raised to 7.4 and 9 the SECs started to release their full contents into the buffer solution in 12 hours. This is understandable as diclofenac sodium salt is a weakly acidic drug with a pK_a around 4.9. Its carboxylic acid group will be protonated easily at a $pH < 5$, but be largely ionized above this pH. The ionic form of the drug will naturally be more water soluble than the unionized form (the solubility of diclofenac sodium salt is 6 mg/ml, whereas the free acid solubility is 1.4 mg/ml in pH 7.4 buffer) [104]. At pH 7 the SECs needed 12 hours to fully release the diclofenac sodium, whereas in pH 9 the SECs released its contents fully in 6 hours. These results suggested that SECs could retain around 75-80 % of diclofenac in the first 2 hours in the acidic pH of the stomach, and release this percentage into the basic pH of the small intestine, where the absorption would take place. Table 16, shows the incubation time of SECs in the buffer solutions and the percentage of diclofenac release.

pH	Release % after 2 h	Release % after 6 h	Release % after 12 h
9	89.4 \pm 4.0	98.8 \pm 0.3	99.6 \pm 0.4
7	61.7 \pm 0.2	83.0 \pm 0.5	98.0 \pm 2.0
1.5	25.4 \pm 0.6	35.2 \pm 2.0	40.3 \pm 2.5

Table 16: Diclofenac sodium salt release from SECs in solutions of different pH. $n=3$.

These findings were similar to a study which was done using commercially available sustained controlled release tablets of diclofenac [105]. Therefore the natural, renewable and relatively cheap SECs could replace the conventional enteric coated

Results and Discussion

tablets and microcapsules for drug controlled release, especially they have the carboxylic acid functional groups that is favored when choosing a drug carrier.

To study the effect of solubility and ionization state of the encapsulated therapeutics in drug release, the free acid form of diclofenac was encapsulated and released in different buffers to compare with the salt form. Figure 44 shows the free acid form of diclofenac released from AH-SECs of *L. clavatum* in comparison to the salt form, which indicates that the solubility and ionization of the encapsulated therapeutics is a vital factor in drug release. For example, the salt form of diclofenac release was greater than the acid form in each pH point, and even the salt form release at pH 7.4 was greater than the acid form at pH 9 point. The diclofenac free acid might have changed into salt when the pH is raised and that might helped the acid to released in pH 7.4 and pH 9.

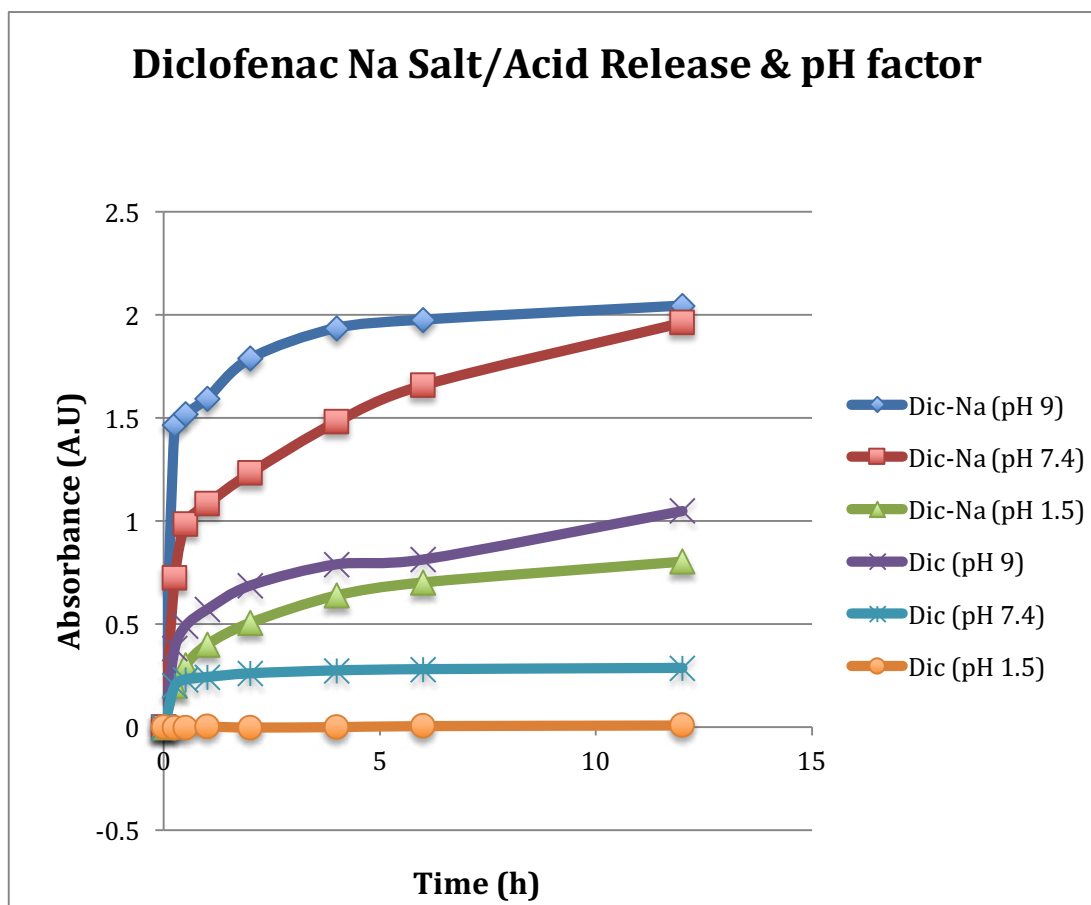


Figure 44: Release of free acid (Dic) and salt (Dic-Na) form of diclofenac from AH-SECs of *L. clavatum* into buffered solutions by time at different pH. $n = 3$.

4.3.1.1 The Controlled Release of Diclofenac sodium

During the study of diclofenac release discussed in the above (Section 4.3.1), it was found that the SECs showed an interesting feature of controlled drug release. The mechanism of release from the SECs was found to be very sensitive to the concentration of drugs in the dissolution medium. For example, when 10 mg of SECs containing 3 mg of diclofenac sodium salt was placed in 1 ml buffer of pH 9, only 15-17 % was released, in comparison to the previous experiment where a full release

of diclofenac sodium salt was achieved when the same amount of SECs and drug was placed in 6 ml of buffered medium. This indicates that the SECs will release a maximum of 0.5 mg of drug in 1 ml of buffered medium, and when the concentration of the drug decreased in the buffered medium the SECs will release the rest of their content of the drug. This process continues until the SECs release all its contents of the therapeutics.

Figure 45, shows the results obtained which support this release mechanism hypothesis. It is believed that release is related to the SECs behavior and not simply the solubility of the drug. For example, the solubility of diclofenac sodium is 6 mg/ml in the buffer, and the 10 mg of SECs contains only 3 mg of diclofenac, so even if the SECs contains 6 mg of diclofenac sodium they should release it fully in 1 ml of the buffer. However, it was found that SECs released 15-20 % of their contents of drug and retained 80-85 % of drug until the surround concentration decreased, and then the next dose was released, or if in sufficient volume of fluid, e.g. in GIT fluid, the SECs will fully release its contents (at least 1 ml of dissolution medium for 0.5 mg of diclofenac). In comparison, a study reported in the literature used 60 ml of dissolution medium to release 3 mg of diclofenac [106]. This study used a larger volume for drug release as the GIT fluid continues to secrete and in addition to the fluid that patient consumes during the ingestion and dissolution of the tablets containing the actives.

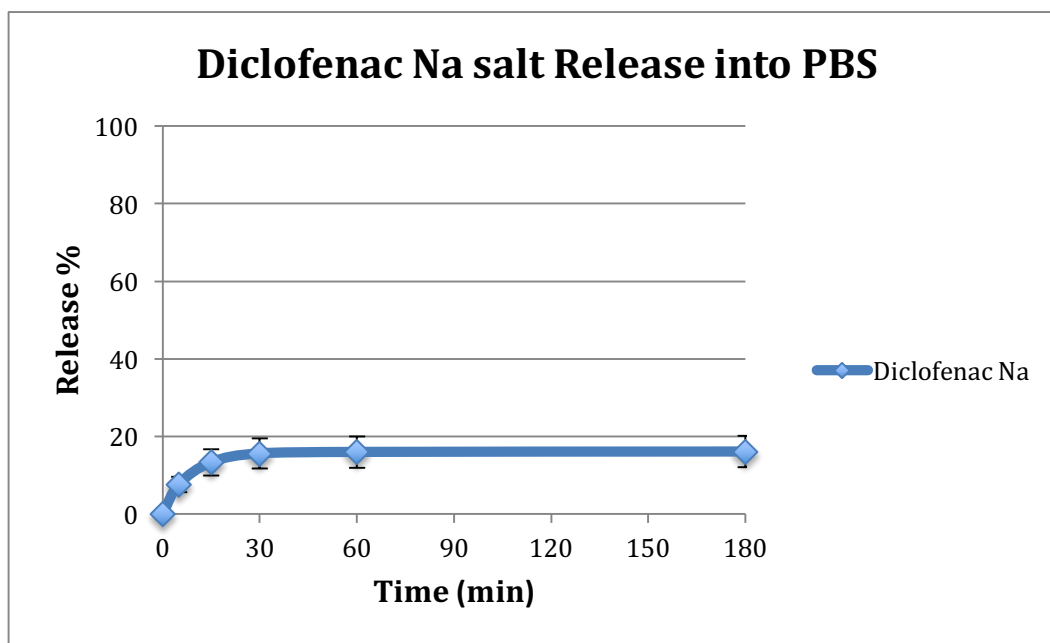


Figure 45: Release of diclofenac Na from AH-SECs of *L. clavatum* into PBS (pH 7.4) over time. 10 mg of SECs (containing 3 mg of diclofenac) was allowed to release its content in 1 ml of PBS at room temperature over time. $n = 3$.

4.3.1.2 Comparison of Diclofenac Na Release with Different SECs species

As stated earlier (in Section 1.6) almost extracted exines from spores and pollens of different plant species have a similar chemical structure to each other, even though they differ in their morphology. Therefore, it was of interest to try another species of pollen for releasing the diclofenac sodium salt and to compare it to the SECs of *L. clavatum* spore. *H. annuus* (sunflower) pollen SECs were chosen since they differ markedly in their morphology. Also, *H. annuus* have a larger pore that might help to release the drug more rapidly. Figure 46 shows the SEM images of *H. annuus* AH-SECs and their larger pores.

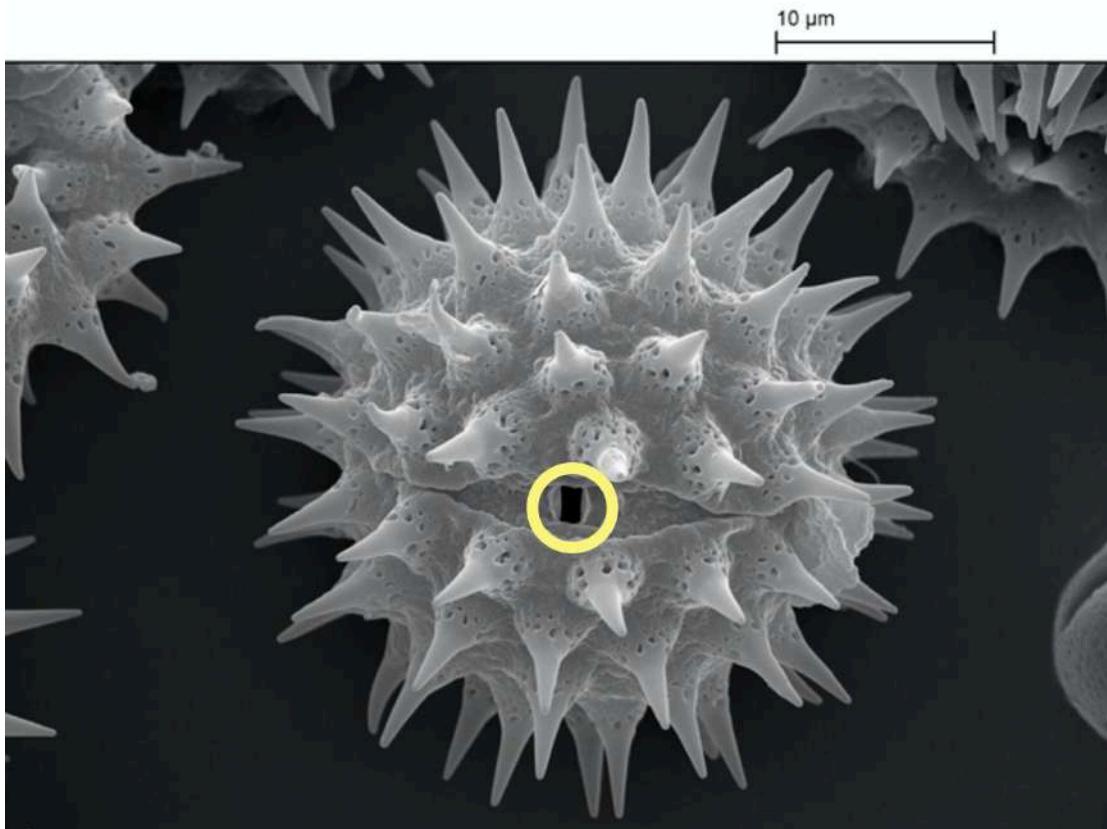


Figure 46: SEM image of *H. annuus* AH-SECs showing their relatively large pore (yellow circle).

Figure 47, shows the diclofenac sodium release from AH-SECs of *L. clavatum* and *H. annuus*. From the graph and the spread of error bars it seems there is no difference between the *L. clavatum* and the *H. annuus* AH-SECs, as both of them released the same amount of diclofenac in the same period of incubation time and same pH 7.4.

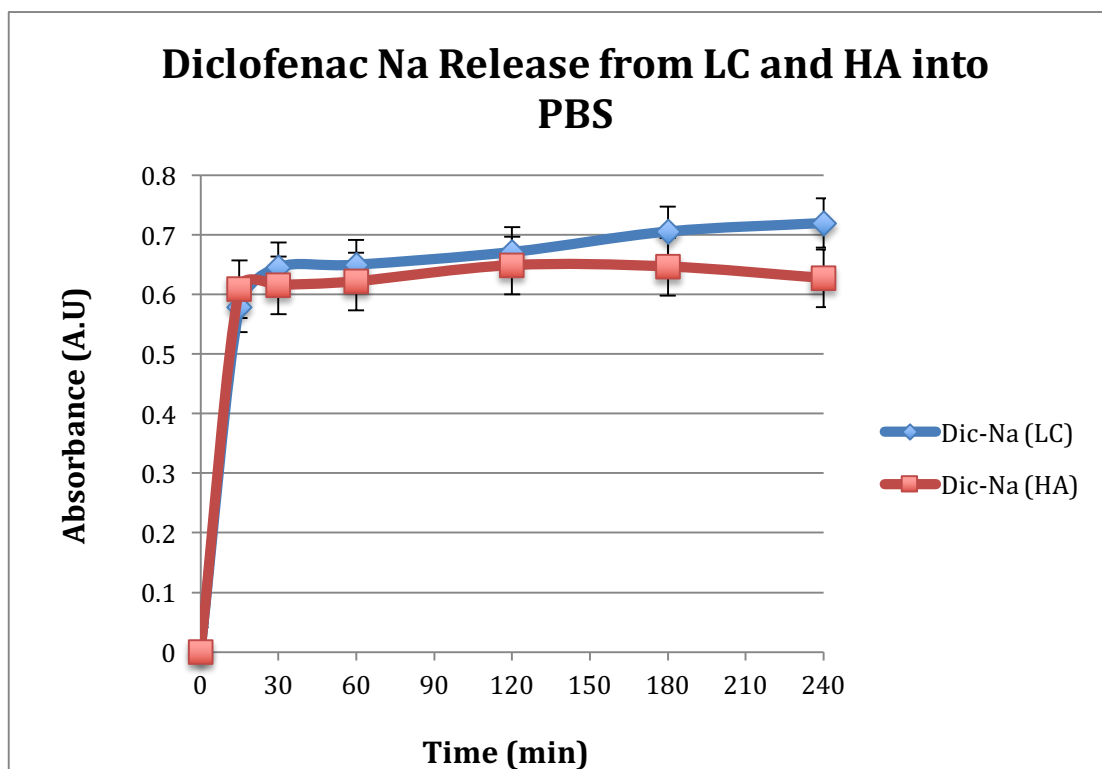


Figure 47: Release of diclofenac sodium salt form AH-SECs of *L. clavatum* (LC) and *H. annuus* (HA) into PBS pH 7.4 by time. $n = 3$.

4.3.1.3 Adsorption of Diclofenac sodium salt on SECs

One of the applications for sporopollenin SECs is in water treatment and cleaning [107], as the hydrophobic chemical structure of SECs makes them attract other chemicals such as hydrocarbon pollutants that contaminate water. This indicates that a small percentage of an encapsulated drug may stick to the SECs and retained. Therefore, it was considered important to quantify the amount of drug that can be adsorbed “irreversibly” to the SECs’ surface in these conditions in order to fully evaluate the application of SECs as drug carrier. This would enable the quantification

of wasted / unreleased drug and also the minimum level of loading that would be feasible.

In this experiment, diclofenac sodium salt aqueous solution (5 mg/L) (0.016 mM) was added to empty SECs in order to observe the “stickiness” of the drug to the SECs (see Section 8.9). After 20 minutes of agitation at 240 rpm at room temperature, the drug-SECs mixture was filtered using 0.22 μm centrifugal micro-tubes. The filtrate was then analyzed by UV-Vis spectroscopy over the range 200-350 nm and the adsorbed concentration of diclofenac sodium was calculated using a standard calibration curve. In another, follow-on experiment the same batch of SECs was recycled five times using new diclofenac sodium solution each time. Figure 48, shows the diclofenac Na percentage that was adsorbed in each cycle of adding 1 ml of diclofenac solution using the UV-Vis spectroscopy.

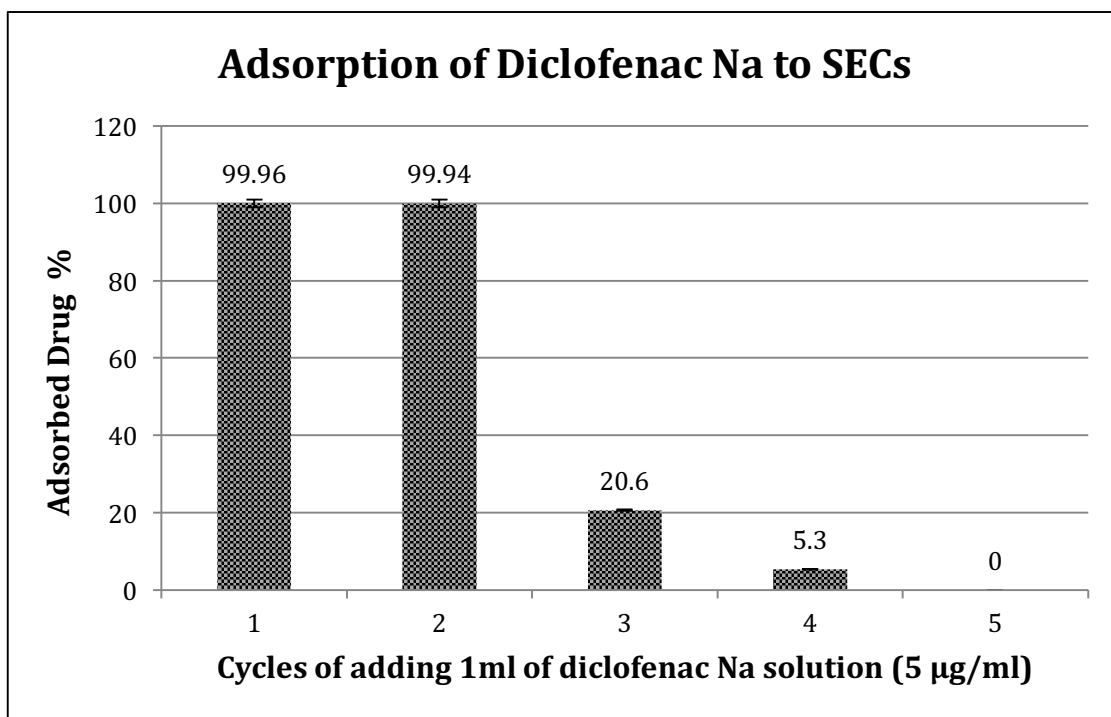


Figure 48: Showing the ability of SECs of *L. clavatum* to extract diclofenac sodium salt from a water solution. Each run contained 10 mg of SECs in 1 ml of diclofenac solution (5 µg/ml) at the naturally buffered pH of the AH-SECs. $n = 3$.

The first cycle of removing diclofenac by adsorption to the SECs' surface was nearly 100 %. The "loaded" SECs from the first cycle were then added to fresh drug-water solution in order to test the SECs' adsorption (as opposed to encapsulation) capacity. Upon recycling the SECs for the second time was shown that they still had the capacity to soak-up more drugs from the aqueous solution, and could still efficiently adsorb nearly 100 % of the drug. Table 17 shows the amount of drug that was removed from the solution.

Results and Discussion

Aliquot of diclofenac Na salt solution added (5 $\mu\text{g}/\text{ml}$)	Mass of diclofenac Na salt adsorbed to SECs (μg)	% Adsorbed for each ml aliquot
1	4.985 \pm 0.015	99.960 \pm 0.040
2	4.984 \pm 0.012	99.940 \pm 0.030
3	1.030 \pm 0.034	20.600 \pm 0.090
4	0.265 \pm 0.056	5.300 \pm 0.150
5	0.000 \pm 0.000	0.000 \pm 0.000

Table 17: Illustrates the amount of diclofenac adsorbed by one sample of *L. clavatum* AH-SECs (10 mg) from five 1 ml aliquots of a diclofenac sodium salt (5 $\mu\text{g}/\text{ml}$). $n=3$.

The total cumulative mass of the adsorbed diclofenac sodium salt was 11.264 μg out of 25 μg , which was the total cumulative mass of diclofenac sodium that was added to the SECs (10 mg) in the five cycles (total cumulative volume 5 ml). This amount of adsorbed drug is very small compared to the 3 mg of diclofenac, which was encapsulated in the same weight of SECs (10 mg) in the release studies that were described in the previous (Section 4.3.1). The adsorbed amount of diclofenac sodium is less than 0.4 % of diclofenac sodium salt used for encapsulation and release, i.e. the adsorption capacity of diclofenac sodium for AH-SECs of *L. clavatum* is less than 0.4 %, therefore, more than 99.6 % of diclofenac sodium would be released freely and would not stick or adsorbed to the SECs' surface.

4.3.2 Mesalamine

Mesalamine, or 5-amino salicylic acid, is an anti-inflammatory drug structurally related to the salicylates [108, 109]. It is used mainly for ulcerative colitis and metabolized in the gut [110, 111]. Figure 49 shows the chemical structure of mesalamine.

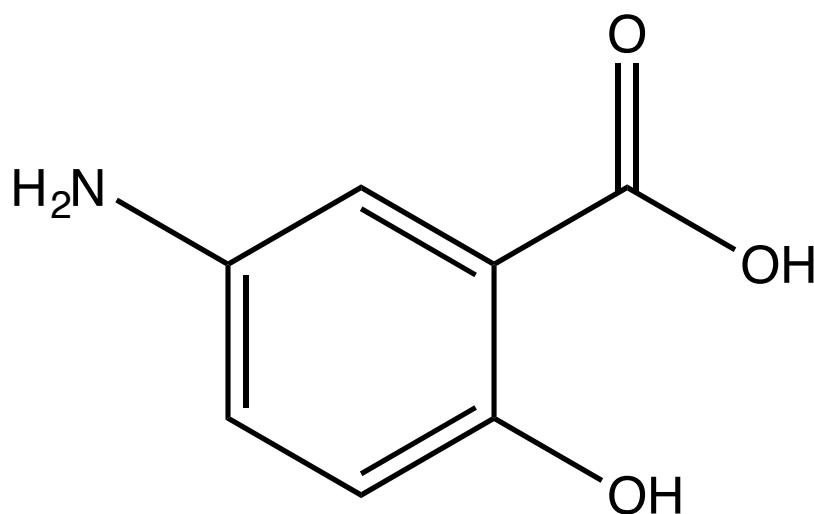


Figure 49: The structure of mesalamine, showing the basic amino group and acidic carboxylic group that it possesses.

Mesalamine (53 mg) was dissolved in 1 M HCl (1 ml) to give a final concentration of 346.09 mM. the solution was added to 1 g of AH-SECs of *L. clavatum* and mixed manually with a spatula for 1 minute to obtain a homogenous mixture. The mixture was left in vacuum desiccator overnight and dried to a constant weight to produce AH-SECs of mesalamine (see Section 8.8.4.2). Figure 50 shows the SEM images of *L. clavatum* SECs after mesalamine encapsulation, and as can be seen the surface of the SECs shows no drug crystals around or on the surface of the SECs. This indicates that the drug encapsulated successfully inside the SECs.

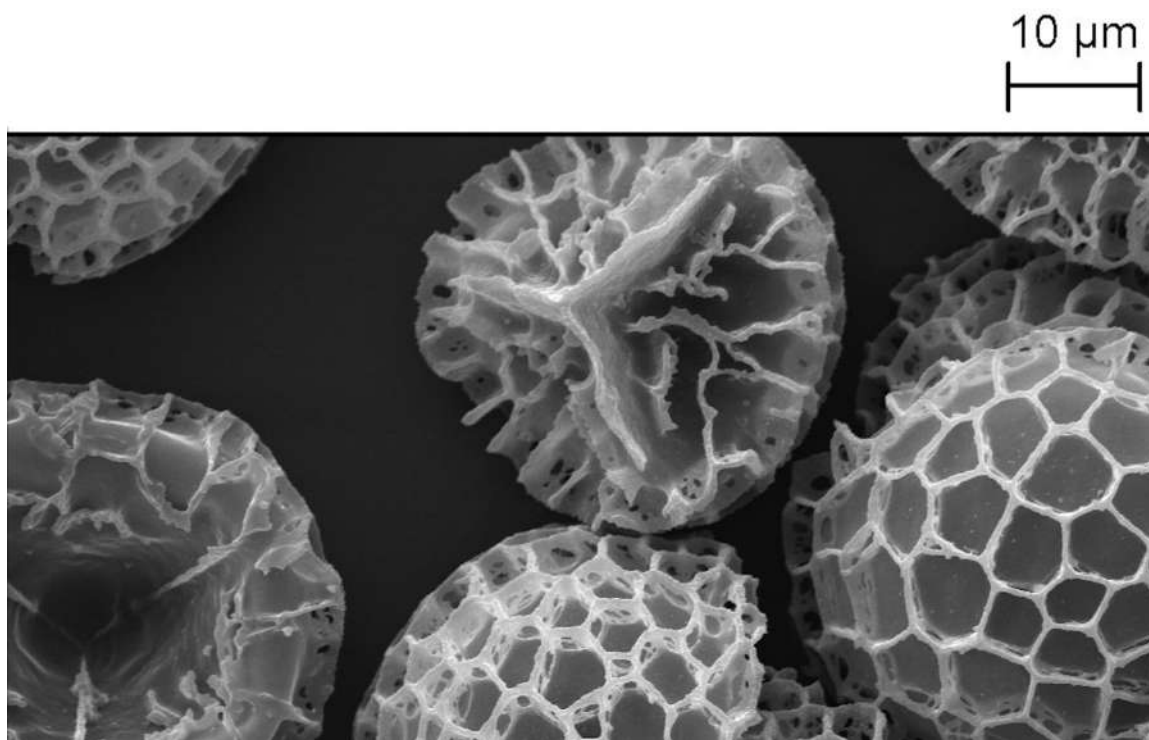


Figure 50: SEM images of *L. clavatum* AH-SECs after encapsulating mesalamine with a loading of (0.05:1 w/w).

After confirmation of mesalamine encapsulation, the same types of release experiments were conducted as described for diclofenac. Thus, the mesalamine filled SECs (10 mg of SECs containing 500 μg of mesalamine) were left for a period of time, agitated in a buffer solution of different pH (pH 1.5 to mimic stomach gastric fluid, pH 7.4 to mimic intestinal fluid and pH 9 to compare the release at higher pH) at room temperature (see Section 8.8.4.3). Figure 51 shows the percentage release of mesalamine in these buffer solutions.

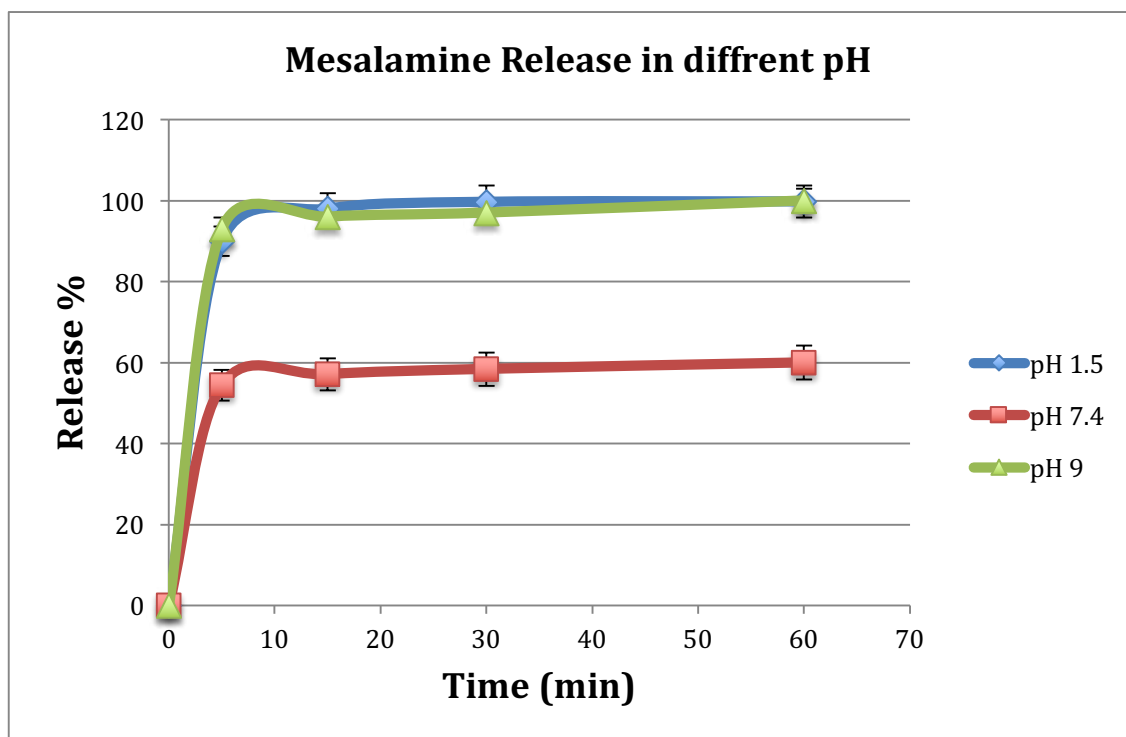


Figure 51: Mesalamine release from AH-SECs of *L. clavatum* (10 mg of SECs containing 500 µg of mesalamine) into buffer solution (1 ml) by time at different pHs. $n = 3$.

In the acidic (pH 1.5) and basic (pH 9) solutions, there was a full release of all of mesalamine within 60 minutes. In the first 5 minutes there was an immediate release of 93 % of mesalamine in pH 9 and 90 % in pH 1.5. However, in the neutral pH 7.4 the initial release in the first 5 minutes was less than 55% and reached 60% within 60 minutes.

Table 18, shows the incubation time of SECs in the buffer solutions and the mesalamine release percentage.

pH	Release % after 30 min	Release % after 60 min
1.5	99.7 ±0.4	99.8 ±0.1
7	58.4 ±2.5	60.0 ±3.3
9	97.0 ±2.1	99.9 ±0.2

Table 18: Mesalamine release % from AH-SECs of *L. clavatum* (10 mg of SECs contains 500 µg of mesalamine) into 1 ml buffer solution by time at different pHs. *n*=3.

This release profile can be explained by considering the functional groups on the mesalamine. It possesses both acidic and basic groups, one of which will be ionized under both low and high pH conditions. The ionized form of the drug is expected to be more water soluble and thus released easily from the SECs' cavity. Taking this observation to a clinical setting, it would mean that most of the mesalamine would be released in the stomach within an hour before it can reach the intestine. Therefore without a co-encapsulant or coating on the SECs (providing a protecting layer), this system could not be used to keep the mesalamine inside the SECs' cavity until it reaches the targeted organ in the GIT and that is mean the in the market formulation of mesalamine capsules are superior in retained most of the mesalamine in the low pH 1.5 [112], as the mesalamine release percentage in these industrial formulations was ranging from 1-20 % in pH 1.5.

Chapter 5. Mucoadhesion Studies of SECs

SECs have a promising future in drug delivery applications. SECs as microcapsules have been used as drug [73] and MRI contrast agent [21] carrier. Also, they can encapsulate living cell [76]. Their biodegradability and non-toxicity has inspired many scientists to use them in pharmaceutical and food industries as described previously (in Section 2.4). There is evidence that mucoadhesion could play a role in the mechanism by which SECs can be used in targeted drug delivery, and allow slow drug release, as SECs have been found in contact with the villi of small intestine of mice [49] following oral ingestion. However, the mucoadhesion properties of SECs have not been studied before the writing of this thesis. Mucoadhesion is another way for targeted drug delivery, which is used in delivering various drugs due to its effective slow drug release (Section 2.4.6.1). The interaction between various mucoadhesive polymers and mucus is related to the physical entanglement and the secondary bond formation, mainly, hydrogen bonds and van der Waals attractions and it is related to the chemical structure of the bioadhesive polymers [113], as discussed before (in Section 2.4.6.1.1).

Generally, a suitable bioadhesive polymer has functional groups (such as carboxyl, hydroxyl, amine and amide) that contribute in mucoadhesion [114]. SECs are known to have hydroxyl and carboxyl functions; therefore, their mucoadhesion ability was investigated. There are different mucoadhesive polymers that are used in drug delivery systems, for example carbopol and chitosan. Carbopol 934, is an anionic poly-acrylic acid cross linked by allyl-sucrose polymer. It is commonly used in

mucoadhesion drug delivery due to its ability to exhibit strong hydrogen bonding with mucin present in mucosa, and its properties of biocompatibility and biodegradability [115, 116]. On the other hand, chitosan is a cationic mucoadhesive polymer. It has also been widely used to develop a mucoadhesive polymer, due to its biocompatibility and biodegradability [117], and its strong interaction with the negatively charged mucin chains [118]. Therefore, SECs' mucoadhesion properties were evaluated and compared to these commercial polymers. Figure 15 (Section 2.4.5.1.2) shows the chemical structure of chitosan and poly-acrylic acid.

5.1 Evaluation the Interaction between Mucin and SECs using Differential Scanning Calorimetry (DSC)

One of the common methods used to study mucoadhesion in the early stages of an investigation is to determine if there is an interaction between the mucin and the polymer chains in a material. Differential scanning calorimetry (DSC) is a well-established method used to show interaction between mucin and a mucoadhesive polymer [119]. Simply, the DSC compares the temperatures involved in heating samples against a reference at a linear increase of temperature [120]. The thermal behavior of mucin, test polymer individually, and both together are normally compared. The differences in thermal behaviour between the pure samples and the mixture can indicate if there is some cross-linking and interaction between the mucin and peripheral chains on a test material.

Firstly, mucin powder was analyzed as received in its commercial form, and then it was hydrated with pure water to obtain a 5% mucin solution (5 g mucin / 95 ml

water), and then freeze-dried (24 hours) to obtain solid mucin for DSC test. This to ensure that the mucin had the same environment when mixed with SECs. This because it will be in a solution form rather than solid powder to mimic the mucous of GIT, and it facilitate the adhesion between the SECs and the mucin. The freeze-dried mucin was used as a reference sample, to compare the mixture of mucin and SECs (mucin-SECs) samples.

Mixing the hydrated mucin with SECs was done by adding 50 μ l of 5% mucin to 10 mg of SECs of *L. clavatum* and *A. artemisifolia* respectively. The mixture was treated for 2 hours at 37 °C in an orbital shaker at 120 rpm. The mixture was freeze-dried later to have a dry powder of mucin-SECs mixture, as the DSC analyzes samples in solid form rather than liquid. The DSC was performed with cooling of 3 mg of sample in aluminum pan from room temperature to 0 °C, then heating it to 300 °C at 20 °C/min. Figures 52 and 53 show the DSC thermogram of the mucin sample as it was received and after hydration then lyophilization, respectively. At 217 °C there was an endothermic peak for the commercial form of mucin (Figure 52) which represents the melting of mucin. The endothermic peak at 125 °C simply represents the water removal.

After hydration and lyophilization of mucin, the endothermic peak was split into many peaks and the highest intensity peak was around 153 °C (see Figure 53). The reason behind these changes in the peak characteristics of freeze-dried mucin could be due to the rehydration and then lyophilization of mucin [121], which can change the inter- and intra-chains bonds of mucin, and then alter the thermal properties of the sample.

Results and Discussion

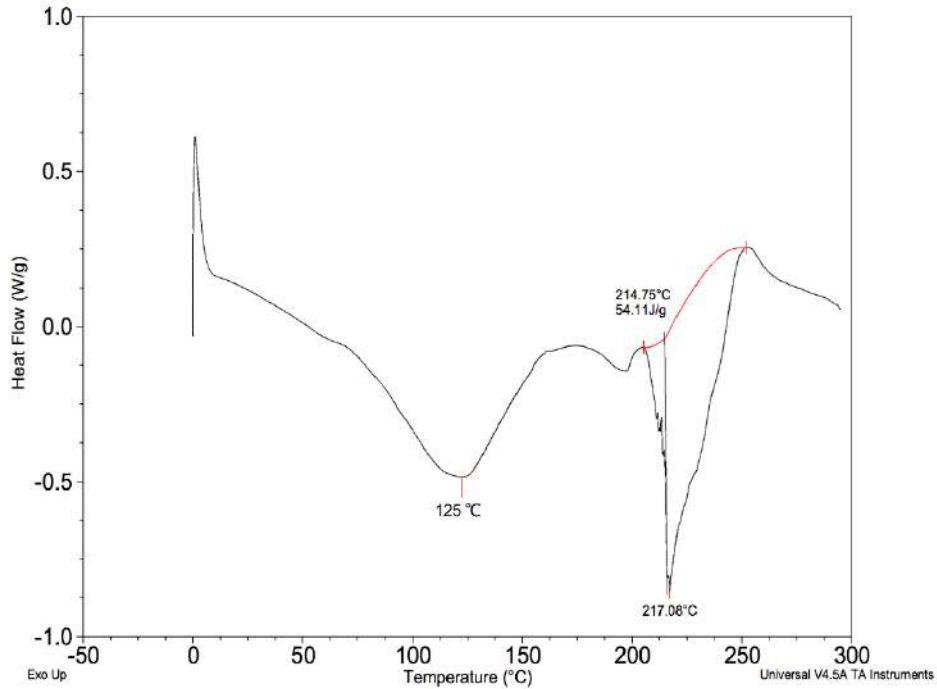


Figure 52: A DSC thermogram of mucin as received shows an endothermic peak around 217 °C (54.11 J/g) representing mucin melting. The endothermic peak at 125 °C simply represents the water removal.

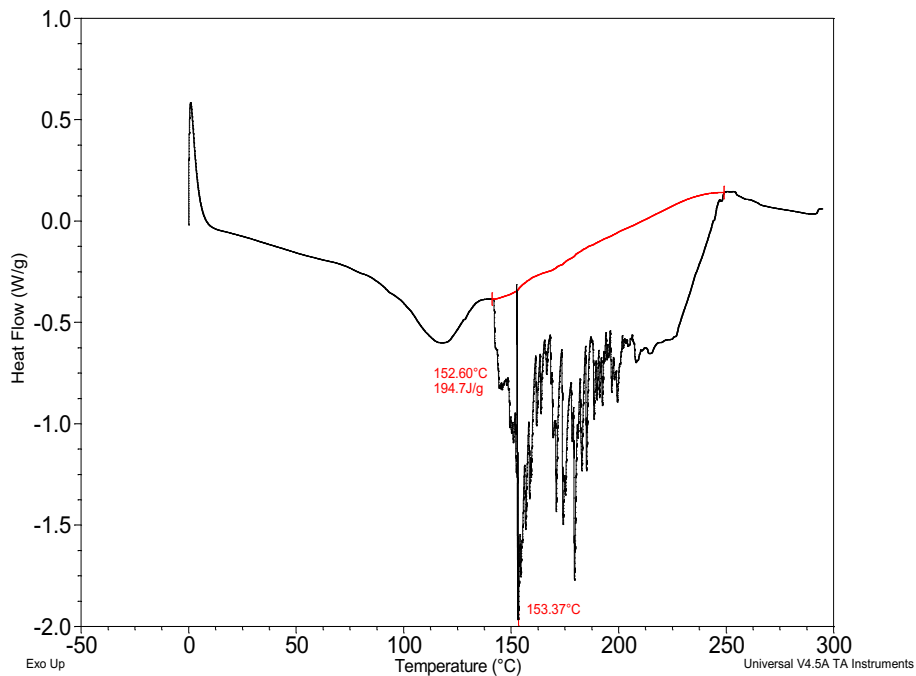


Figure 53: A DSC thermogram of freeze-dried mucin showing that the peaks were spread into many small peaks between 145-230 °C, but with a main peak around 153 °C.

Results and Discussion

After analyzing the mucin samples (powder as received and after rehydration then freeze-drying) by DSC, the *A. artemisifolia* AH-SECs were similarly analyzed by DSC before and after freeze-drying (Figures 54 and 55 respectively) to observe any changes in their thermal behavior before mixing with mucin. The Figures 54 and 55 show no difference in thermograms of the SECs before and after freeze-drying. The endothermic peak at 275 °C represents the water loss from the framework of the SECs at this high temperature.

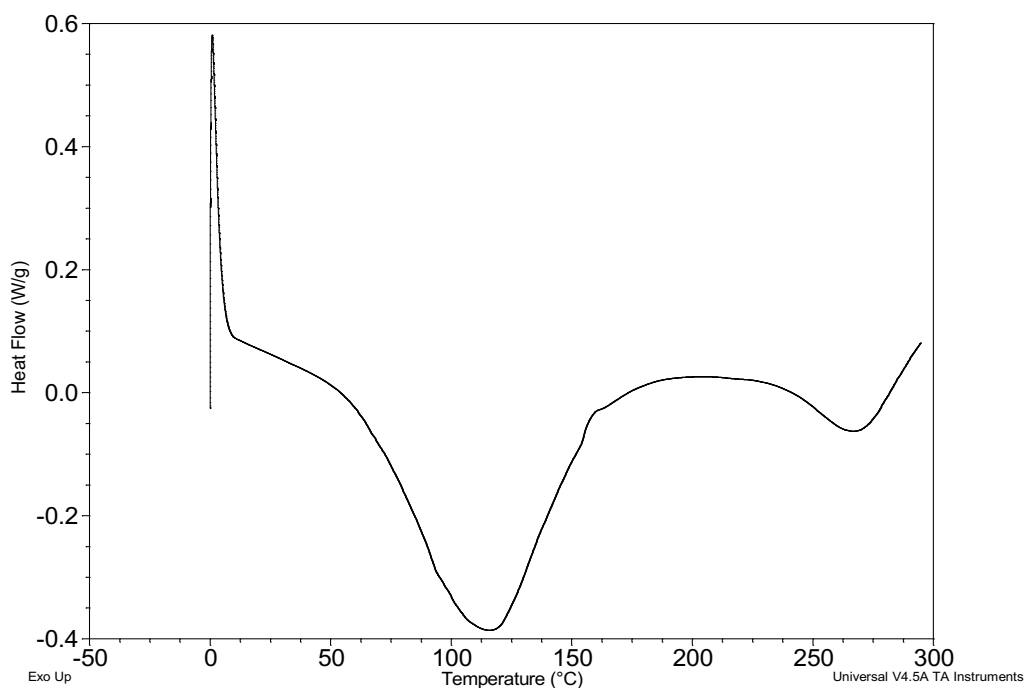


Figure 54: A DSC thermogram of AH-SECs of *A. artemisifolia*. An endothermic peak can be observed around 110 °C indicating dehydration of the pollen and peak at 275 °C represents the water loss from the framework of the SECs at this high temperature.

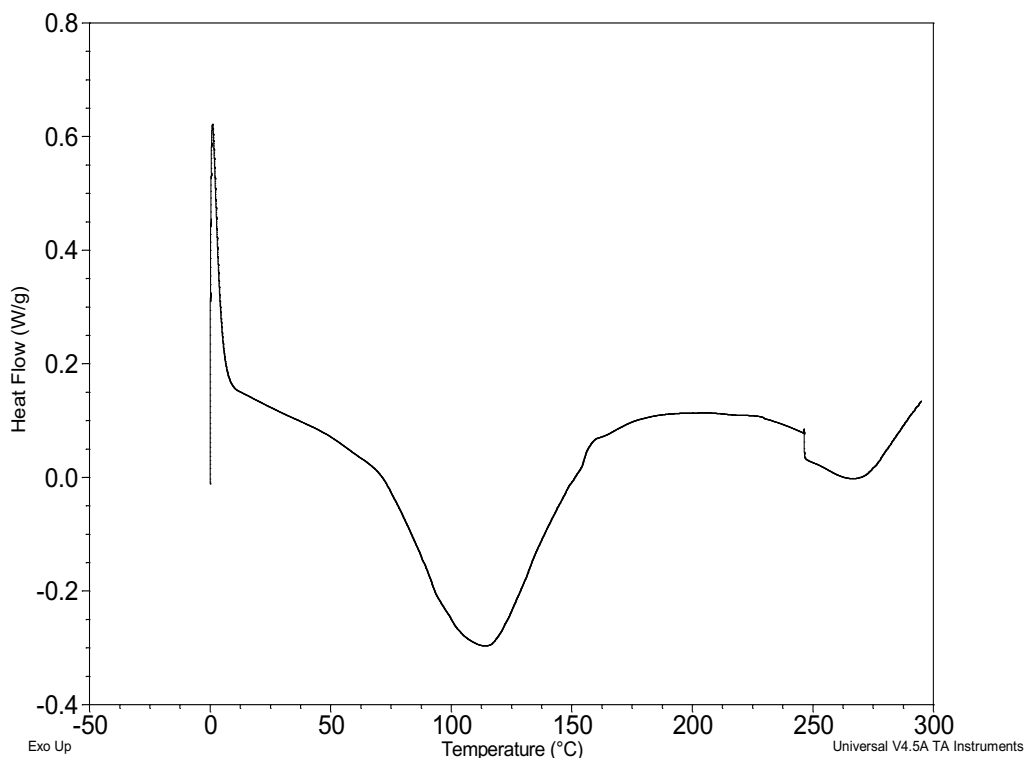


Figure 55: A DSC thermogram of freeze-dried *A. artemisifolia* showing the same behaviour as the non freeze-dried sample shown in Figure 53.

When mucin solution was mixed with the AH-SECs of *A. artemisifolia* and freeze-dried, the sharp peaks of mucin disappeared from the thermogram (Figure 56). Instead of the sharp peaks, there was a short broad peak at 225 °C. This indicates that there was an interaction between the SECs and the mucin that could be attributed to a change in the mucin chain conformations, which alter the thermal properties of mucin. Figure 57 shows an overlay of the thermograms from mucin, freeze-dried mucin, SECs and the mucin-SEC mixture, and the resulting change in mucin thermal behavior after the interaction between the mucin chains and the SECs of *A. artemisifolia*.

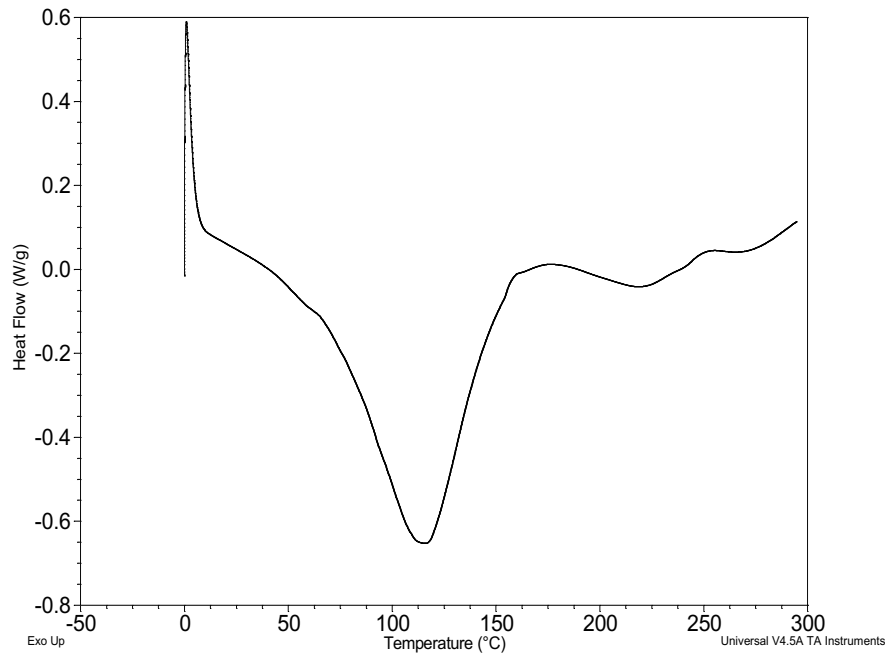


Figure 56: A DSC thermogram of *A. artemisifolia*. SECs-mucin freeze-dried, indicates an interaction between SECs and the mucin chains, since the mucin peaks do not appear after mixing mucin with the SECs.

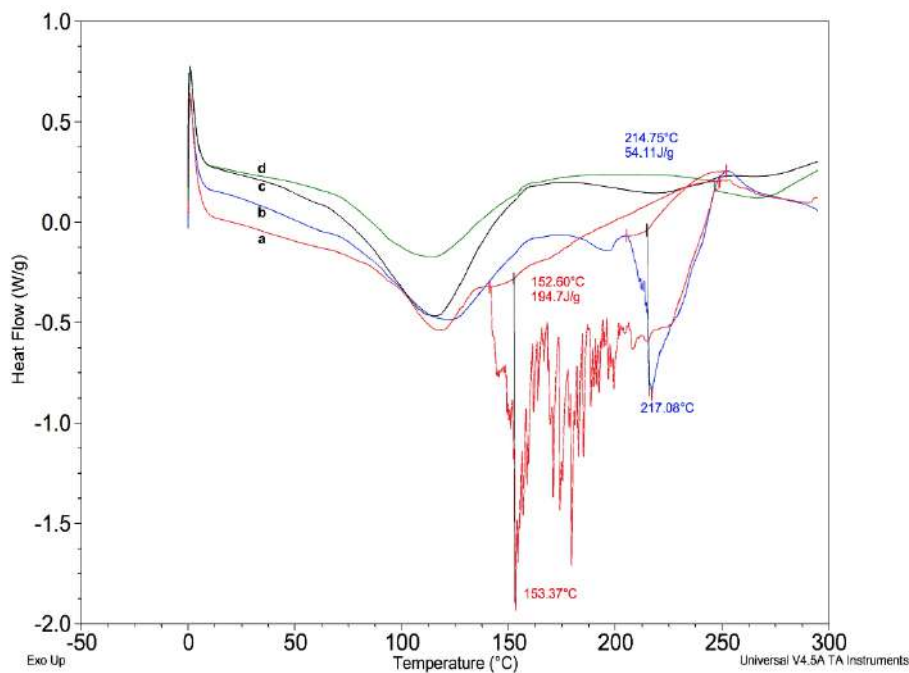


Figure 57: Overlay of the DSC thermograms of AH-SECs *A. artemisifolia*, SECs and mucin show: (a) freeze-dried mucin, (b) mucin powder as received (c) mucin-SECs freeze-dried and (d) freeze-dried SECs.

The type of this interaction between the SECs' surface and mucin is likely to be non-covalent. Possibly an accumulation of, hydrogen bonding, electrostatic, and hydrophobic interactions play a role in binding which are well-known features of mucoadhesivity of mucin [123]. Both SECs and mucin have hydrophobic (mainly lipids), and hydrophilic functional groups. Carboxylic acid groups are found in mucin and SECs and can be deprotonated, easily, in water and alkali to form carboxylates [74], and the phenol on the surface of SECs can form phenoxide anion. Moreover, mucin has an amino group that can form a cation when protonated and bind by a salt bridge to carboxylate groups [124].

After it was shown that there is an interaction between the *A. artemisifolia* SECs and mucin, the study was extended to SECs obtained from *L. clavatum* spores. These were mixed with mucin and analyzed by DSC using a similar procedure that used to test the AH-SECs of *A. artemisifolia* in order to verify that the interaction between the mucin and assess whether this property of SECs was not simply a function of one species of plant spore or pollen. Figures 58 and 59 show that there were no observable differences in the DSC thermograms of the AH-SECs of *L. clavatum* before and after freeze-drying respectively.

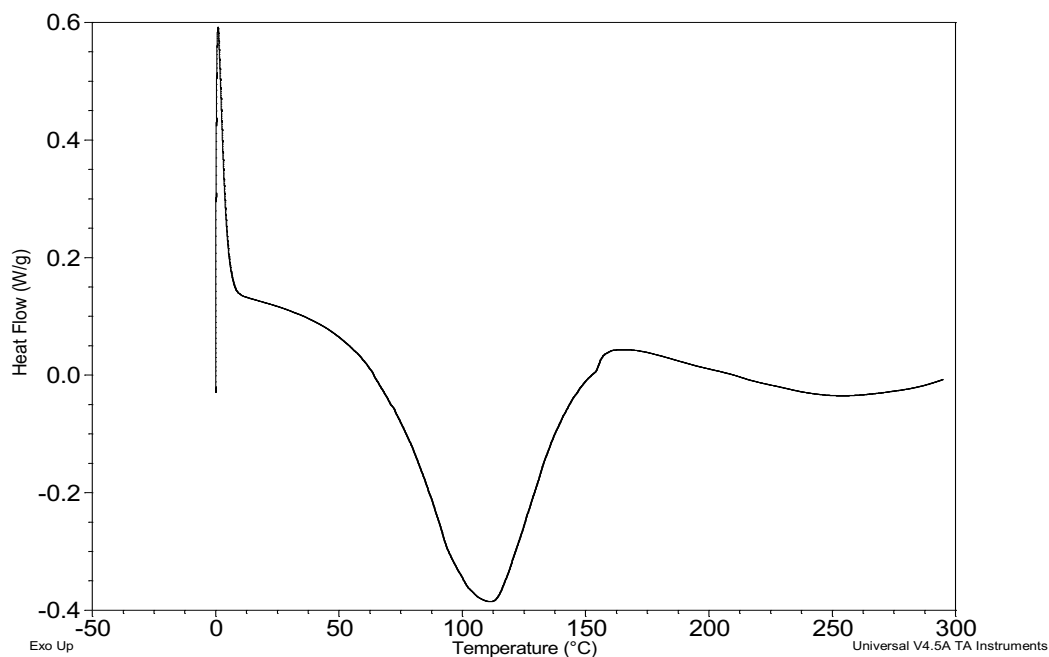


Figure 58: A DSC thermogram of AH-SECs of *L. clavatum*. There is an endothermic peak around 110 °C indicating dehydration of the SECs.

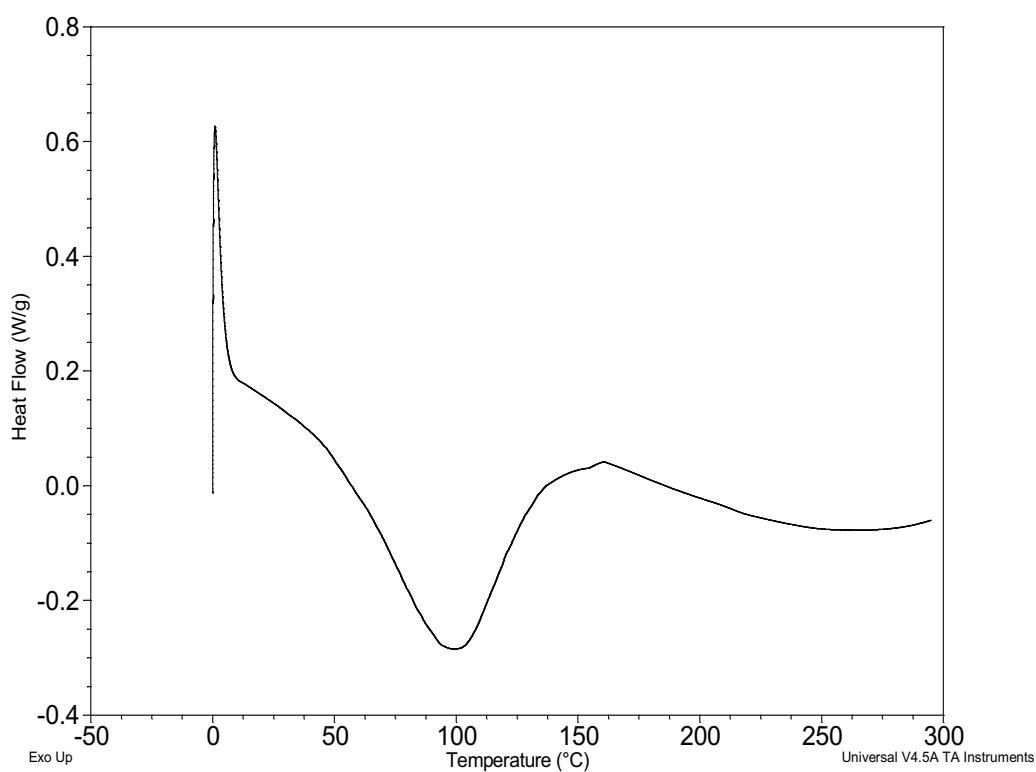


Figure 59: A DSC thermogram of freeze-dried AH-SECs from *L. clavatum* show the same behaviour of the non freeze-dried one.

However, when the *L. clavatum* SECs were mixed with mucin, the mucin peaks changed and showed similar thermal behaviour of mucin that observed in the sample of mucin mixed with *A. artemisifolia* SECs, i.e. there was a short broad peak at 225 °C indicating that there was an interaction between the mucin and the SECs as shown in Figure 60. The DSC experiments of the two different species of SECs towards mucin showed that SECs possess mucoadhesive properties that could be a common feature and is not related to simply one species of plant.

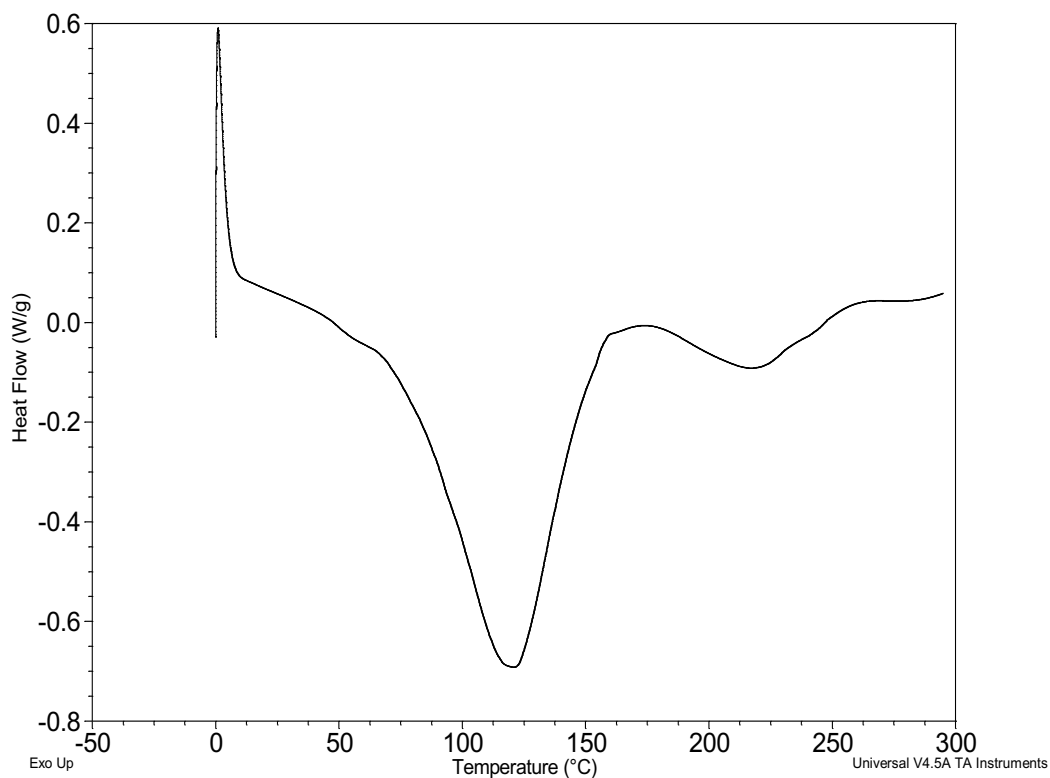


Figure 60: A DSC thermogram of AH-SECs of *L. clavatum*-mucin freeze dried, indicating an interaction between SECs and mucin, as the mucin peaks did not appear after mixing mucin with SECs.

Figure 61 shows overlay of mucin, freeze-dried mucin, SECs and mucin-SECs thermogram and the change in mucin thermal behaviour after the interaction between the mucin chain and the SECs of *A. artemisifolia*.

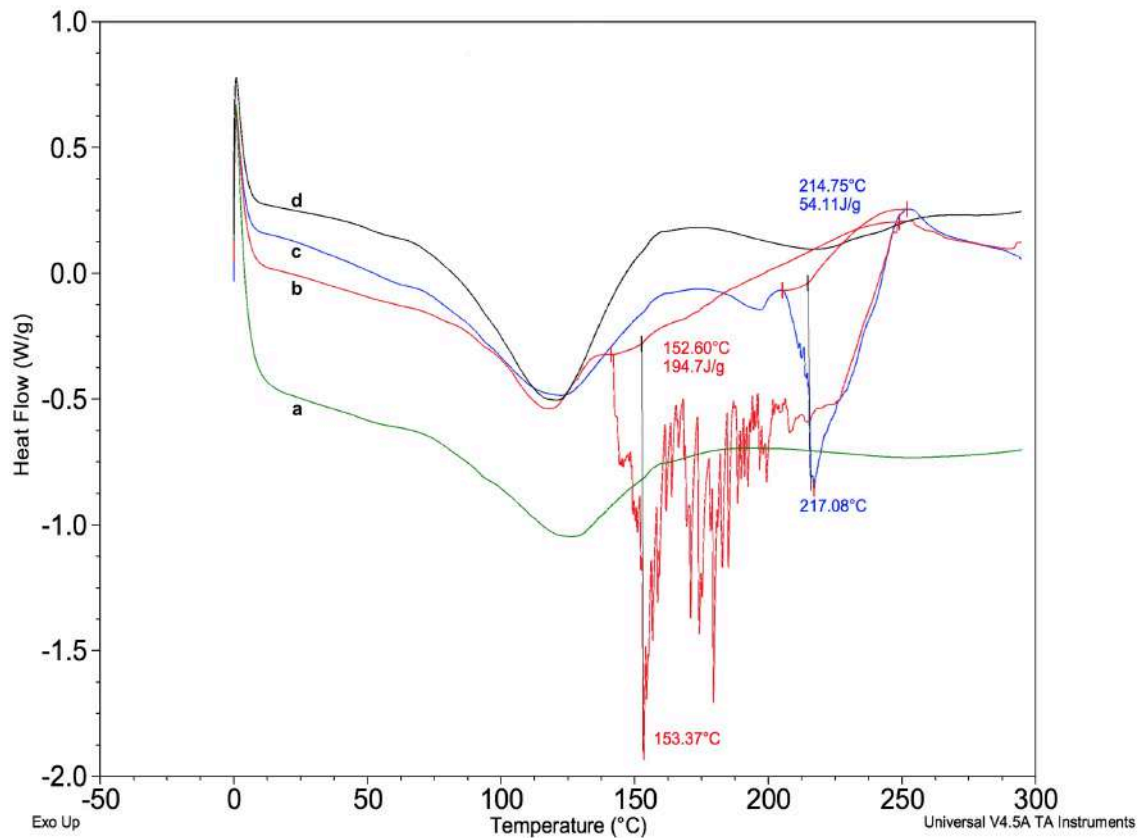


Figure 61: Overlay DSC thermograms of AH-SECs of (a) *L. clavatum* freeze-dried, (b) mucin freeze-dried, (c) mucin powder as received and (d) mucin-SECs freeze-dried.

5.2 *In vitro* Evaluation of Mucoadhesion Properties of SECs using Texture Analyzer

The applications of tensile test, or tension test, using the texture analyzer instrument have been reported as a useful technique commonly used to study the mechanical properties of materials and to evaluate the pharmaceutical mucoadhesive profile of solid and semisolid dosage forms [125]. Texture analyzer consists mainly of two parts: (i) a mobile load cell that holds a probe to which the mucoadhesive polymer sample is attached; (ii) a sample test area that holds the natural or artificial mucus tissue. The probe moves downwards to the sample area until it touches the mucus, then a known force is applied for a specific time. The probe is then moved upwards away from the mucus and the ‘mucoadhesive strength’, also known as the ‘peak detachment force’, is measured by the maximum force required to separate the mucoadhesive polymer from the surface of the mucus layer [126, 127]. The area under the ‘peak force’ curve represents another parameter that measures the adhesion strength and is known as ‘work of adhesion’ or ‘work area’. Figure 62 shows an example of peak force and the work of adhesion graph.

The ‘peak detachment force’ is related to the formation of hydrogen bonds between the functional groups of the bioadhesive material and the surface of the mucus. ‘Work of adhesion’ in turn is more dependent on the interpenetration of the adhesive chains of the bioadhesive material into the mucus [128].

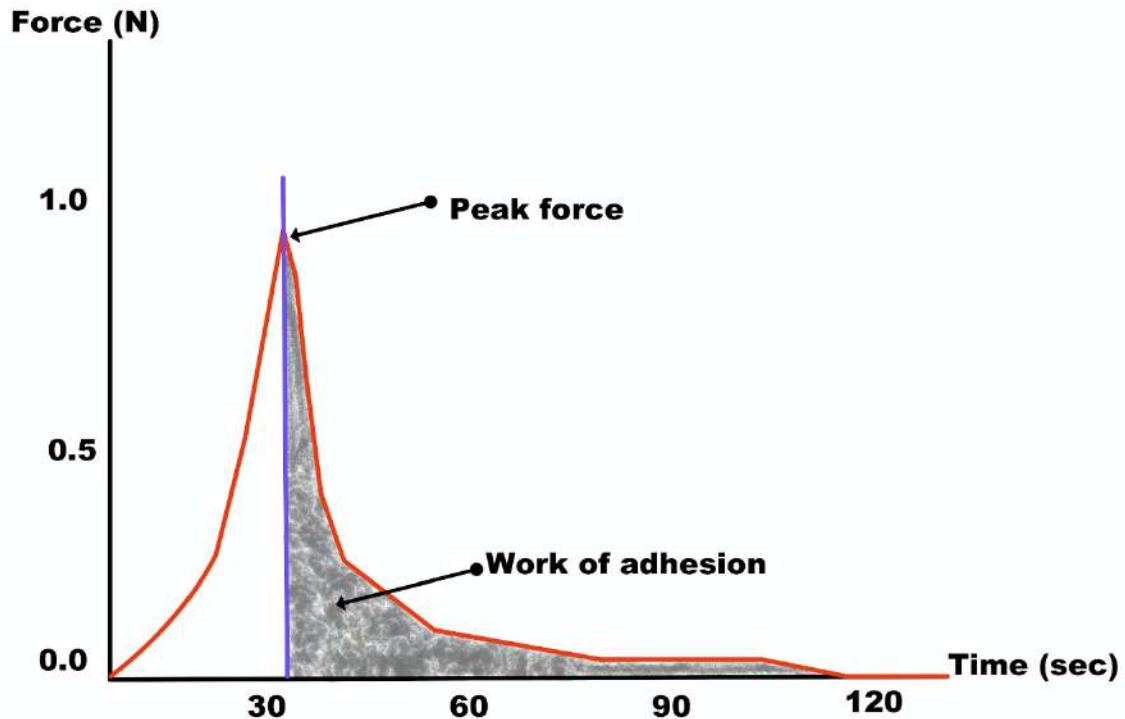


Figure 62: Schematic curve shows peak force and work of adhesion parameters that are measured by a texture analyzer

In this study four samples of SECs were used to measure and evaluate their bioadhesive properties and compare them to the mucoadhesive polymers controls chitosan and carbopol-934. The types of SECs studied were from *L. clavatum* (AH-SECs and BH-SECs), *A. trifida* (AH-SECs) and *A. artemisifolia* (AH-SECs). It was considered that the BH-SECs should be more hydrophilic than the AH-SECs as they have sodium salts of the surface functional groups, as discussed before in (Section 3.4.8), whereas the uncharged AH-SECs would be more hydrophobic.

All the samples were tested in powder and tablet forms, and were prepared for the texture analysis as described in the experimental Chapter 8 (in Section 8.10.2).

5.2.1 Powder form samples

Each sample of SECs and the controls was used in a powder form. A small amount of the sample was spread evenly on one side of a sticky pad manually by spatula. The other side of the sticky pad was adhered to the texture analyzer probe. Each sample was left in contact with the 5% mucin (50 μ l) in nutrient agar for a period of time (see Section 8.10.2). Figures 63 and 64 show the peak force and work of adhesion, respectively, for the SECs and the controls. The detachment force of the four SECs samples (powder form) shows strong bioadhesive properties, which was 75% of carbopol after 60 and 120 seconds contact time. After 240 seconds contact time, AH-SECs of *L. clavatum* and *A. trifida*, show mucoadhesivity greater than carbopol after the 120 seconds contact time.

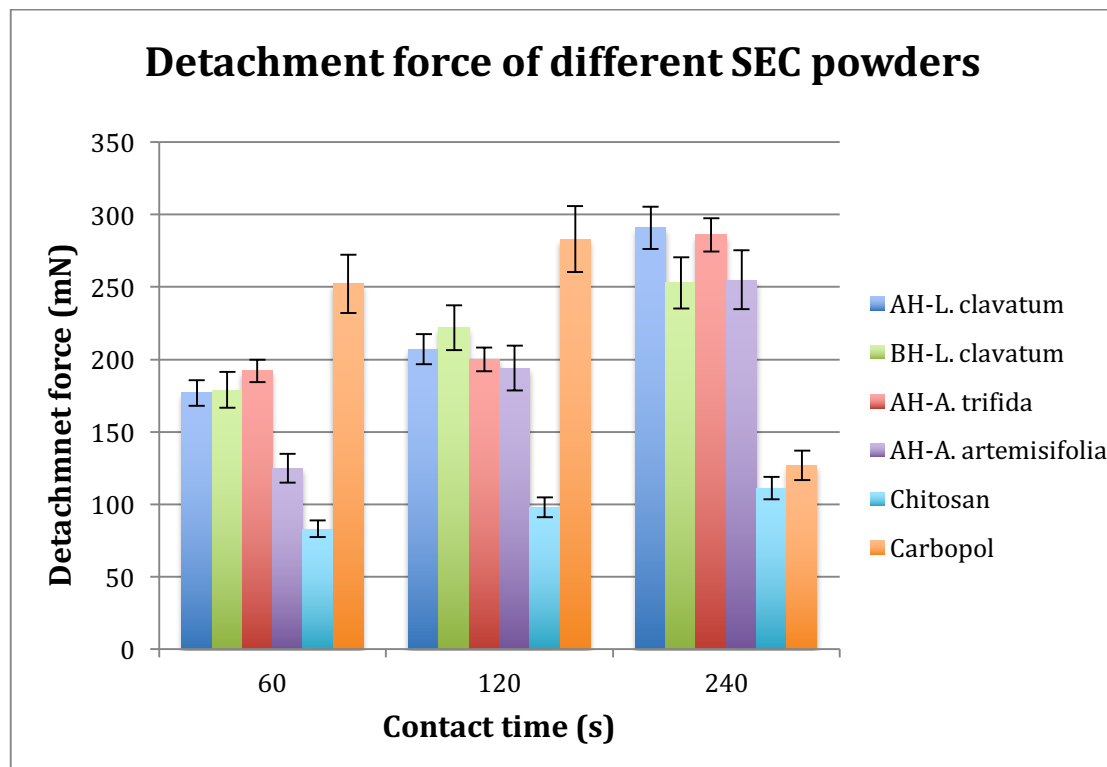


Figure 63: The detachment force of the four SEC samples and the two controls (all in powder form). $n = 3$.

The results in Figure 63 show that there was a reproducible increase in peak force for all the powders up to 240 seconds with the exception of carbopol, due to the absorption of water at this last time point. Thus, it was shown (Figure 63) that the SECs possess mucoadhesive properties within the range of the well-recognized mucoadhesive material, such as carbopol and chitosan. From these data it can be seen that the mucoadhesive properties of SECs are more than twice those of chitosan. Also, All the SECs showed a 'peak force' that is twice that of chitosan at the 120 seconds time point, and they showed that they have a similar 'peak force' when taking error bars in account. However, AH-SECs and BH-SECs of *L. clavatum* and AH-SECs of *A. trifida* showed higher adhesion strength than *A. artemisifolia* at the 60 seconds time point

Also, these data showed that when contact time between the mucin and the SECs increased, the gap between chitosan and SECs in peak force was increased significantly. For example, the mucoadhesion strength for *L. clavatum* between 60s and 120s was statistically significant (p-value = 0.030).

This result demonstrated that by increasing contact time, SECs can form additional binding interactions with the mucin chains. As stated in (Section 5.1) pertaining to the DSC results, these bonds are likely to be non-covalent bonds such as electrostatic, hydrophobic and hydrogen bonding. Furthermore, in these experiments SECs were found to resist hydration more than carbopol and chitosan and the resistance of SECs to hydrate makes them more preferable as mucoadhesive material than carbopol and chitosan for mucoadhesion drug release. This is because materials that form a bioadhesive hydrate the fastest are also the fastest to lose their bioadhesivity [85].

Results and Discussion

This behaviour of SECs in comparison to the controls can also be applied to the ‘work of adhesion’. The ‘work of adhesion’ values obtained for the SECs were higher than those obtained for chitosan and were found to increase with increasing time of contact (Figure 64), This observation may be explained by an increase in secondary bond formation between the polymers and mucus with an increase in contact time. Also it was observed that the gap in the ‘work of adhesion’ between the chitosan and SECs was increased by time similar to that found for the peak force (Figure 63).

Powder SECs ‘work of adhesion’ shows strong bioadhesive properties. In the 240 seconds contact time, AH-SECs of *A. trifida* ‘work of adhesion’ was greater than the other SECs. That indicates that they have more physical entanglement with mucin chains.

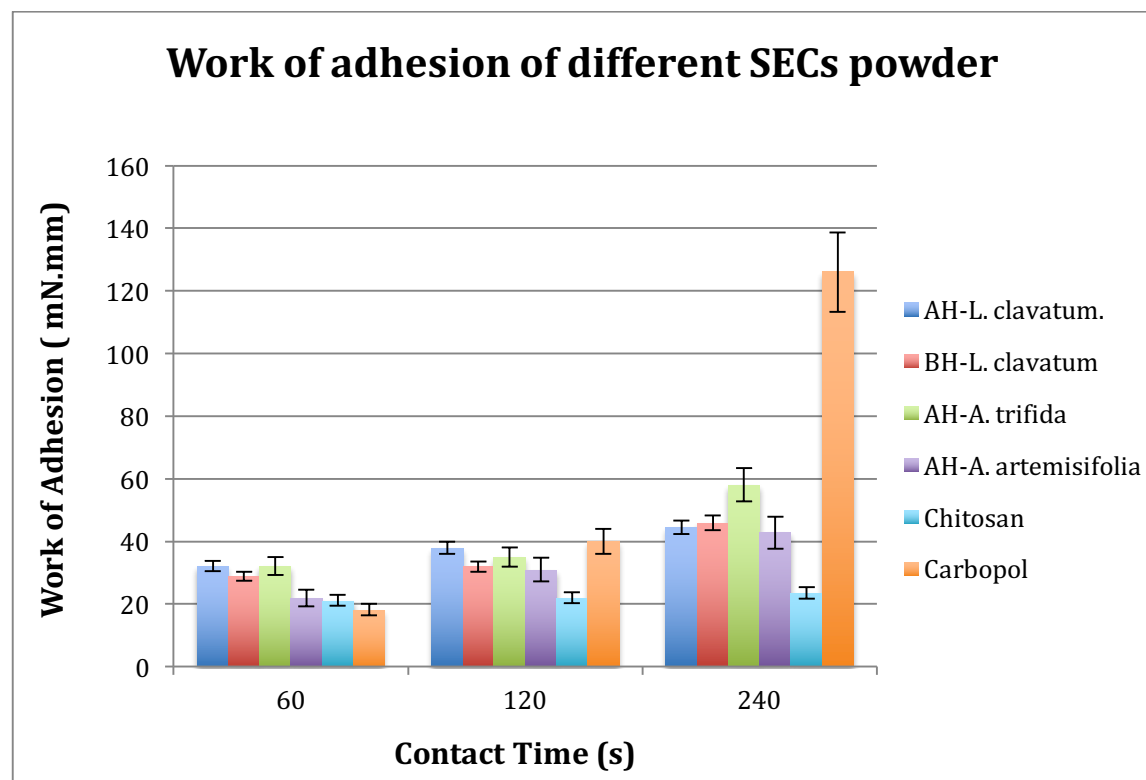


Figure 64: Work of adhesion of SECs in powder form, $n = 3$.

5.2.2 Tablet form samples

Since the powder form of SECs from different plant sources showed significant mucoadhesive properties (in Section 5.2.1) that were comparable to known mucoadhesive polymers, it was of interest to compare each in tablet form. The tablet form has the advantage that the mass and surface area of the samples can be fixed accurately, which is a little more difficult in powder form.

The same four SECs samples in addition to the two controls powders were compressed to form 150 mg tablet with 40-100 Newtons (see experimental Section 8.10.2)

Figures 65 and 66 show the ‘peak force’ and the ‘work of adhesion’ data, respectively, for tablets samples. The characteristics observed were similar to those obtained for the powder form of the samples. The peak force values of the tablet forms of the SECs showed mucoadhesive properties in the range of those found for established mucoadhesive materials. Also all the samples were contact time dependent and showed an increase in peak force that corresponded to an increase in contact time. However, at the 120 seconds contact time, the carbopol began to jellify resulting in a decrease in peak force. Similarly, it was observed that chitosan began to jellify at 240 seconds contact time interval, and this distorted the peak force value. Also, by the same time point the *A. trifida* AH-SECs tablet was fractured, hence gave unreliable peak force readings in 120 and 240 seconds time points. The mucoadhesion strength for *L. clavatum* tablets between 60s and 120s was statistically significant (p-value = 0.003).

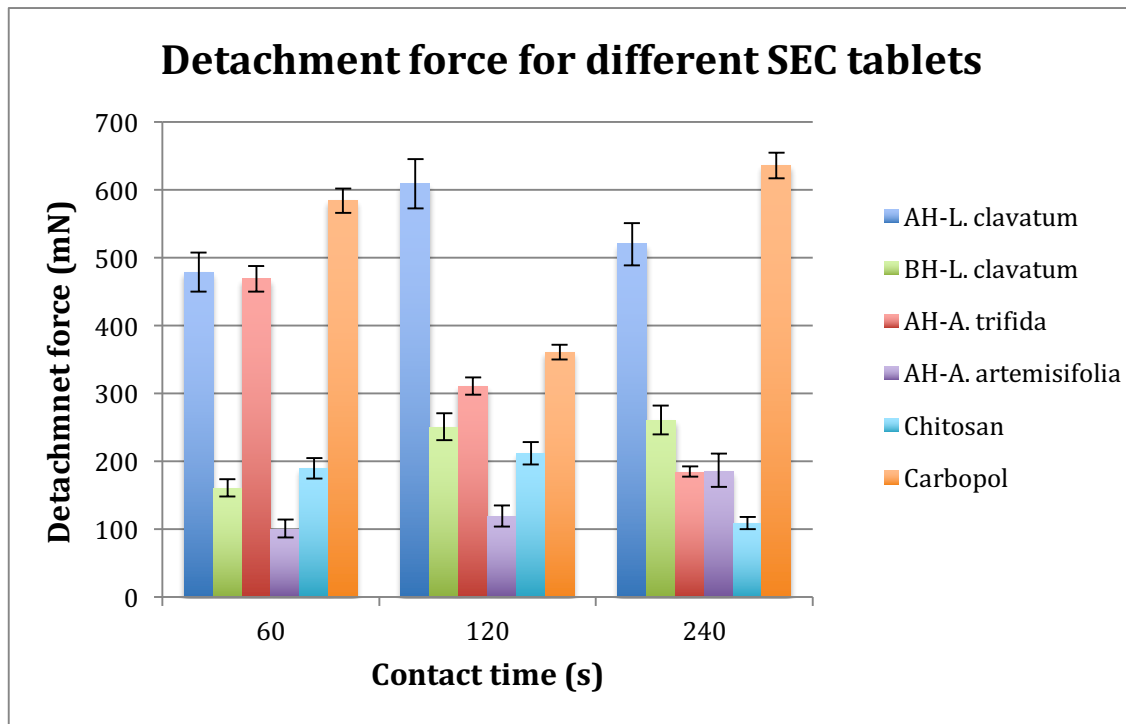


Figure 65: Tablets of SECs show an increase in ‘detachment force’ for all types of SECs when contact time increased (at 60 and 120 seconds), except *A. trifida* AH-SECs which showed a decrease in the detachment force within 120 seconds. This may be due to the fracture of the tablet, since the ‘detachment force’ would have been measuring the fracture force of tablet and not the mucoadhesion force. Also, at the 240 seconds contact time, the observed increase in the carbopol detachment force is misleading, since the carbopol goes into conformation change from solid to gel at this point due to rehydration from mucus and lose of mucoadhesion. $n = 3$.

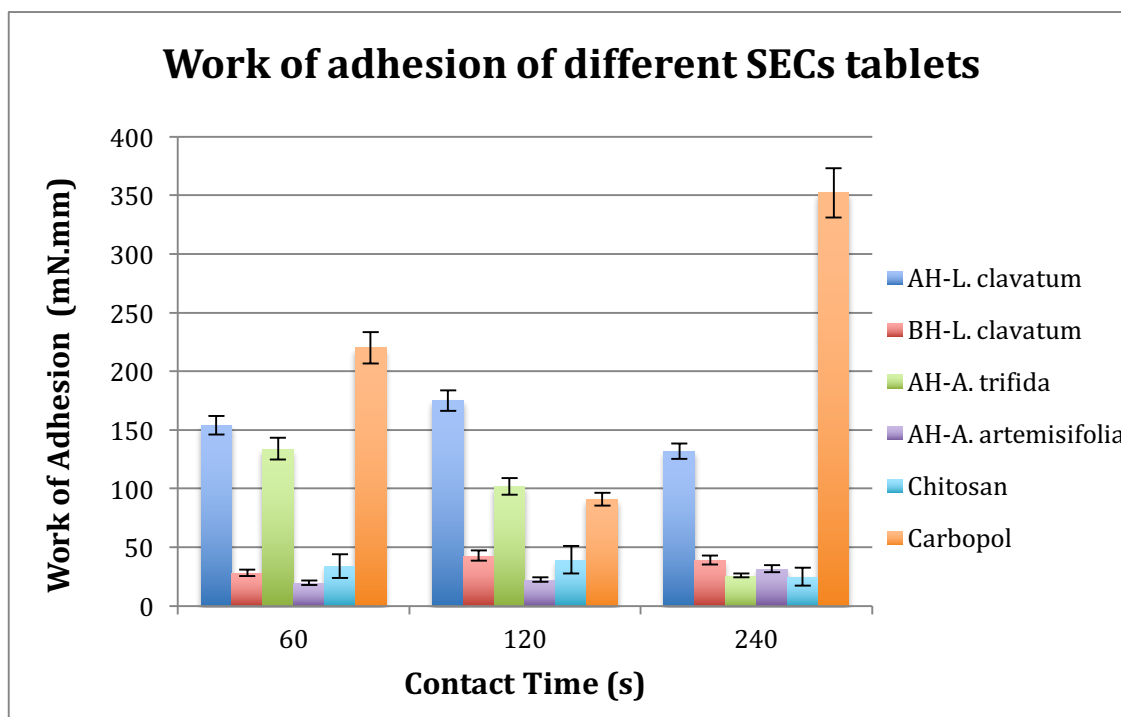


Figure 66: ‘Work of adhesion’ vs different contact times for SEC tablets and controls. $n = 3$.

It is worth noting that the ‘peak force’ observed for all of the samples in tablet form was greater than the respective samples in powder form (when $n = 2$). This is because the tablet forms have a greater mass and surface area than the respective powder forms, which means they have more available functional groups that increase the chance of forming additional secondary bonds.

The ‘work of adhesion’ for all of the SECs was higher than observed for chitosan and found to increase with increasing contact time. This can be interpreted as being due to an increase in contact time increasing the chance of secondary bond formation between the polymers and mucus. Also it was observed that the gap in the ‘work of adhesion’ values observed between chitosan and SECs increased with time, in a similar manner to the peak force values (Figure 66).

In conclusion, the ‘peak force’ and ‘work of adhesion’ showed that the SECs from all of the plant sources namely, *L. clavatum*, *A. artemisifolia* and *A. trifida*, have bioadhesive properties that exceed the bioadhesivity of chitosan but overall less than carbopol. DSC and ‘texture analyzer’ results indicated there is an interaction between the SECs and mucin. Hydrogen bonding, electrostatic, van der Waals and hydrophobic interactions are responsible for the bioadhesivity of these polymers with mucin. Also, it seems from this study that different SECs from different plant species have different levels of mucoadhesion strength. Further studies of functional group characterization as has been performed on the SECs of *L. clavatum*, (see Section 1.6), should be performed on *A. artemisifolia* and *A. trifida* to gain a more complete understanding of the major differences in the functional groups involved which may have an effect on the mucoadhesivity of SECs.

The elasticity of SECs might also have a role in the adhesion, as most of the known mucoadhesive polymers have some sort of elasticity to withstand the muscularity activity GIT and its secretions [129]. Also, the resistance of SECs to hydrate makes them more preferable to carbopol and chitosan because the quicker a bioadhesive material hydrates the faster it will lose its bioadhesivity [85].

Chapter 6. SECs' Morphology and Lipids role in their Mucoadhesivity

6.1 The Role of SECs' Morphology in their Mucoadhesivity

In the previous section (Section 5.2), SECs from different species of spores and pollens showed mucoadhesion properties, which were greater than those of the well-known pharmaceutical mucoadhesive polymer, chitosan. The 'peak force' was found to vary between the different types of SECs that that led to the investigation described in this section. The topology of pollens and spores and consequently their extracted SECs are different. To this extent the individual morphological characteristics have proved invaluable to forensic scientists, geologists and archaeologists [130]. Therefore, it was of interest to investigate the importance of SECs' morphology to the mucoadhesive properties of SECs in particular those obtained from *L. clavatum* and *H. annuus*. Importantly, these types of SECs are characterized by very distinct and jagged topological features that could assist in the physical binding to a surface (see Figure 67). It is possible that such features have evolved for role of adhesion in the process of pollination and plant reproduction. In respect of such as drug delivery, the most bioadhesive type of SEC could be important in choosing the best microcapsules for such a purpose. Figure 67.A shows *H. annuus* SECs, which differ in surface decoration features from those seen in *L. clavatum* SECs (Figure 67.B). The long spikes of *H. annuus* SECs may help in enhancing the mucoadhesion and increase the contact surface area, which may lead to an enhancement of the drug absorption.

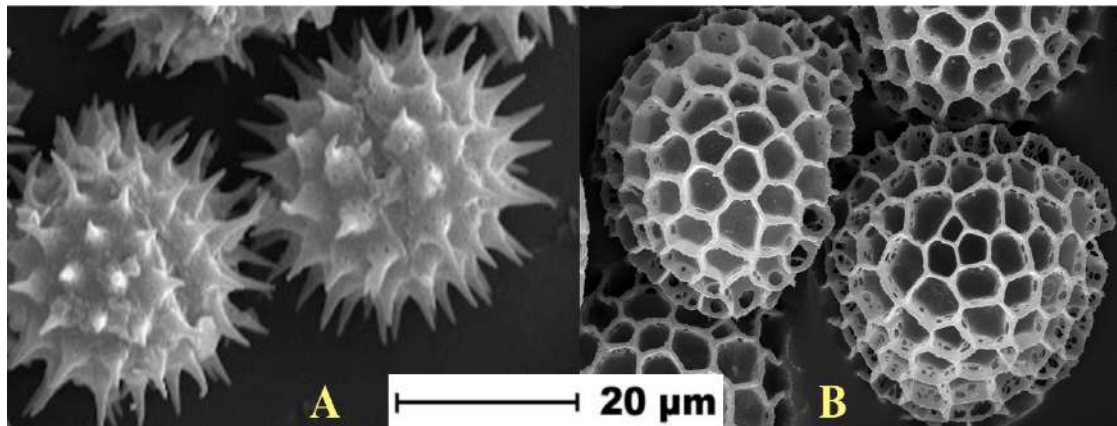


Figure 67: SEM images of *H. annuus* SECs (A) showing their long spikes in comparison to *L. clavatum* (B).

Figure 68, shows the ‘peak force of detachment’ of the tablets of SECs from *L. clavatum* and *H. annuus* in comparison to the two controls used previously. In the first two contact time points (at 60 seconds and 120 seconds) *L. clavatum* SECs showed a greater adhesion strength than that found for the *H. annuus* SECs. However, at the 240 seconds time interval *H. annuus* SECs gained a greater ‘peak force’. This result might mean that the *H. annuus* SECs need longer contact time to form a stronger adhesion, and the *L. clavatum* needs less contact time for initial bonds to form with the mucus. Also, it was observed that in the last point of time (at 240 seconds), *H. annuus* SECs were more resistant to hydration, and their surfaces in contact with the mucus were therefore dryer. In contrast the surface of *L. clavatum* SECs appeared to be wet. From this study it can be seen that the morphology and the surface architecture can influence and enhance mucoadhesion at longer contact times. The mucoadhesion strength for *L. clavatum* and *H. annuus* tablets between 60s and 120s was statistically significant (p-value = 0.003 for *L. clavatum*, and p-value = 0.007 for *H. annuus*).

however, from the results obtained such an influence is relatively small, and the mucoadhesion was not statistically significant (p-value = 0.075).

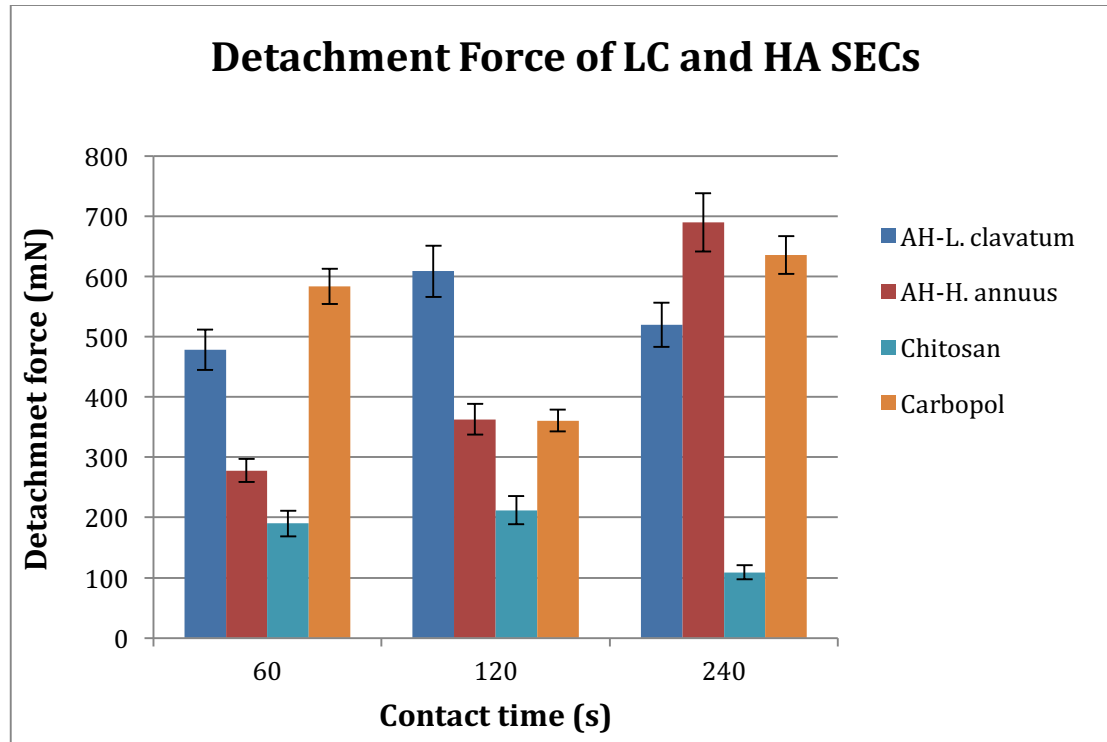


Figure 68: Peak force of tablet AH-SECs of *H. annuus* (HA), *L. clavatum* (LC) and controls (carbopol and chitosan). $n = 3$.

6.2 The Role of SECs' Lipids in their Mucoadhesivity

As note earlier (Section 2.4.6.1.1), hydrophobic bonding is one of the bonding interactions that have been used to explain mucoadhesion. With this in mind it was thought to develop another method to explore the role of SECs lipids in mucoadhesion. The idea was to compare two forms of AH-SECs from *L. clavatum* spores, one with their natural lipids and the other in which their lipids had been fully

removed (lipid-free SECs), and use texture analysis to compare adhesion strength using peak force (see Section 3.4.3 for more details about these lipids and lipid-free SECs). Figure 69 and Table 19 show the ‘peak force’ of these two samples in addition to the controls. As it was expected, removing the lipids from the SECs made them more hydrophilic, with the consequence of enhancing their mucoadhesion slightly. This is because hydrophilic groups on the SECs can establish a mucoadhesive bonds quickly with the aqueous mucin mixture. The mucoadhesion was statistically significant for *L. clavatum* without their lipids (p-value = 0.011), and with their lipids (p-value = 0.030).

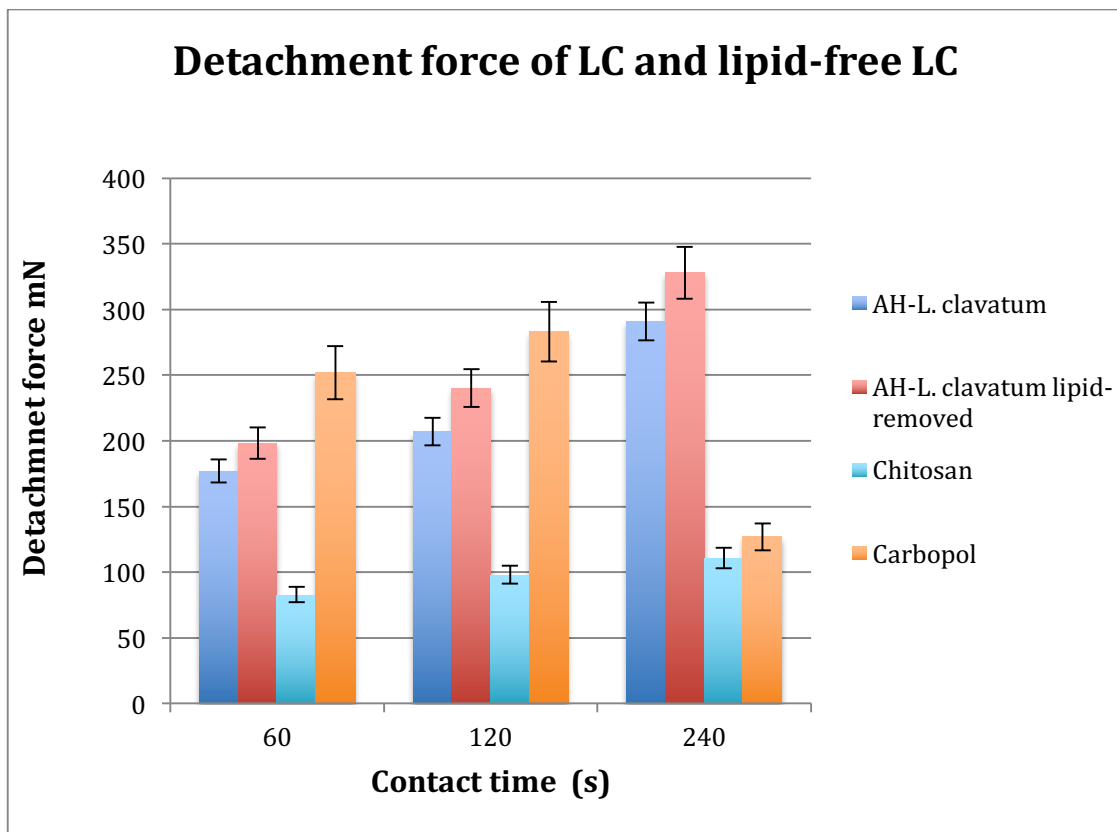


Figure 69: Peak force of powder AH-SECs of *L. clavatum* (LC) with and without their lipids and the control polymers of chitosan and carbopol. $n = 3$.

		Peak force mN			
Polymer Contact Time (s)	LC AH-SECs	LC AH-SECs lipid-free	carbopol	chitosan	
60	177.0 ±12.2	198.4 ±8.1	252.3 ±32.9	83.6 ±1.9	
120	206.3 ±12.4	240.0 ±10.3	287.6 ±34.6	94.3 ±2	
240	291.0 ±20.3	328.1 ±24.1	126.6 ±1.5	111.0 ±4.7	

Table 19: Summary of Peak force of powder AH-SECs of *L. clavatum* (LC) with and without their lipids and the control polymers of chitosan and carbopol. *n* =3.

6.3 *Ex vivo* Evaluation of SECs' Morphology and Lipids in Mucoadhesion

The aim of this study was to use a biological tissue sample instead of the nutrient agar to study the mucoadhesivity of SECs from two different plant species. Three cow cheek tissues were smeared with 5% mucin solution (400 µl), and then 150 mg of one of the three types of SECs (AH-SECs and AH-SECs-lipids-free of *L. clavatum* and AH-SECs of *H. annuus*) were spread on the surface of separate cow cheek tissue samples. Each one of SECs was left for one minute to give it a time to form bonds between the SECs and mucus, then they were put in a bowl with water that just touch the surface of the cheek where SECs adhere to, and left for 2 hours agitated at 37 °C see Figure 70.

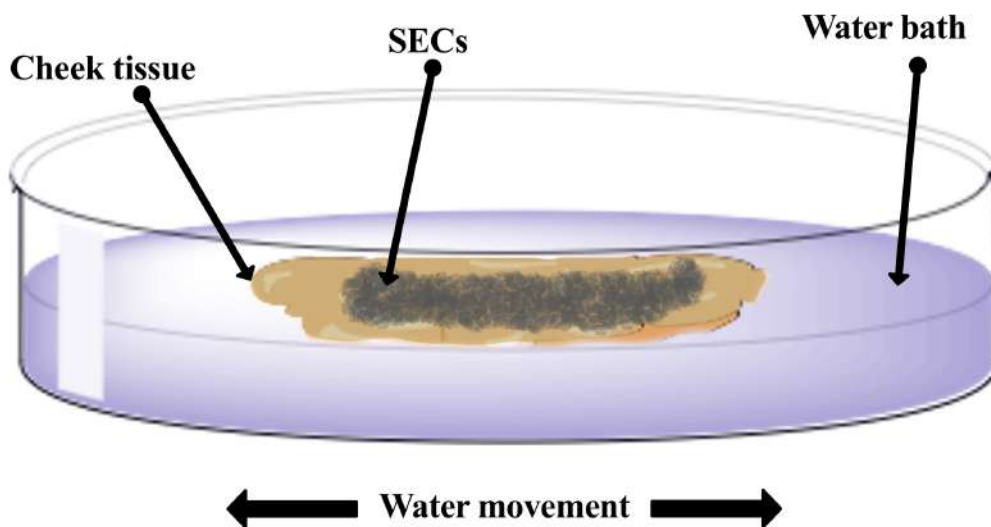


Figure 70: A mucus layer was spread over a cheek tissue surface and SECs were spread over that mucus on the cheek, then they were put in bowl that was filled with water until the water just touch the surface of the cheeks and the SECs that adhere to it. After that the bowl was agitated which cause the water in the bowl to wash the surface of the cheek tissue in every movement.

After that time, the cheeks were removed from the water, and the water was filtered using centrifugal tubes. The precipitates, which are the SECs and some of the cheeks fibers, were collected and freeze-dried overnight. On the second day, the dried precipitates were broken into powder and filtered through the sieve (20 μm). Then the recovered SECs were collected, weighted and their percentage was calculated from the initial weight of the SECs that was spread in the cheek surfaces (see Section 8.11).

The *ex vivo* results (Table 20 and Figures 71, 72 and 73) showed similar findings to the texture analyzer results for SECs discussed previously (in Section 6.1 and 6.2). For example, the lipid-free AH-SECs of *L. clavatum* showed strong adhesion to the

Results and Discussion

cheek surface and the SECs lost only 1 mg of their initial mass (150 mg) when they were agitated in a water bath, i.e. 99.33 % of the lipid-free SECs were retained in contact with the cheek surface (Figure 71.a and 71.b). Interestingly, this was the same sample that showed higher mucoadhesivity properties in texture analyzer in the powder form (Figure 69, Section 6.2).

On the other hand, the AH-SECs of *L. clavatum* (with their original lipids still in) lost 15.4 mg of its initial weight, i.e. 89.73 % of the AH-SECs were retained in contact with the cheek surface (Figure 72.a and 72.b). The AH-SECs of *H. annuus* lost only 17.2 mg of its initial weight, i.e. 88.54 % of the AH-SECs were retained in contact with the cheek surface (Figure 73.a and 73.b), which was relatively equal to the AH-SECs of *L. clavatum* (with their original lipids in). The last two samples (AH-SECs of *L. clavatum* and *H. annuus* with their lipids in) suggested that hydrophilic SECs possessed greater mucoadhesivity than the hydrophobic SECs, which was the find in the *in vitro* study described earlier (in Section 6.2). Table 20 summarizes the recovered mass of each sample in these experiments.

AH-SECs	Initial mass mg	Recovered mass mg	Recovered %
<i>L. clavatum</i> (lipids-free)	150.00	1.00	0.67 %
<i>L. clavatum</i>	150.00	15.40	10.26 %
<i>H. annuus</i>	150.00	17.20	11.46 %

Table 20: *Ex vivo* experiments of mucoadhesion of different SECs. *n* =3.

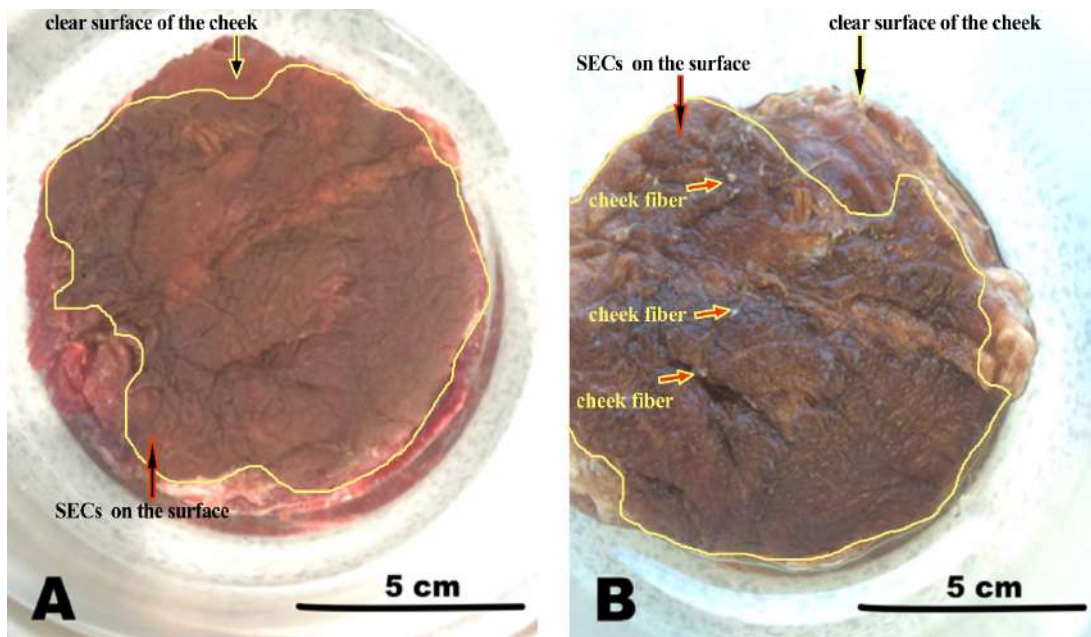


Figure 71: (A) AH-SECs of *L. clavatum* (lipids-free) spread over the cow cheek tissue, and (B) after shaking in water bath for 2 hours at 37 °C.

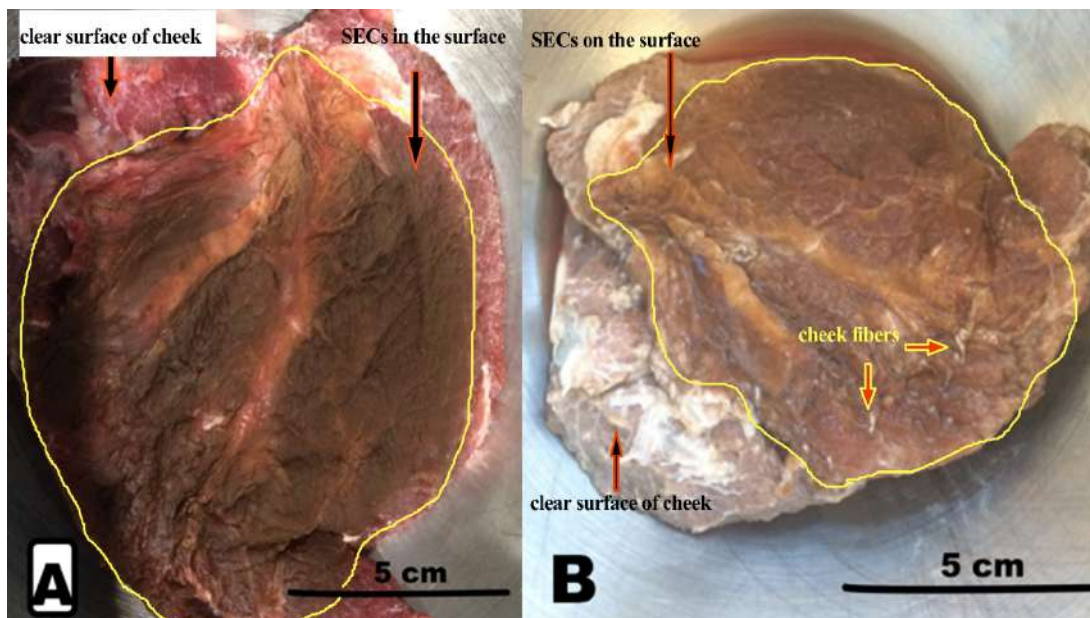


Figure 72: (A) AH-SECs of *L. clavatum* spread over the cow cheek tissue, and (B) after shaking in water bath for 2 hours at 37 °C.

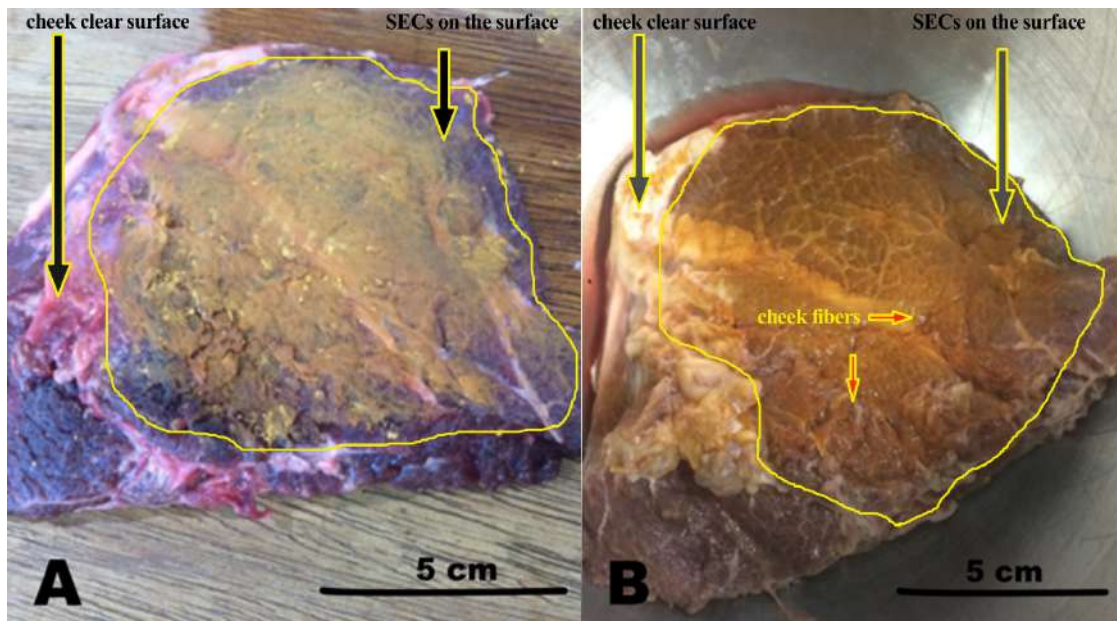


Figure 73: (A) AH-SECs of *H. annuus* spread over the cow cheek tissue, and (B) after shaking in a water bath for 2 hours at 37 °C.

In conclusion, this *ex vivo* study supports the *in vitro* studies that were performed using mucus on the agar surface and texture analyzer instrument (in Section 6.2), where the results suggested that lipid-free SECs showed relatively higher mucoadhesivity due to their greater hydrophilicity, which facilitates their hydrogen bond formation in the aqueous mucin.

6.4 Disintegration Test of SECs' Tablets

Disintegration is a measure of the quality of the oral dosage form in respect to the stability of tablets and capsules. The disintegration test is performed to find out the time that it takes for a solid oral dosage form, such as a tablet or capsule, to completely disintegrate [131] (see Figure 74). If the disintegration time is too long for the tablet to disintegrate, it is likely to pass through the stomach and intestine without releasing its content. Alternatively, if the time is too short, the tablet is likely to release its therapeutic agent quickly when it is swallowed [132].

From the mucoadhesion studies that were discussed previously in (Sections 7.1 and 7.2), it was found that some SECs were able to hydrate more rapidly than others depending on their species, extraction and lipids content. Hydration must be taken into consideration when choosing SECs for vitamins or therapeutics delivery as hydration of SECs tablets would decrease the disintegration time i.e. likely release the therapeutic agent quickly when reach the upper GIT, i.e. stomach where the tablets may stay for 1-2 hours during the normal process of digestion and absorption.

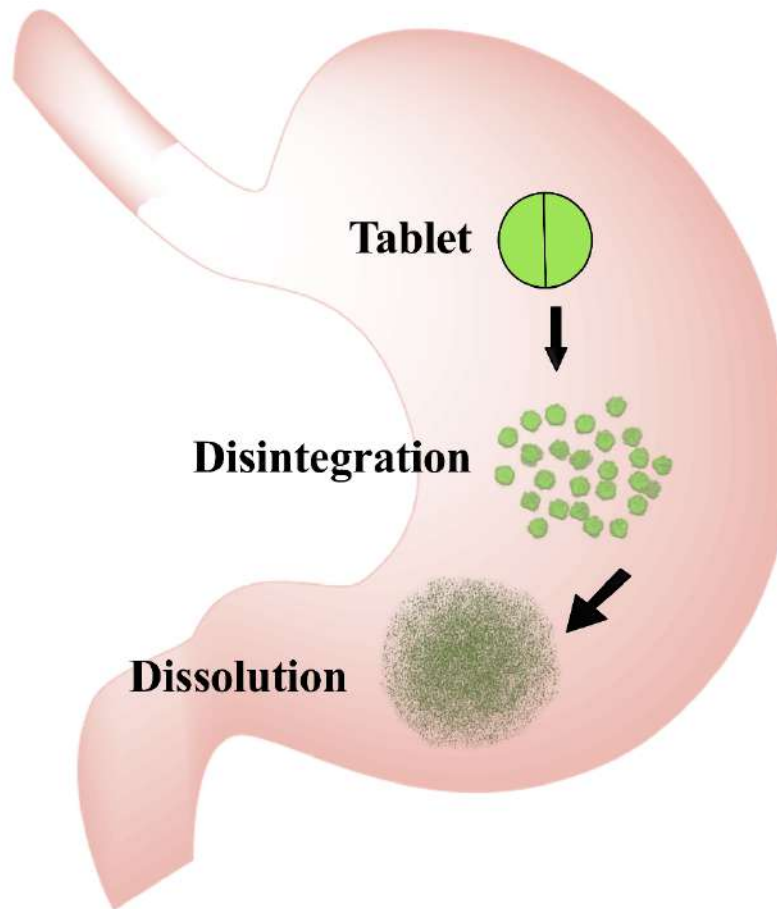


Figure 74: Tablet disintegration in upper GIT (stomach).

The disintegration test was done by placing tablets in a basket-rack assembly in a Copley disintegration apparatus, immersed in water several times, and then visually observed to determine disintegration completion by time.

For this study, three tablets were made for each sample of AH-SECs and BH-SECs of *L. clavatum* in addition to the AH-SECs of *H. annuus* (150 mg, 10 mm diameter) (see Section 8.12). The three tablets for each sample were left inside the Copley disintegrator at 37 °C and 30 cycle per minute for 2 hours (Figure 75). In each cycle, the flat probe was lowered to a beaker full of water, immersed in the tablet and then raised up again.

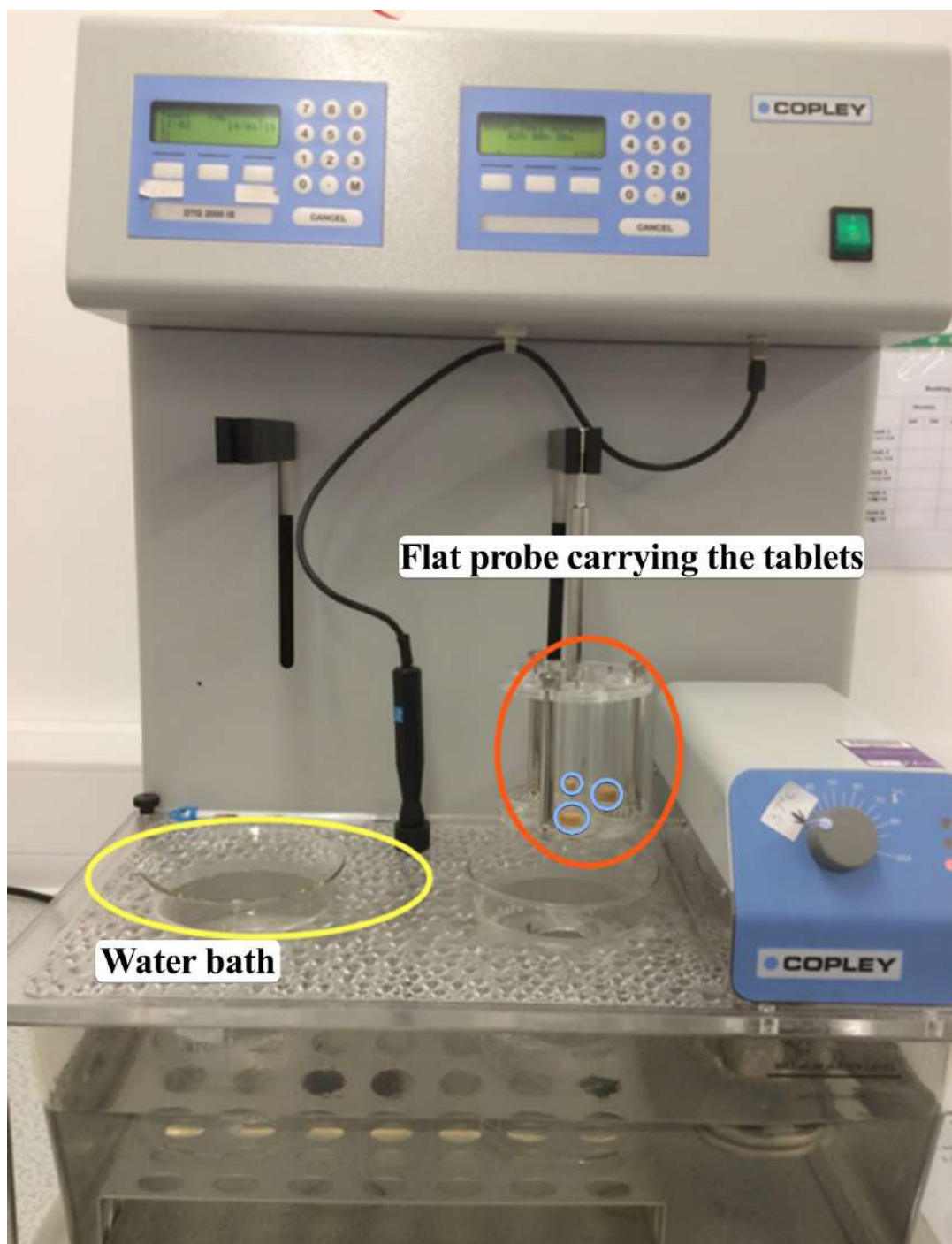


Figure 75: Disintegration apparatus used to study *H. annuus* tablets (blue circles) at the start of the experiment. The red circle shows the flat probe, and the yellow circle shows the beaker that full of water.

Results and Discussion

After 2 hours in the disintegrator (Figure 76) the AH-SECs of *H. annuus* did not show any signs of disintegration. The weight of the tablets was monitored before and after the disintegration test.

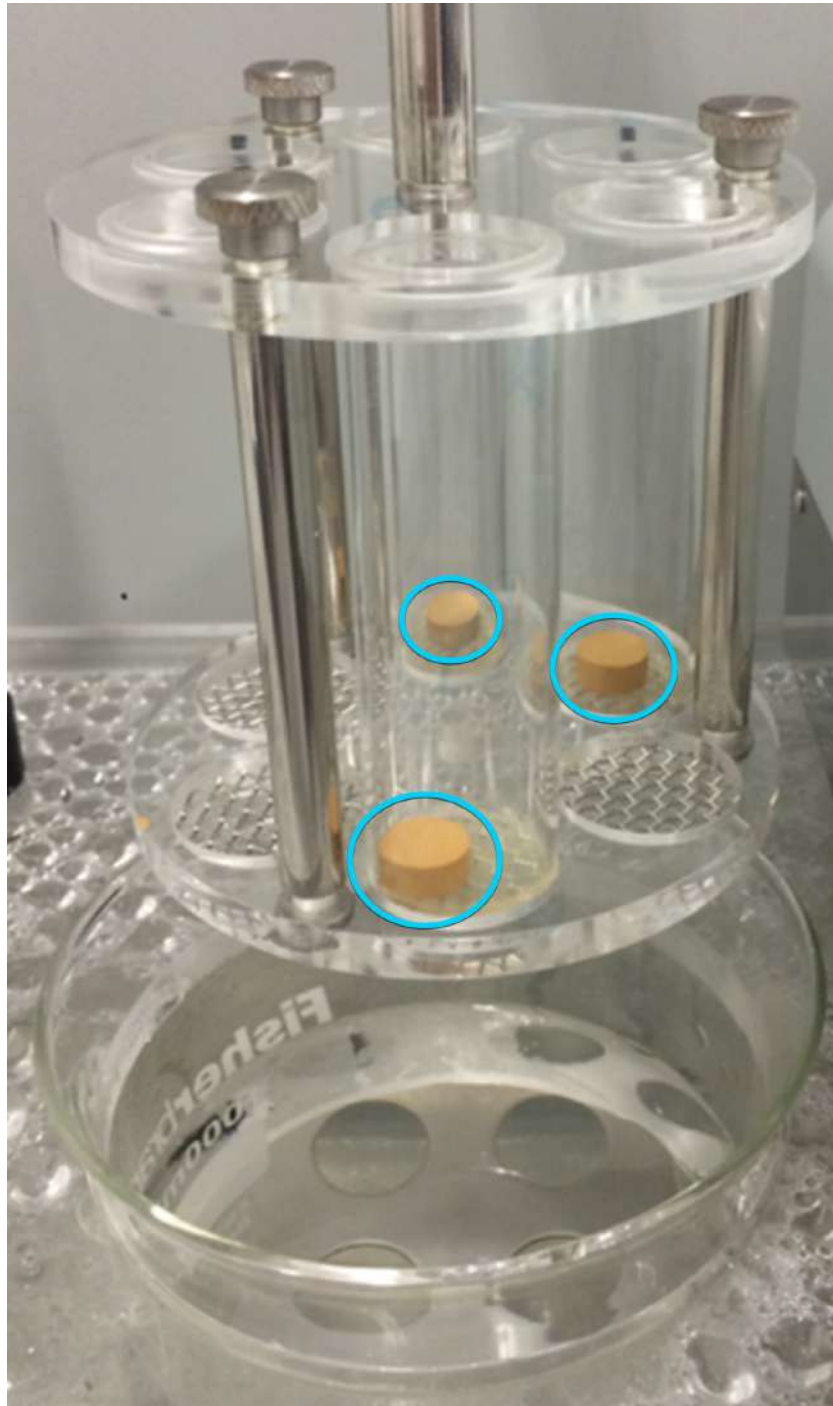


Figure 76: AH-SECs of *H. annuus* tablets after 2 hours in disintegrator instrument.

It was found that the AH-SECs of *H. annuus* tablets preserved their shape after the disintegration test; however, they lost some of weight during the test (around 23 ± 3 mg i.e 15.33 % of their initial weight was lost in the water bath) (See Figure 77). The lost mass of the SECs was calculated by freeze-drying the tablets after disintegration, then taking the weight of the dried samples and compare it to the initial mass before disintegration.

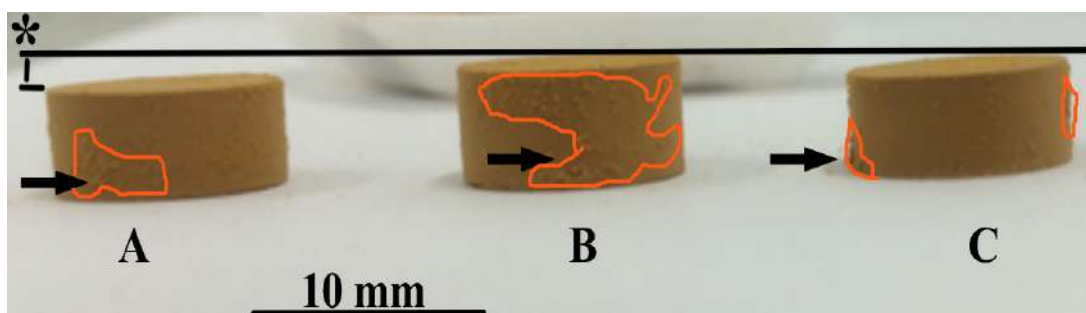


Figure 77: AH-SECs of *H. annuus* tablets preserved their structure even after subjecting to the disintegration for 2 hours; however, they lost some of their mass as seen in (*). Also, the surface of the tablets (in red circles) shows rough marks due to the disintegration. These experiments were repeated in triplicate.

The second sample that was chosen to study was the AH-SECs of *L. clavatum*. It was disintegrated for 2 hours as described above. In contrast to *H. annuus* tablets, the AH-SECs of *L. clavatum* tablets were disintegrated and deformed (Figure 78). This is could be related to their hydrophobicity which is greater than *H. annuus* pollen (as discussed in Section 6.1 were *L. clavatum* hydrated faster than *H. annuus*). The mass loss of AH-SECs tablets of *L. clavatum* was (35 ± 3 mg i.e. 23.33 % of their initial weight was lost in the water bath).

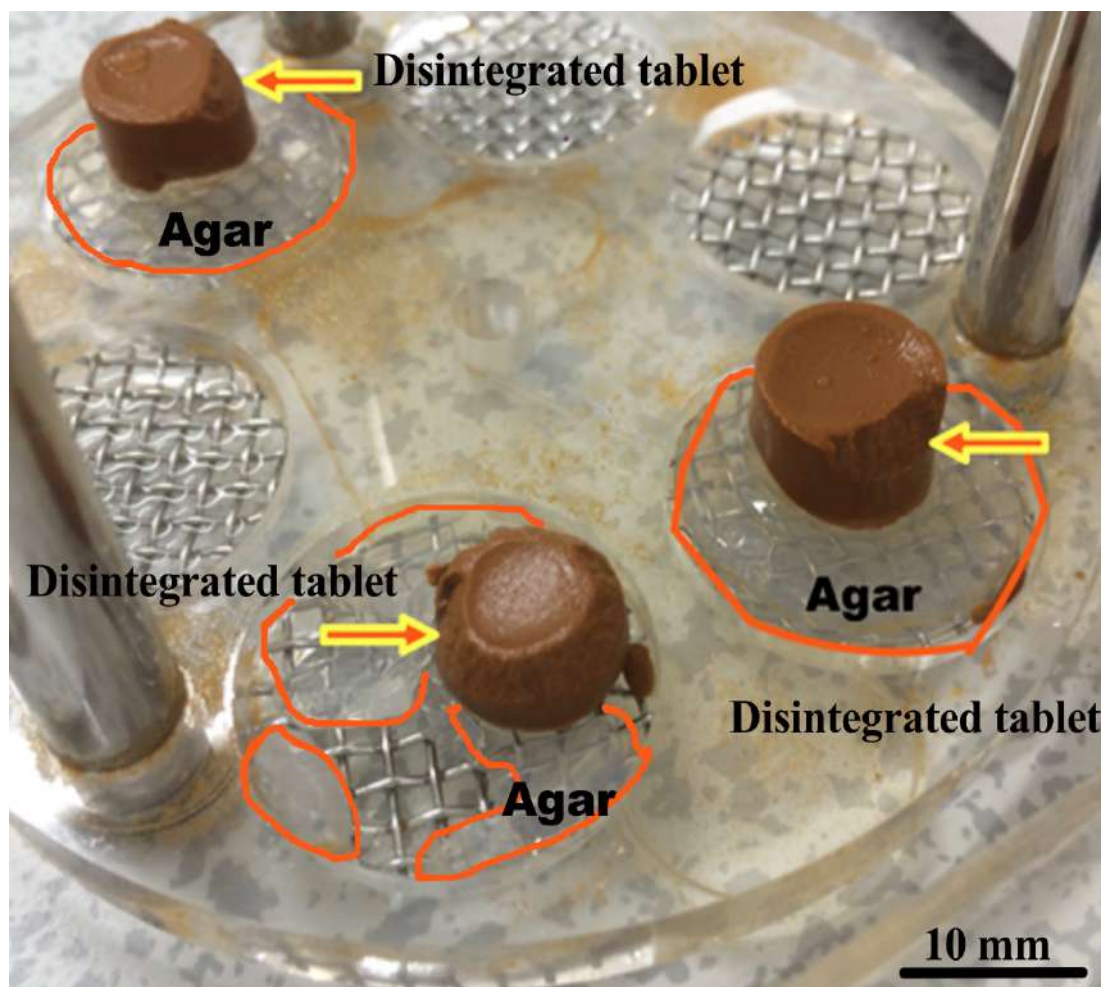


Figure 78: AH-SECs of *L. clavatum* tablets after disintegration for 2 hours. The picture shows that all of the tablets lost their tablets shape and started to disintegrate and absorb water. The tablets were placed in 15 mm diameter nutrient agar disc (red circle) to mimic the mucosa. These tests were repeated in triplicate.

The third sample that was chosen to test disintegration times was the BH-SECs of *L. clavatum*. After two hours of being subjected to the disintegration test, they completely lost their tablet form, and dispersed in the water in less than an hour. This is because they are more hydrophilic than the AH-SECs of *L. clavatum* and *H. annuus*. As explained earlier in (Section 3.4.8), the base extracting method (Section 8.6.6) gives a salt form of the SECs, which easily hydrate and disperse in water.

Figure 79 shows the BH-SECs of *L. clavatum* tablets before disintegration, whilst there was no identifiable remnant of the tablet left after disintegration; just a yellowish suspension was observed.



Figure 79: BH-SECs of *L. clavatum* tablets before disintegration. These tests were repeated in triplicate.

In conclusion, different type of SECs could be chosen to deliver drugs by the oral route, depending on the therapeutic agent that is intended to be released into the GIT. For example, if the encapsulated drug is required to be released quickly into the stomach in less than an hour, BH-SECs *L. clavatum* tablets might be preferred. Alternatively, if the therapeutic agent intended to be released over a long period of time, then the *H. annuus* tablets would be a better choice since they disintegrate over a longer period. However, for this study, AH-SECs of *L. clavatum* tablets is considered the best choice for common drug releasing as they can be disintegrated within 2 hours while they still in the stomach. In this way they will be in dispersed state before entering the intestine where the most drugs are absorbed there into blood stream. Hence, that will facilitate the releasing and then enhance the absorption, as

was the case when AH-SECs of *L. clavatum* were used to encapsulate and release EPA in an earlier study [73].

6.5 An attempt to Explain the Role of SECs Mucoadhesivity, the ‘dry liquid’ Lipids and the Controlled Release in Absorption Enhancement

SECs have many attributes that may be used to explain the mechanism of absorption enhancement. For example, it has been shown that they have mucoadhesion properties that can help in keeping SECs and the mucosa of the GIT in contact for a longer period of time at the site of absorption (Sections 5.2, 6.1, 6.2 and 6.3). This will lead to continued release of the actives from the SECs cavity to the site of absorption. Also, the controlled release that was discussed earlier in (Section 4.3.1.1) can help in increase the half-life time of the encapsulated therapeutics by its slow release effect, as SECs will stop releasing the encapsulated actives when the first release reached a fixed level, and then start the second dose release when the first dose level decreased. Furthermore, the ‘dry liquid’ lipids of SECs that could not be removed during the SECs extraction by 9 M HCl (in Section 3.4.4), which were found to be oleic and linoleic acids (mainly), have the ability to enhance the absorption by disruption the tight junction between the epithelial cells of the GIT, which responsible for the paracellular transport pathway, and enhance the cell permeability [133]. All these factors are important in absorption enhancement and are found in a natural, non-toxic, mono-dispersed, commercially available and relatively cheap mucoadhesive polymer (see Section 2.4). Figure 80 illustrates the possible role of SECs in absorption enhancement.

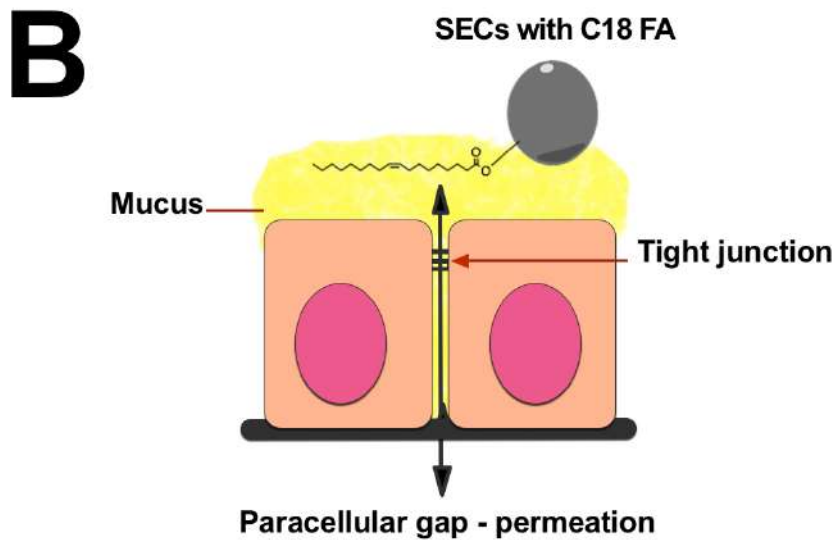
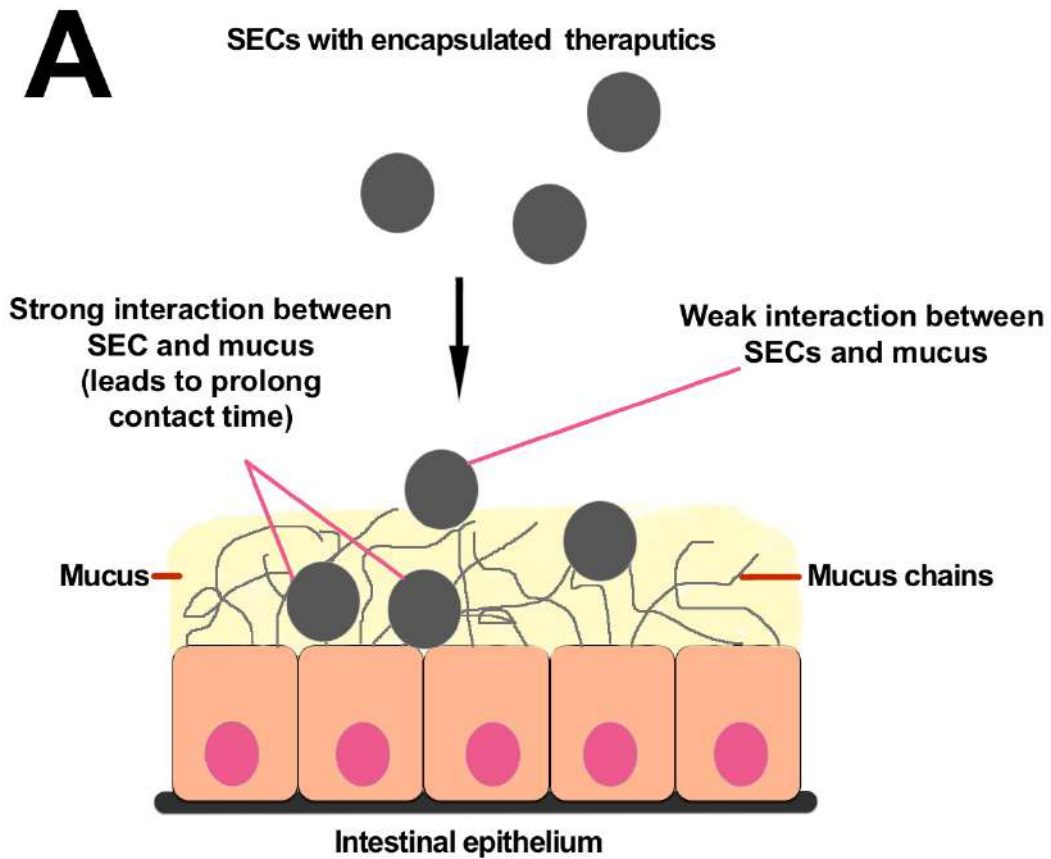


Figure 80: Role of SECs in absorption enhancement. (A) Mucoadhesion play main roles in keep the SECs adhered to GIT epithelium, while the C18 fatty acids of SECs disturb the tight junction and enhance the paracellular permeation (hypothesis).

Chapter 7. Conclusion

Plant spores and pollen grains have amazed many scientists since the 18th century. The outer shell, exine, was the main interest of many studies due to their inertness to wide range of chemicals. Sporopollenin is the secret behind this inertness. Sporopollenin is classified as one of the most durable and resistant natural organic material that can be found in the exines of spores and pollens. Treating spores with strong acids such as, phosphoric acid and strong alkali such as sodium hydroxide could not affect the sporopollenin and exines structures. Moreover, sporopollenin can resist extremely high temperatures of up to 200 °C. Also, it has the capability to survive many types of enzymes.

The SECs of *L. clavatum* spores were used over the last two centuries in traditional medicine and in pharmaceutical applications. These SECs were found in human food sources and have not shown any harmful affects on the human body. After ingestion, SECs can resist all the enzymatic attacks of GIT and reach small intestine then release their contents into the blood stream.

Sporopollenin can be used as a microcapsule to encapsulate many medical substances for protection then controlled release into the site of absorption. In this study vitamin D, diclofenac acid, diclofenac sodium salt and mesalamine were encapsulated in *L. clavatum* SECs, and then released into buffer solutions at different pHs that mimic the GIT pH. The release of such kind of vitamin and drugs showed the direct effect of pH factor on the release of the SECs contents. For example, vitamin D was not released in acidic pH but was released pH 7.4. This was an interesting point, especially, for protecting the encapsulated vitamin D from the harsh acidic environment of stomach.

Conclusion

Thus, the encapsulated vitamin could reach the small intestine and the SECs release their contents in the mildly basic environment of small intestine. Also, diclofenac sodium was released fully in pH 7.4 within 12 hours, whereas less than 40 % was released in pH 1.5. However, the mesalamine showed a full release in acidic pH which showed that SECs need coating to be used for mesalamine.

The adsorption of the drugs to the SECs was shown to be very low (0.4 %), which means almost all the drug will be released and would not adsorb to the SECs surface, especially in the GIT when they would be flushed with fluid continuously.

SECs have the ability to dry their original liquid fatty acid (C16 and C18) or have one added (by adsorption or chemical attachment), and they still show a liquid state behaviour in the SS-NMR spectra. These 'dry liquid' lipids composed 20% of the SECs mass and are attached covalently to either the exines surface or inside the sporopollenin matrix; however, when hydrolyzing them with strong acid or base they lose their covalent bonds and can be dissolved easily with a simple hydrocarbons solvent such as dodecane. These 'dry liquid' lipids may play a role in absorption enhancement as they disturb the intercellular tight junction and enhance the paracellular permeability of the encapsulated actives.

The bioadhesivity properties of SECs can be used to understand the drug release and absorption enhancement mechanism of SECs in intestinal mucosa. The SECs showed greater mucoadhesivity than the common used mucoadhesive polymer in pharmaceutical industries. For instance, *L. clavatum* SECs mucoadhesion strength was twice of those of chitosan. The mucoadhesion strength for *L. clavatum* powder polymer was statistically significant either with their lipids in (p-value = 0.03), or when their lipids were removed (p-value = 0.01).

Conclusion

The disintegration time of SECs tablets gives an idea about the best extraction protocol to use to increase the time of disintegration or decrease it depending in the site of absorption. For example, AH-SECs of *L. clavatum* was disintegrated within 2 h and lost 23.33 % of their mass, which is a preferable SECs type to be used for EPA release.

As further work, more studies should be done on the pH and their role in the SECs behaviour for drug releasing and bioadhesivity. Also, functionalizing the surface of SECs with different groups that can make them polar or non-polar and more or less hydrophilic will be of interest and important to encapsulate different chemicals to affect their release. For drug delivery, encapsulating different kinds of drug can help in understanding the mechanism of releasing and absorption enhancement and the role of drugs' pK_a . Also, encapsulating drug into SECs, then release it into mucosal tissue with simulated intestinal fluid can help in determining the mucoadhesivity of SECs in real time. *In vivo* studies of release for the encapsulated vitamins and drugs in laboratories animals could give more accurate data as the SECs will face the pH, the enzymes and the temperature of the GIT in a living body.

Chapter 8. Materials and Methods

8.1 Materials

8.1.1 Chemicals

Raw *Lycopodium clavatum*, *Ambrosia artemisifolia*, *Ambrosia trifida*, *Pinus sylvestris* and *Helianthus annuus*, were purchased from Unikum (Copenhagen, Denmark).

Ergocalciferol (vitamin D₂) analytical grade, diclofenac sodium salt, mesalamine (5-aminosalicylic acid), Nile red, deuterium oxide (D₂O) ≥ 99.99 %, mucin from porcine stomach, 100 mm diameter Petri dishes containing nutrient agar, carbopol-934, chitosan and dichloromethane were purchased from Sigma-Aldrich (Dorset, UK).

Sodium hydroxide (NaOH) ≥ 98%, Hydrochloric acid (HCl) ≥ 37%, Phosphate buffer solution (PBS) pH 7.4, Buffer pH 9, Buffer pH 1.5, absolute ethanol, acetone, hexane, dodecane, dimethyl sulfoxide, triethylamine, oleic acid, oleoyl chloride and mPEG-tosylate were purchased from Fisher Scientific (Loughborough UK).

1,2-Dioleoyl-*sn*-glycero-3-phosphocholine (DOPC) was purchased from Avanti Polar lipid inc. (USA).

All studies were carried in the Chemistry Department, University of Hull, Hull, excluding mucoadhesion studies as they were carried in the School of Pharmacy and Life Sciences, Robert Gordon University, Aberdeen.

8.1.2 Apparatus

8.1.2.1 Magic Angle Spinning solid-state proton Nuclear Magnetic Resonance (MAS SS-¹H-NMR)

MAS SS-¹H-NMR was performed using 500 MHz Bruker BioSpin NMR (Germany). The SECs samples were packed in 4 mm NMR rotor, and analyzed using the MAS SS-¹H-NMR. The MAS SS-¹H-NMR was performed with 8 KHz speed spinning rate at 283 Kelvin temperature, $\pi/2$ pulse length and 2 seconds of relaxation delay. The spectra were collected using 16 scans.

8.1.2.2 Ultraviolet-Visual (UV-Vis) Spectroscopy

UV-Vis spectroscopy was performed using PerkinElmer lambda UV-Vis (Massachusetts, USA).

8.1.2.3 Scanning Electron Microscopy (SEM)

SEM was performed using Lecia Cambridge Stereoscan 360 SEM by Tony Sinclair.

8.1.2.4 Texture Analyzer

Texture analysis was performed using a Stable Micro Systems texture analyzer (Surrey, UK). The loaded probe (9 mm) movement downward to the sample palate surface at a speed of 1 mm/sec, with contact force of 0.5 Newton and probe withdrawn speed of 10 mm/sec.

8.1.2.5 Differential Scanning Calorimetry (DSC)

DSC was performed using PerkinElmer (Massachusetts, USA). 3 mg of sample in aluminum pan was cooled from room temperature to 0 °C, then heat it until 300 °C at 20 °C/min rate.

8.1.2.6 Elemental Composition Analysis

Elemental composition analysis was performed using Fisons instrument Carlo Erba EA 100 C H N S analyser by Carol Kennedy.

8.1.2.7 Inductively Coupled Plasma- Optical Emission Spectrometer (ICP-OES)

ICP-OES was performed using Perkin Elmer Optima 5300DV spectrometer by Bob Knight to detect Na in the PEGylated SECs samples. A calibration curve was prepared with 1000 ppm of Na standard. An amount of 30 mg of SECs was added to 4 ml of nitric acid (HNO₃) in a teflon vessel and sealed. The samples were then digested with nitric acid at 200 °C in high pressure (approximately 250 psi) for 15 minutes and then diluted with purified water by weight.

8.1.2.8 pH Testing

The pH of SEC-water filtrates was conducted using a Hanna HI 2210 pH Meter. Direct pH measurement of the suspension was affected by SECs sticking to the probe so it was essential to filter the suspension before testing.

8.1.2.9 Gas Chromatography Mass Spectrometry (GC-MS)

GC-MS was performed by Kevin Welham, using Agilent 5973N single quadrupole Mass Selective Detector (MSD) with Agilent 6890+ Gas Chromatograph (GC) and Agilent 7683 Automated Liquid Sampler (ALS). Agilent HP-1 GC column 0.2 mm (id) x 12 m (length) x 0.33 μm (film thickness). Helium Carrier gas at 1 mL min^{-1} , split injection with 100:1 split ratio, 1 μL sample used. Injector Temp $250\text{ }^{\circ}\text{C}$ and the Interface Temp $250\text{ }^{\circ}\text{C}$. The temperature programmed GC method was as the following: $40\text{ }^{\circ}\text{C}$ for 3 min, then $40\text{ }^{\circ}\text{C}$ to $310\text{ }^{\circ}\text{C}$ at $15\text{ }^{\circ}\text{C min}^{-1}$, held at $310\text{ }^{\circ}\text{C}$ for 12 min. For the main samples, four drops were taken and made up to 1.5 mL with methanol. For FAMES analysis the samples (0.5 mL) were converted to Fatty Acid Methyl Esters (FAMES) using methanolic KOH (1.0 mL), the FAMES were then extracted into DCM (1.5 mL) for analysis using the method as described above.

8.1.2.10 Disintegration Testing

The Disintegration testing was performed using a Copley Disintegration Tester DTG Series. Samples were left inside the Copley disintegrator at $37\text{ }^{\circ}\text{C}$ and 30 cycle per minute for 2 hours. In each cycle, the flat probe was lowered to a beaker full of water, immersed in the tablet and then raised up again.

8.2 Extraction of Sporopollenin exine capsules (SECs) from Raw spores

8.2.1 Protocol A: Extraction of *L. clavatum* SECs using Base

Hydrolysis

Raw *L. clavatum* spores (500 g) were suspended in 6% (w/v) sodium hydroxide aqueous solution (NaOH)_{aq} (156 g, 2.6 L), then heated at 80 °C overnight. The next day, the mixture was filtered with porosity grade 3 filter (20 µm), and the isolated SECs then washed with 3 L of pure water (H₂O) three times to remove the excess NaOH, until the solution became neutral. The extracted SECs were washed with 1 L of absolute ethanol three times to remove the excess, and then refluxed in ethanol (2.6 L) at 80 °C for four hours. The SECs were filtered using vacuum and washed three times with absolute ethanol, then left in vacuum to dry overnight to a constant weight to give the base hydrolyzed sporopollenin exine capsules (BH-SECs).

This protocol was repeated three times to avoid any technical error and get the average net weight of SECs after extraction. The average weight of dried extracted BH-SECs of *L. clavatum* was 225 ±0.01 g. Then, the samples were sent for elemental analysis, which showed no nitrogen in the sample indicating a successful extraction. The details of this elemental analysis data is shown in Table 21.

Element	% Found
C	60.70 ±3.0
H	7.30 ±1.3
N	0.00 ±0.0

Table 21: Elemental analysis of BH-SECs *L. clavatum*. The elemental analysis was run in triplicate. $n = 3$.

8.2.2 Protocol B: Extraction of sporopollenin using Acid Hydrolysis

Raw spores (500 g) from *L. clavatum*, *A. artemisifolia*, *A. trifida*, *P. sylvestris* or *H. annuus* were suspended in 9 M hydrochloric acid aqueous solution (HCl)_{aq} (2.25 L), then heated at 100 °C for a period of time (1 hour and 24 hours) The next day, the mixture was filtered with porosity grade 3 filter (20 µm), and the isolated SECs then washed with 3 L of H₂O three times to remove the excess HCl, until the solution became neutral. The SECs were filtered using vacuum and washed three times with 1 L of absolute ethanol, then left in vacuum to dry overnight to a constant weight.

Also, this protocol was repeated three times to avoid any technical error and get the average of SECs net weight after extraction. The average weight of dried AHS was 270 ±0.015 g. $n = 3$.

8.2.3 Protocol C: Treatment of Base hydrolyzed SECs of *L. clavatum* (BH-SECs) with acid

BH-SECs of *L. clavatum* (40 g, prepared using Protocol A) were suspended in 9 M HCl_{aq} (0.36 L), then heated at 100 °C overnight. In the next day, the mixture was filtered with porosity grade 3 filter (20µm), then the SECs washed with 3 L of H₂O three times to remove the excess HCl, until the solution became neutral. The SECs were filtered using vacuum and washed three times with 3 L of absolute ethanol, then left in vacuum to dry overnight to a constant weight. This protocol was run in triplicate and the net weight of dried extracted SECs was 31 ±0.01 g.

8.3 Chemical Resistance Study

The AH-SECs of *L. clavatum* (1 g) (which refluxed for 1 hour and 24 hours in 9 M HCl -Protocol B) was sent to obtain SEM images and MAS SS-¹H-NMR to check any morphological or chemical changes after exposure to such corrosive acid.

8.4 Thermal Resistance Study

AH-SECs of *L. clavatum* (1 g) was left in oven at 200 C for 3 hours and 24 hours. After that period of time, the SECs were collected and left to cool down in open air, and then they were sent to obtain SEM images and MAS SS-¹H-NMR to check any morphological or chemical changes after exposure to such a high temperature.

8.5 A study of *L. clavatum* SECs' Elasticity

AH-SECs of *L. clavatum* was grinded with a hard object, namely 70-110 μm glass beads, to break them. The SECs and the glass beads were mixed together and grinded manually using mortal and pestle until having a fine powder (5 minutes). Then, SEM images were taken for the mixture of the resulted fine powder of the SECs and the glass beads.

8.6 A study of *L. clavatum* SECs' Lipids

8.6.1 An Attempt to Dissolve Raw SECs Lipids with Different Solvents

1. Raw *L. clavatum* spores and *P. sylvestris* pollens (1 g) were treated individually with acetone, ethanol, dodecane and chloroform (10 ml) at 100 C for 24 h. the next day, the reaction was filtered (and the filtrate were collected and sent to obtain GC-MS), whereas the spores and pollens were washed with absolute ethanol (10 ml x 3), and left to dry at desiccator to constant weight.
2. The previous raw *L. clavatum* spores and *P. sylvestris* pollens that were treated with the lipid dissolving solvents (200 mg) were treated individually with dodecane (2 ml) at 60 C for 4 h. After that, the spores/pollens were filtered (and the filtrate were collected and sent to obtain GC-MS), whereas the spores and pollens were washed with absolute ethanol (10 ml x 3), and left to dry at desiccator to constant weight.

8.6.2 An Attempt to Dissolve AH-SECs Lipids with Different

Solvents

AH-SECs of *L. clavatum* spores and *P. sylvestris* pollens (1 g) were treated individually with dodecane (10 ml) at 60 °C for 4 h. After that, the reactions were filtered (and the filtrate were collected and sent to obtain GC-MS), whereas the AH-SECs of spores and pollens were washed with absolute ethanol (10 ml x 3), and left to dry at desiccator to constant weight.

8.6.3 An Attempt to Quantify the AH-SECs Lipids using MAS SS-

¹H-NMR

In this method water (5 mg) was added to an accurately weighed sample of AH-SECs of *L. clavatum* (75 mg) in a SS-NMR 4 mm rotor, to compare the integration area of the lipid peaks in relation to the water peak.

8.6.4 Nile red Staining of SECs

AH-SECs of *L. clavatum*, an access amount (1 ml) of 31.41mM Nile red (1 mg/ml) was added to SECs in acetone (1g/ml stain/acetone solution). The mixture was left in orbital shaker at 240 rpm for 20 minutes at room temperature, and then filtered, washed with PBS and vacuum dried overnight. The stained SECs were spread in glass slide and kept in kitchen foil to protect from light, then sent directly to fluorescence microscopy to obtain an image for the stained SECs and their lipids.

8.6.5 An Attempt to Add C18 fatty acid to the Lipid-free AH-SECs

Physically

Oleic acid (400 mg) mixed with 7 ml of water, was shaken for 20 minutes in orbital shaker at 900 rpm. AH-SECs of *L. clavatum* or *P. sylvestris* (200 mg) were added to the (202.28 mM) oil-water emulsion, and shaken for 1 min by hand, then left at room temperature for 4 hours. The emulsion was filtered using vacuum and filter (porosity grade 3) and the SECs were washed with hexane (10 ml x 3) to remove the excess of the oil, then left to dry under vacuum overnight.

8.6.6 Modifying the Surface of SECs with NaOH

AH-SECs of *L. clavatum* or *P. sylvestris* (5 g) were added to 100 ml of 2 M NaOH, then left stirring at room temperature overnight. Then the mixture was filtered and the SECs washed with water until neutral, then washed with ethanol and left overnight to dry under vacuum.

8.6.7 An Attempt to Add C18 fatty acid to the Lipid-free AH-SECs

Chemically

(A) Oleic acid (10 ml) was added to the lipid-free AH-SECs of *L. clavatum* (1 g) in toluene (50 ml), and then 5 drops of concentrated sulfuric acid (H₂SO₄) was added to the mixture. The mixture was heated at 170 °C overnight. The mixture was filtered, washed thoroughly with hexane (20 ml x3) and dried in desiccator until constant weight.

(B) The lipid-free AH-SECs of *L. clavatum* (1 g) were suspended in dichloromethane (DCM) (10 ml), then triethylamine (Et₃N) (0.3 ml) and oleoyl chloride (10 ml) was added to the SECs-DCM suspension at 0 °C (ice bath). The mixture was left after that stirring for 4 hours at room temperature, then filtered, washed with 2 M HCl (20 ml), pure water until neutral (30 ml x3), ethanol (30 ml) and acetone (30 ml) respectively and vacuum dried overnight to constant weight.

8.6.8 Attempted PEGylation of SECs

First method: AH-SECs (1 g) of *L. clavatum* were stirred in dimethyl sulfoxide (DMSO) (20 ml) for 5 minutes in room temperature, and then anhydrous potassium carbonate (K₂CO₃) (1 g) (126.08 mM) was added to the SECs-DMSO mixture with a catalytic amount of potassium iodide (0.05 g) (33.53 mM). mPEG-tylosate (0.5 g) was added in portion over 10 minutes at room temperature to give final concentration of (0.025 mM). After that the mixture was left for 4 hours at 170 °C to complete the reaction at nitrogen atmosphere, then filtered, washed thoroughly with water (20 ml x 3) then ethanol (20 ml x 3) and dried overnight in desiccator.

Second method: AH-SECs (1 g) of *L. clavatum* were stirred in dimethyl sulfoxide (DMSO) (20 ml) for 5 minutes in room temperature, and then sodium hydride (NaH) (1 g) (2083.53 mM) was added to the SECs-DMSO mixture with a catalytic amount of potassium iodide (0.05 g) (33.53 mM). mPEG-tylosate (0.5 g) was added in portion over 10 minutes at room temperature to give final concentration of (0.025 mM). After that the mixture was left for 4 hours at 170 °C to complete the reaction at

nitrogen atmosphere, then filtered, washed thoroughly with water (20 ml x 3) then ethanol (20 ml x 3) and dried overnight in desiccator.

8.7 A study AH-SECs and BH-SECs of *L. clavatum* Acting as a

Buffer Particles

BH-SECs and AH-SECs of *L. clavatum* (200 mg) were added to deionized water (100 ml) and left for a period of time (1 h, 6 h and 24 h) in orbital shaker at 120 rpm, and then the SECs-water mixture was filtered using 0.22 μm centrifugal filter tube (at 10,000 rpm, for 1 minute) and the water pH was measured using pH conductivity meter.

8.8 Vitamin and Other Drugs Encapsulation and Release

8.8.1 Encapsulation of Vitamin D₂ (ergocalciferol) into BH-AH-SECs of *L. clavatum*

Vitamin D₂ (ergocalciferol) (300 mg) was suspended in 1 ml of absolute ethanol to give final concentration of 756.33 mM, and then mixed in ultrasonic bath for two minutes until the vitamin D₂ had dissolved.

The solution was added to 1 g of BHS-AHS SECs of *L. clavatum*, and then mixed manually for a few minutes to ensure equal distribution. The final mixture (vitamin D₂ encapsulated SECs) was covered with kitchen foil to protect vitamin D₂ from exposure to light, and left under vacuum overnight to evaporate the ethanol.

8.8.2 Mixing DOPC with Vitamin D₂

DOPC (10 mg) was mixed with 10 mg of vitamin D manually using spatula, and then 10 μ l of deuterium oxide (D₂O) was added to the DOPC-vitamin D mixture in 4 mm NMR rotor, and analyzed using the MAS SS-¹H-NMR. The MAS SS-¹H-NMR was performed with 8 KHz speed spinning rate at 283 Kelvin temperature, $\pi/2$ pulse length and 2 seconds of relaxation delay. The spectra were collected using 16 scans for measuring the DOPC and vitamin D₂.

8.8.3 Mixing DOPC with Vitamin D₂ encapsulated SECs

DOPC (10 mg) was mixed with 10 mg of vitamin D₂-encapsulated SECs., and 10 μ l of the buffered deuterium oxide (D₂O) (10 ml D₂O with 9.7 mg phosphate buffer pH 7.4 (0.01 mM)) was added to the above mixture in 4 mm NMR rotor. The next day, the NMR experiment was carried out with 8 KHz speed spinning rate at 310 K, $\pi/2$ pulse length and 2 seconds relaxation delay. The spectra were collected using 8 scans the temperature was optimized to meet the normal human body temperature 37 °C, i.e. 310 K.

8.8.4 Diclofenac and Mesalamine Encapsulation and Release

8.8.4.1 Encapsulation of Diclofenac in AH-SECs of *L. clavatum*

Diclofenac sodium salt (450 mg) was added to 1 ml ethanol to give 1414.51 mM final solution. Then the diclofenac solution was added to 1 g of AH-SECs of *L. clavatum* and mixed manually with a spatula for 1 minute to obtain a homogenous

mixture. The mixture was left in vacuum desiccator overnight until dried to a constant weight.

8.8.4.2 Encapsulation of Mesalamine in AH-SECs of *L. clavatum*

Mesalamine (53 mg) was dissolved in 1 M HCl (1 ml) to give a final concentration of 346.09 mM, then was added to 1 g of AH-SECs of *L. clavatum* and mixed manually with a spatula for 1 minute to obtain a homogenous mixture. The mixture was left in vacuum desiccator overnight until dried to a constant weight.

8.8.4.3 Release of Encapsulated Drugs into Buffer Solutions

A sample of SEC-encapsulated drug (10 mg) was added to known volume of buffer solution (1 ml and 6 ml) and left for a period of time in an orbital shaker (240 rpm) at room temperature. The above mixture was filtered using 0.22 μm centrifugal filter (at 10,000 rpm, for 1 minute) and the concentration of the drug in the filtrate was calculated by comparing it to a standard calibration curve of the drug using a UV-Vis spectrophotometer.

8.9 Drug Adsorption Study of Diclofenac sodium salt

AH-SECs of *L. clavatum* (10 mg) were mixed with 1 ml of an aqueous solution (5 mg/L) (0.016 mM) of diclofenac sodium salt. The above mixture was left in an orbital shaker at 240 rpm for 20 minutes. The mixture was filtered using 0.22 μm centrifugal filter tube (at 10,000 rpm, for 1 minute) and the concentration of the drug in the filtrate (the recovered mass) was measured by comparing it to a standard calibration curve of the diclofenac Na using a UV-Vis spectrophotometer. The

adsorbed drug was calculated by subtracting the drug remaining in the filtrate from the amount in the original sample.

8.10 Mucoadhesion Studies (*in vitro*)

8.10.1 Preparation DSC samples

AH-SECs of *L. clavatum* or *A. artemisifolia* were mixed with hydrated mucin by adding 200 μ l of 5% mucin in water to 10 mg of SECs to get 1:1 ratio of mucin/SECs and then was left for 2 hours at 37 °C in orbital shaker at 120 rpm. The mixture was freeze-dried to have a dry powder of mucin-SECs mixture. The DSC was performed with cooling of a 3 mg of sample in aluminum pan from room temperature to 0 °C, then with heating to 300 °C at a rate of 20 °C/min.

The following combinations were prepared for DSC analysis:

- AH-SECs of *L. clavatum* freeze-dried
- AH-SECs of *L. clavatum* / mucin freeze-dried
- AH-SECs of *A. artemisifolia* freeze-dried
- AH-SECs of *A. artemisifolia* / mucin freeze-dried
- Mucin powder in commercial form as received
- Mucin freeze-dried

8.10.2 Preparing samples for Texture Analysis

The AH-SECs of (*L. clavatum*, *A. artemisifolia*, *A. trifida* and BH-SECs of *L. clavatum*) in addition to the two controls (carbopol-934 and chitosan) were prepared in two forms (powder and tablet) to be analyzed by the texture analyzer. The tablets were made using a Manesty F3 tablet press, to generate a 150 mg tablet with hardness between 40-100 Newtons (using ERWEKA-TBH28 hardness tester). The two forms of each sample were stuck to one of the face of a double-sided sticky pad, and the other face was stuck to the 9 mm probe of the texture analyzer (Stable Micro Systems, Surrey, UK). A mucin solution (50 μ l, 5% mucin in water) was dropped on to a nutrient agar surface. The loaded probe was moved downward to contact the mucin-agar surface at a speed of 1 mm/sec, and after touching it a constant force of 0.5 Newton was applied for 60, 120 and 240 seconds. After the specified time the probe was withdrawn at a speed of 10 mm/sec.

8.11 Preparing the *ex vivo* Experiments of Mucoadhesion

Three cow cheek tissues were smeared with 400 μ l of 5% mucin solution manually using spatula., and then 150 mg of the three types of SECs (AH-SECs and AH-SECs- lipids removed of *L. clavatum* and AH-SECs of *H. annuus*) were spread on the surface of the three cow cheek tissue samples separately. Each one of SECs was left for one minute to give it a time to form bonds between the SECs and mucus, then each sample of tissue was put in a separate bowl with the SECs on the uppermost surface. Each bowl was then filled with water until it just reached the upper, "SEC loaded" tissue surface.

The “SEC-loaded” tissues were left agitating in water bath at 37 °C for 2 hours. After that time, the cheek tissues were removed from the water, and the water was collected into centrifugal tubes and centrifuged at 8000 rpm for 30 minutes. The supernatant was discarded and precipitates (which included the SECs and some of the cheek fibers) were collected and freeze-dried overnight. The second day, the dried precipitates were smashed using mortar and pestle and filtered through 20 µm sieve. Then the free SECs were collected, weighted and subtracted from the initial weight of the SECs that was spread in the cheek surface.

8.12 Preparing Tablet Disintegration Experiments

Three tablets were made for each sample of AH and BH *L. clavatum*, in addition to the AH of *H. annuus*. Each tablets weighed 150 mg. The three tablets were left resting in nutrient agar (15 mm diameter) inside a Copley disintegrator at 37 °C and 30 cycle per minute for 2 hours. In each cycle, the flat probe immerses the tablet in a beaker of water then lifts the tablet out again. After 2 hours, which is the disintegration test time, the tablets were freeze-dried then weighted to calculate the mass loss after disintegration.

References

- [1] *Encyclopædia Britannica* (2006) Chicago: Encyclopædia Britannica, Inc.
Available from: <http://search.eb.com>. accessed January 2015.
- [2] W. Punt, S. Blackmore, S. Nilsson and A. Le Thomas, *Glossary of Pollen and Spore Terminology*. P. Hoen (ed.) (1999) Utrecht: Laboratory of Palaeobotany and Palynology.
- [3] J. Heslop-Harrison, “*Sporopollenin in the biological context.*” in J. Brooks *et al.* (eds.) *Sporopollenin*. (1971) London & New York: academic press, p. 1-30.
- [4] Sporomex, *Our Technology*, available: <http://www.sporomex.co.uk/technology>
accessed January 2015.
- [5] R. Kessler and M. Harley, *Pollen. The hidden sexuality of flowers*. (2004) London: Papadakis, 264 pp.
- [6] I. Orhan, E. Küpeli, B. Şener and E. Yesilada, *J. Ethnopharmacol.*, **109** (2007) 146-150.
- [7] J. F. John, *Journal für Chemie und Physik*, **12**(3) (1814) 244-252.
- [8] F. Zetsche and K. Huggler, *Justus Liebigs Annalen der Chemie*, **461** (1928) 89-108.
- [9] J. W. De Leeuw, G. J. M. Versteegh and P. F. Van Bergen, *Plant Ecology*, **182**(1-2) (2006) 209-233.

References

- [10] J. M. Pettitt, *Protoplasma*, **88** (1976) 117-131.
- [11] J. R. Rowley, J. J. Skvarla and G. El-Ghazaly, *Canadian Journal of Botany*, **81**(11) (2003) 1070-1082.
- [12] J. Brooks and G. Shaw, *Grana*, **17** (1978) 91-97.
- [13] J. Brooks and G. Shaw, *Nature*, **220** (1968) 678-679.
- [14] G. Erdtman, *Svensk Botanisk Tidskrift*, **54**(4) (1960) 561-564.
- [15] G. Shaw, "The chemistry of sporopollenin." in J. Brooks *et al.* (eds.) *Sporopollenin*. (1971) London & New York: Academic Press, p. 305-348.
- [16] J. Brooks and G. Shaw, *Chem. J Geol.*, **10**(1) (1972) 69-87.
- [17] K. Schulze Osthoff and R. Wiermann, *J. Plant Physiol.*, **131**(1-2) (1987) 5-15.
- [18] K. Faegri, "The preservation of sporopollenin membranes under natural conditions." in J. Brooks *et al.* (eds.) *Sporopollenin*. (1971) London & New York: Academic Press, p. 256-272.
- [19] R. G. Stanley and H. F. Linskens (eds.) *Pollen: biology, biochemistry, management*. (1974) Berlin, Heidelberg & New York: Springer-Verlag, 307 pp.
- [20] G. Shaw and D. C. Apperley, *Grana*, **35**(2) (1996) 125-127.
- [21] M. Lorch, M. J. Thomasson, A. Diego-Taboada, S. Barrier, S. L. Atkin, G. Mackenzie and S. J. Archibald, *Chem Commun*, **14**(42) (2009) 6442-4.

References

- [22] E. Domínguez, J. A. Mercado, M. A. Quesada and A. Heredia, *Grana*, **37**(2) (1998) 93-96.
- [23] F. A. Loewus, B. G. Baldi, V. R. Franceschi, L. D. Meinert and J. J. McCollum, *Plant Physiol.*, **78**(3) (1985) 652-654.
- [24] K. E. Espelie, F. A. Loewus, R. J. Pugmire, W. R. Woolfenden, B. G. Baldi and P. H. Given, *Phytochemistry*, **28**(3) (1989) 751-753.
- [25] E.M. Friis, K.P Pedersen, P.R. Crane, *Nature*, **410** (2001) 357–360.
- [26] W. J. Guilford, D. M. Schneider, J. Labovitz and S. J. Opella, *Plant Physiol.*, **86**(1) (1988) 134-136.
- [27] Wiermann R, Ahlers F, Schmitz-Thom I (2001) Sporopollenin. In A Stenbuechel, M Hofrichter, (eds), *Biopolymers*, Wiley-VCH Verlag, Weinheim, Germany **1** (2001) 209–227
- [28] G. Shaw and A. Yeadon, *J. Chem. Soc.*, (1966) 16-22.
- [29] F. Ahlers, I. Thom, J. Lambert, R. Kuckuk and R. Wiermann, *Phytochemistry*, **50**(6) (1999) 1095-1098.
- [30] E. Domínguez, J. A. Mercado, M. A. Quesada and A. Heredia, *Sex.Plant Reprod.*, **12**(3) (1999) 171-178.
- [31] H. Bubert, J. Lambert, S. Steuernagel, F. Ahlers and R. Wiermann, *Zeitschrift Für Naturforschung C-a Journal of Biosciences*, **57**(11-12) (2002) 1035-1041.
- [32] S. Wilwesmeier and R. Wiermann, *Plant Physiol.*, **146** (1995) 22–28.
- [33] A. Meuter-Gerhards, S. Riegert and R. Wiermann, *J.Plant Physiol.*, **154**(4)

References

- (1999) 431-436.
- [34] S. Wilmesmeier, S. Steuernagel and R. Wiermann, *Zeitschrift Für Naturforschung C-a Journal of Biosciences*, **48(9-10)** (1993) 697-701.
- [35] S. Herminghaus, S. Arendt, S. Gubatz, M. Rittscher and R. Wiermann, in M. Cresti *et al.* (eds.) *Sexual Reproduction in Higher Plants*. (1988) New York: Springer, p. 169–174.
- [36] K. Wehling, C. Niester, J. J. Boon, M. T. M. Willemse and R. Wiermann, *Planta*, **179(3)** (1989) 376-380.
- [37] P.F. Vanbergen, M.E. Collinson and J.W. Deleeuw, *Grana*, **1** (1993) 18–30.
- [38] M. Kawase and M. Takahashi, *Grana*, **34(4)** (1995) 242-245.
- [39] A. R. Hemsley, Courier Forschung-Institute of Senckenberg, **147** (1992) 93-107.
- [40] A. R. Hemsley, P. J. Barrie, W. G. Chaloner and A. C. Scott, *Grana*, **Suppl. 1** (1993) 2-11.
- [41] A. R. Hemsley, P. D. Jenkins, M. E. Collinson and B. Vincent, *Bot. J. Linn Soc.*, **121** (1996) 177-187.
- [42] F. Ahlers, J. Lambert and R. Wiermann, *Zeitschrift Für Naturforschung C-a J. Bioscience.*, **58(11-12)** (2003) 807-811.
- [43] A. Boom, *Ph.D. thesis*, University of Amsterdam, Netherlands (2004).
- [44] N.R. Meychik, N.P. Matveyeva, Y.I. Nikolaeva, A.V. Chaikova and I.P. Yermakov, *Biochemistry (Moscow)*, **71** (2006) 893–899.
- [45] A.A. Dobritsa, J. Shrestha, M. Morant, F. Pinot, M. Matsuno, R. Swanson, B.L. Møller, and D. Preuss, *Plant Physiol.*, **151** (2009) 574–589.

References

- [46] A.A. Dobritsa, Z. Lei, S. Nishikawa, E. Urbanczyk-Wochniak, D.V. Huhman, D. Preuss and L.W. Sumner, *Plant Physiol.*, **153** (2010) 937–955.
- [47] S.S. Kim, E. Grienenberger, B. Lallemand, C.C. Colpitts, S.Y. Kim, C. de A Souza, A. Geoffroy, P. Heintz, D. Krahn, D. Kaiser, M. Kombrink, E. Heitz, T. Suh, M. Legrand and C.J. Douglas, *The Plant Cell*, **22** (2010) 4045–4066.
- [48] C. Jungfermann, F. Ahlers, M. Grote, S. Gubatz, S. Steuernagel, I. Thom, G. Wetzels and R. Wiermann, *J. Plant Physiol.*, **151**(5) (1997) 513-519.
- [49] G. Volkheimer, F. H. Schulz, H. Wendland and E. D. Hausdorf, *Maroc Médical*, **47**(506) (1967) 626-633.
- [50] G. Volkheimer and F. H. Schultz, *Digestion*, **1** (1968) 213-218.
- [51] M. L. Weiner, *Food Chem. Toxicol.*, **26**(10) (1988) 867-880.
- [52] F. Delie and M. J. Blanco-Prieto, *Molecules*, **10**(1) (2005) 65-80.
- [53] A. Fasano, *J. Pharm. Sci.*, **87**(11) (1998) 1351-1356.
- [54] G. Volkheimer, *Pathologie*, **14**(5) (1993) 247-252.
- [55] W. Jorde and H. F. Linskens, *Acta Allergologica*, **29**(3) (1974) 165-175.
- [56] T. Liu and Z. Zhang, *Biotechnol. Bioeng.*, **85**(7) (2004) 770-775.
- [57] A. Maack, "Sporopollenin - A new versatile biopolymer." in Polymerix, held in Rennes, France (2003).
- [58] D. Southworth, M. B. Singh, T. Hough, I. J. Smart, P. Taylor and R. B. Knox, *Planta*, **176** (1988) 482-487.
- [59] B. P. Binks, J. H. Clint, G. Mackenzie, C. Simcock and C. P. Whitby, *Langmuir*, **21**(18) (2005) 8161-8167.
- [60] S.L. Atkin, S. Beckett and G. Mackenzie, UK, *Patent* US 20050002963 (2005).
- [61] E. Yilmaz, M. Sezgin and M. Yilmaz, *J. Mol. Catal. B-Enzym*, **62** (2010) 162–

168.

[62] H. Tutar, E. Yilmaz, E. Pehlivan and M. Yilmaz, *Int. J. Biol. Macromol.*, **45** (2009) 315–320.

[63] M. Ucan, A. Gurten and A. Ayar, *Colloids Surf. A: Physicochem. Eng. Asp.*, **219** (2003) 193.

[64] A. Ayar and B. Mercimek, *Process Biochem.*, **41** (2006) 1553.

[65] M. Ersoz, S. Yildiz and E. Pehlivan, *J. Chromatogr. Sci.*, **31** (1993) 61.

[66] E. Pehlivan, M. Ersoz, S. Yildiz and H. Duncan, *Sep. Sci. Technol.*, **29** (1994) 1757.

[67] E. Pehlivan, M. Ersoz, M. Pehlivan, S. Yildiz and H. Duncan, *J. Colloid Interf. Sci.*, **170** (1995) 320.

[68] A. Ayar and B. Mercimek, *Process Biochem.*, **41** (2006) 1553.

[69] M. Ersoz, E. Pehlivan, H.J. Duncan, S. Yıldız and M. Pehlivan, *React. Polym.*, **24** (1995) 195.

[70] F. Gode and E. Pehlivan, *Bioresource Technol.*, **98** (2007) 904.

[71] S. Barrier, A. S. Rigby, A. Diego-Taboada, M. J. Thomasson, G. Mackenzie and S. L. Atkin, *LWT-Food Sci. Technol.*, **43** (2010) 73-76.

[72] J. B. Aungst, *The AAPS Journal*, **14.1** (2012) 10–18

[73] A. Wakil, G. Mackenzie, A. Diego-Taboada, J. G. Bell and S. L. Atkin, *Lipids*, **45** (2010) 645-649.

[74] A. Diego-Taboada, P. Cousson, E. Raynaud, Y. Huang, M. Lorch, B. P. Binks, Y. Queneau, A. N. Boa, S. L. Atkin, S. T. Beckett and G. Mackenzie, *J. Mater. Chem.*, **22** (2012) 9767-9773.

[75] V. N. Paunov, G. Mackenzie and S. D. Stoyanov, *J. Mater. Chem.*, **17** (2007) 609-612.

References

- [76] S. A. Hamad, A. F. K. Dyab, S. D. Stoyanov and V. N. Paunov, *J. Mater. Chem.*, **21** (2011) 18018-18023.
- [77] P. Forsell, R. Partanen and K. Poutanen, *Food Sci. Technol.*, **20**(3) (2006) 18-20.
- [78] U.S. Vural, M. Ersoz and M. Pehlivan, *J. Appl. Polym. Sci.*, **58** (1995) 2423.
- [79] A. Leone-Bay, D. R. Paton and J. J. Weidner, *Med. Res. Rev.*, **20**(2) (2000) 169-186.
- [80] M. S. Amer and Tawashi (Amer Particle Technologies Inc.), USA, *Patent US* 5,013,552 (1991).
- [81] M. S. Amer and Tawashi (Amer Particle Technologies Inc.), USA, *Patent US* 5,275,819 (1994).
- [82] R. Tawashi, USA, *Patent US* 005648101A (1997).
- [83] A. Diego-Taboada, S. Barrier, M. Thomasson, S. Atkin and G. Mackenzie, *Innovations in Pharm. Technol.*, **24** (2007), 63-68.
- [84] Y. Tao, Y. Lu, Y. Sun, B. Gu, W. Lu, J. Pan, *Int. J. Pharm.*, **378** (2009) 30-36.
- [85] J. D. Smart, *Adv. Drug Delivery Rev.*, **57**(11) (2005) 1556-1568.
- [86] A. Ahuja, R. Khar and J. Ali, *J. Pharm. Bioal. Sci.*, **3**(1) (2011) 89-100.
- [87] C. R. Park and D. L. Munday, *Int. J. Pharm.*, **237**(1-2) (2002) 215–226.
- [88] J.K Vasir, K. Tambwekar, and S. Garg, *Int. J. Pharm.*, **255** (2003) 13-32.
- [89] K. Edsman and H. Hagerstrom, *J. Pharm. Pharmacol.*, **(57)** (2005) 3–22

References

- [90] Lee, J.W., Park, J.H. & Robinson, J.R. *J. Pharm. Sci.*, **89**(7) (2000) 850-866.
- [91] G. Mackenzie, *internal report*, University of Hull, UK (2015).
- [92] K.E. Cooksey, J.B. Guckert, S.A. Williams, P.R. Callis, *J Microbiol Methods*, **(6)** (1987) 333-345.
- [93] P. van Gijzel, *Proceeding of the Koninklijke Nederlandse Akademie Van Wetenschappen*, **64**(1) (1961) 56-63.
- [94] M. T. M. Willemse, “Morphological and fluorescence microscopical investigation on sporopollenin formation at *Pinus sylvestris* and *Gasteria verrucosa*” in J. Brooks et al. (eds.) *Sporopollenin*. (1971) London & New York: Academic Press, p. 68-91.
- [95] F. De Jaeghere, E. Allémann, R. Cerny, B. Galli, A.F. Steulet, I. Müller, H. Schütz, E. Doelker and R. Gurny, *Pharm. Technol.*, **3** (2001) 1-8.
- [96] M.F. Holick, *N Engl J Med*, **357** (2007) 266–281.
- [97] A. Zittermann, *Prog Biophys Mol Biol*, **92** (2006) 39–48.
- [98] S.J. Singer, G.L. Nicolson, *Science*, **175** (1972) 720-731.
- [99] V.P Torchilin, *Annu Rev Biomed Eng.*, **8** (2006) 343-375.
- [100] McGettigan P, Henry D., *PLoS Med.*, **10**(2) (2013) e1001388.

References

- [101] Briefing Documents for FDA Joint Meeting of the Arthritis Advisory Committee (AAC) and Drug Safety and Risk Management Advisory Committee (DSARM). Iroko Pharmaceuticals, LLC: Silver Spring; 2014.
- [102] P.A. Todd, E.M. Sorkin, *Drugs*, **35**(3) (1988) 244-285.
- [103] P. Derry, S. Derry, R.A Moore and H.J McQuay, *Cochrane Database Syst Rev.*, **2** (2009) CD004768
- [104] C. Durairaj, S.J Kim, H.F Edelhauser, J.C Shah and U.B Kompella, *Invest. Ophth. Vis Sci.*, **50**(10) (2009) 4887-4897.
- [105] F. Zafar, H. Ali, S.N Shah, R. Bushra, R. Yasmin, G.R Naqvi and H. Shareef, *Lat. Am. J. Pharm.*, **33**(5) (2014) 759-765.
- [106] R. Kozakevych, Y. Bolbukh and V. Tertykh, *World J. Nano Sci. Eng.*, **3**(3) (2013) 69-78.
- [107] O. Gezici and A. Ayar, *CLEAN Soil, Air, Water*, **37**(4-5) (2009) 349-354.
- [108] B. G. Feagan, N. Chande, and J. K. MacDonald, *Inflammatory Bowel Diseases*, **19**(9) (2013) 2031–2040.
- [109] A. C. Moss and M. A. Peppercorn, *Expert Opinion on Drug Safety*, **6**(2) (2007) 99-107.
- [110] S. N. Rasmussen, S. Bondesen and E. F. Hvidberg, *Gastroenterology*, **83**(5) (1982)1062–1070
- [111] R. N. Brogden and E. M. Sorkin, *Drugs*, **38**(4) (1989) 500-523.

References

- [112] A. Abinusawa, S. Tenjarla, *Advances in Therapy*, **32**(5) (2015) 477-484.
- [113] D. Duchene, F. Touchard and N.A. Peppas, *Drug Dev. Ind. Pharm.*, **14** (1988) 283–318.
- [114] R. Gurny, J.M. Meyer, N.A. Peppas, *Biomaterials*, **5** (1984) 336–340.
- [115] G.P Andrew, T.P Lavery and D.S Jones, *Euro. J. Pharm. Biopharm*, **71**(3) (2009) 505-518.
- [116] S. Rossi, M.C Bonferoni, F. Ferrari and C. Caramella, *Pharm. Dev. Technol.*, **4**(1) (1999) 55-63.
- [117] A. Portero, D.T Osorio, M.J Alonso and R.C López, *Carbohydr. Polym.*, **68**(4) (2007) 617-625.
- [118] A. Ludwig, *Drug Deliv. Rev.*, **57**(11) (2005) 1595-1639.
- [119] J. Modi, G. Joshi and K. Sawant, *Drug Dev. Ind. Pharm.*, **39**(4) (2013) 540-547.
- [120] G.W.H. Hohne, W.F. Hemminger, H.-J. Flammershein, *Differential Scanning Calorimetry*, second ed., Springer-Verlag, Berlin, Heidelberg, New York, 2003.
- [121] R. Ruiz-Caro and M.D Veiga-Ochoa, *Molecules*, **14** (2009) 4370-4386.
- [122] R. Sobel, eds., 2014. *Microencapsulation in the Food Industry* *Microencapsulation in the Food Industry* 1st ed., San Diego: Elsevier Science Publishing Co Inc.
- [123] S. Harding, S. Davis, M. Deacon and I. Fiebrig, *Biotechnol Genet Eng Rev*, **16** (1999) 41-86.

References

- [124] X. Cao, *Ph.D. thesis*, Boston University, USA (1997).
- [125] C. Eouani, P. Piccerelle, P. Prinderre, E. Bourret and J. Joachim, *Euro. J. Pharm. Biopharm.*, **52**(1) (2001) 45-55.
- [126] N. Thirawong, J. Nunthanid, S. Puttipipatkachorn and P. Sriamornsak, *Eur. J. Pharm. Sci.*, **67** (2007) 132-140.
- [127] N. Thirawong, R.A. Kennedy and P. Sriamornsak, *Carbohydr. Polym.*, **71** (2008) 170-179.
- [128] C.R Park and D.L Munday, *Int. J. Pharm.*, **237**(1-2) (2002) 215–226.
- [129] N.A Peppas and P.A Buri, *J. Control. Release*, **2** (1985) 257-275.
- [130]: Palynology, *World of Forensic Science*. 2005. Available from <http://www.encyclopedia.com>, accessed April 2015
- [131] S. Anwar, J.T. Fell, P.A. Dickinson, *Int. J. Pharm.*, **290**(1-2) (2005) 121-127.
- [132] N. Donauer, R. Lobenberg, *Int. J. Pharm.*, **345**(1-2) (2007) 2-8.
- [133] W.G Jiang, R.P Bryce and D.F Horribin, *Biochem Biophys Res Comm*, **244** (1998) 414-420.
- [134] S.L Atkin, S.T Beckett and G. Mackenzie, *Patent WO Patent 2005000280* (2005).
- [135] R. Batchelor, C. J. Windle, S. Buchoux and M. Lorch, *J. Biol. Chem.*, **285** (2010), 41402-41411.
- [136] L. Brannon-Peppas, *Med Plastics and Biomaterials*, **4** (1997), 34-44.

References

- [137] C.-H. Zheng, J.-Q. Gao, Y.-P. Zhang and W.-Q. Liang, *Biochem. Bioph. Res. C.*, **323** (2004), 1321-1327.
- [138] G. Gregoriadis, *Liposome Technology*. Boca Raton CRC Press, (1984).
- [139] A. Gabizon, *Cancer Invest.* **19** (2001), 424-436.
- [140] E. Donath, *Angew. Chem. Int. Ed Eng.*, **37** (1998), 2202-2205.
- [141] R. Hejazi, and M. Amiji, *Journal of Controlled Release*, **89** (2003), 151-165.
- [142] F.L. Mi, Y. M. Lin, Y. B. Wu, S. S. Shyu, and Y. H. Tsai, *Biomaterials*, **23** (2002), 3257-3267.
- [143] X. Zhao, K. Kato, Y. Fukumoto and K. Nakamae, *Int. J. Adhes. Adhes.*, **21** (2001), 227-232.
- [144] S. Miyazaki, H. Yamaguchi and M. Takada, *Acta Pharm. Nord.*, **2** (1990), 401-406.